INVESTIGATION ON THE FRICTIONAL BEHAVIOUR OF ALUMINIUM AA4032 ALLOY USING EXPERIMENTAL AND NUMERICAL APPROACH

A Thesis Submitted in Partial Fulfillment of the Requirements for the Degree of MSc in Manufacturing Engineering

Under the Supervision & Guidance of
Dr. Desalegn Wogaso

A Thesis Submitted by

Mohammed Hamda
ID No: GSR/0103/09

MSc Manufacturing Engineering

Program of Mechanical Design and Manufacturing Engineering

School of Mechanical Chemical and Materials Engineering

ADAMA SCIENCE AND TECHNOLOGY UNIVERSITY

Adama, Ethiopia

September, 2019

ADAMA SCIENCE AND TECHNOLOGY UNIVERSITY

School of Mechanical, Chemical and Materials Engineering

Program of Mechanical Design and Manufacturing Engineering

MSc in Manufacturing Engineering

INVESTIGATION ON THE FRICTIONAL BEHAVIOUR OF ALUMINIUM AA4032 ALLOY USING EXPERIMENTAL AND NUMERICAL APPROACH

BY

Mohammed Hamda

ID No: GSR/0103/09

Approved by Board of Examiners

Chairman, Department Graduate Committee	Signature	Date
Major Advisor	Signature	Date
Co-Advisor	Signature	Date
Internal Examiner	Signature	Date
External Examiner	Signature	Date

DECLARATION

I certify that research work titled "Investigation on the Frictional Behavior of Aluminum AA4032 Alloy Using Experimental and Numerical Approach" submitted in partial fulfillment of the requirement for the award of the degree of Masters of Science in Manufacturing Engineering is my own work carried out from November to September 2019 under the supervision of Dr. Desalegn Wogaso**,** Mechanical Design and Manufacturing Engineering Program, Adama Science and Technology University, Adama, Ethiopia. The work has not been submitted for the award of any other degree or diploma. All relevant resources of information used in this thesis have been properly acknowledged.

______________________	______________	___________
Candidate	Signature	Date

This is to certify that the above declaration made by the candidate is correct to the best of my knowledge and belief. This thesis has been submitted for examination with my approval.

______________________	______________	___________
Advisor	Signature	Date

ACKNOWLEDGEMENT

I would like to express my sincere gratitude to my advisor **Dr. Desalegn Wogaso** for his continuous encouragement, supervision and useful suggestions throughout the course of this research work. His vast knowledge, guidance and timely suggestions have been helpful in finding solutions to the problems encountered throughout this research endeavor.

I would also like to extend my sincerest thanks and gratitude to **Mr. Abdulmalik Husein,** Program Chair, Mechanical Design and Manufacturing Engineering Program, and member of the Post-Graduate Committee in the School of Mechanical, Chemical and Material Engineering, for his support and contribution to the success of my thesis work.

In addition, I am here expressing my special thanks to **Mr. Habtamu Ketema**, Mechanical Lab Assistant, Ethiopian Conformity Assessment Enterprise, Ethiopian Standard Agency, for his valuable help during the laboratory work. Mr. Habtamu Ketema provided guidance and insight from his testing experiences on the set up and operation of the lab based hydraulic press used throughout this study.

I would like to thank **Mr. Yilikal Dinkayehu,** Mechanical Lab Assistant, Mechanical Engineering Department, Adama Science and Technology University, for his support during preparation of work piece. I am also thankful to **Mr.Abby Tesfaye,** Material Lab Assistant, Addis Ababa Institute Technology University, for providing the facilities to measure roughness of specimens.

Thank you to all my colleagues and friends of Manufacturing Engineering Stream, Mechanical Engineering Department, Adama Science and Technology University, who supported me in all possible forms. In particular, special thanks go to **Mr. Murtesa Dabesa** and **Mr. Anjelo Lidetu**, for their kind support and helpful suggestions. I am very grateful.

Finally, I wish to express my sincere gratitude to my parents who helped me and encouraged me along the way. However, most of all, I am indebted to my mother, **Wezero Dero Boka**, for her moral support and suggestions that made a great contribution to this work.

ABSTRACT

Nowadays, aluminum 4032 alloy and different non-ferrous material combinations are widely used for applications such as car component production, airplane industry and civil engineering, where lightweight materials are required. In the industrial metal working operations, most of the time, to reduce friction, metal forming industries have been using un-recommended lubricant during metal alloys forged to various components. However, for metallic alloys a realistic friction factor must be specified at the die-work piece interface in order to obtain accurate metal flow. The friction factor of the different metal alloy shows different behavior under different metal forming processes. The aim of this research was to investigate frictional behavior and select suitable lubricant for processing of aluminum 4032 alloy using ring compression test. The investigation was structured into two parts. The first part was to study experimentally the effects of surface roughness of work piece on the friction factor. The experiment was performed using 1.5 µm, 2.5 µm and 3.5 µm work piece roughness to understand how various surface roughness affects the friction behavior during dry conditions. The second experimental study was conducted as the effects of various lubricants on the friction factor by varying the lubricating conditions with respect to selected surface roughness at lower values of interface friction. In order to know the friction behavior of AA 4032, a number of lubricating conditions, including palm oil, grease, and emulsion oil were examined. For both experiment, DEFORM-3D, a commercial finite element simulations were used to analyze the effects of various surface roughness and lubricating conditions on the interface friction factor, in order to evaluate frictional behavior of aluminum 4032 alloy effectively. Ring compression test results indicate that the use of smoother surface roughness of work piece has reduced the friction factor during dry condition. In addition, the friction factor was determined for various lubricating conditions, and palm oil is found to be a suitable lubricant for AA 4032 during cold forging. Effects of various surface roughness and lubricating conditions on the interface friction factor, obtained by finite element simulations are in a good agreement with the experimental data.

Keywords: *friction factor, surface roughness, ring compression test, finite element simulation*

TABLE OF CONTENT

LIST OF TABLES

LIST OF FIGURES

LIST OF ACRONYMS AND ABBREVIATIONS

AA: Aluminum Association

$D_{o:}$ Internal diameter of the ring in the initial stage

D_f : Internal diameter of the ring in the final stage

$H_{o:}$ Initial height of the ring

$H_{f:}$ Final height of the ring for every reduction

OD: Outer diameter of ring specimen

ID: Inner diameter of ring specimen

H : Height of ring specimen

μ : Friction coefficient

m: Friction factor

τ : Tangential stress

σ : Normal stress

F : Sliding force on the interface along the interfacial direction

N : Normal force on the interface along the normal direction

τ_0 : Shear strength of the material

σ_0 : Yield strength

τ_0 : Shear strength

P_{ave} : Average surface pressure on the deformation specimen

ISO : International standardization organization

e : Engineering strain

S : Engineering stress

e_t : True strain

σ_t : Axial true stress

$F_{i:}$ Instantaneous load

F_t : Original load

A_i : Instantaneous area

A_o : Original area

σ_e : Effective stress

n : Strain hardening coefficient

K: Strength coefficient

CHAPTER ONE

INTRODUCTION

1.1 Background and Justification

The metal forming process, such as forging, is one of the manufacturing processes where metal is pressed, pounded or squeezed under high pressures into high strength parts by (Semiatin, 1998). During forging process, the work piece is placed between upper and lower die, and it is deformed under high compressing pressure provided by the power module when the two dies move towards each other. The advantage of metal forming over cutting is that it changes the shape and dimensions of the work pieces without removing material. If used properly, it provides a greater benefit in saving materials as well as extra mechanical merits like higher structural strength gained through strain hardening. Mechanical parts obtained through forging process are very common in industrial practice, and they are stronger than an equivalent cast part or machined part. This is because the macrostructure of the material is continuous throughout the part, giving rise to a piece with improved strength characteristics.

In the compression process, the friction affects the shape of the work piece as reported by (Narayanasamy & Pandey, 1997). When the work piece contacts with the die, the work piece is deformed mainly under the pressure normal to the interface, and at the same time the work piece flows in the tangential direction as well. Such tangential flow depends on the friction condition of the die-work piece interface. It would lead to higher equivalent stress, which reduces the workability of the metal block and generates failure such as cracks so that the metal block is rejected. Thus, for controlling the quality of the product obtained through the compressing process, the friction condition on the die-work piece interface is required to be controlled.

As the ease of metal flow is key to achieving die fill, common industry practice is to minimize interface friction through the use of metal forming lubricants. When the two surfaces are separated by a lubricant layer, the asperities of the two surfaces will not interact each other, as a result a metal can easily flow between die and work piece. Furthermore, proper and adequate lubrication of a correct lubricant is essential to reduce this interface friction. (Rajesh & Siva-Prakash, 2013) conducted experimental study to analysis friction factor under different lubricants. The result show that presence of lubricant at the interface between the tools and work piece reduces the interface friction coefficients. (Wogaso, et al., 2014) utilized ring compression test and finite element simulations to investigate the frictional behavior of powder metallurgical Al-4%Cu preforms under different initial relative densities and lubricating conditions. They concluded that the use of lubricants has reduced the friction. (Shahriari, et al., 2011) also conducted experimental study and finite element simulations to determine effects of lubricant and temperature on the friction coefficient during hot forging conditions. The results revealed that the interfacial friction is significantly dependent on the temperature and type of lubricants used.

However, forging process introduces plastic deformation and an increase in new surface area that causes most of lubricant to be squeezed out, resulting in boundary lubrications to be present at critical locations, even where a thick layer of lubricant is sprayed initially as summarized by (Peterson & Ling, 1966). The lubrication conditions vary a lot during metal forming processes. Therefore, one has to consider the working conditions in order to select the proper lubricants. Under high pressures and reductions the lubricant film often breaks down and causing poor metal flow and wears. In addition, (Isogawa, et al., 1992) suggested that it is not economically practicable or viable to test a large number of lubricants in the production shops, since any failure in lubrication may result in huge losses of money and time. Performance of the lubricants also cannot be predicted accurately. This again leads to wrong usage of lubricants and subsequently losses. Therefore, it is essential to conduct the friction measurement test and find the lubricity of the lubricants in a laboratory setup under actual production conditions.

In contrast to existing applying lubricant practices, it is hypothesized that the coefficient of friction value for each material must be known in a given metal forming processes. (Sofuoglu & Rasty, 1999) utilized ring compression test to investigate the effect of material properties, strain rate sensitivity, and barreling on the behavior of friction calibration curves and concluded that the friction calibration curves are notably influenced by material properties and testing conditions, and every material possesses its own distinctive friction calibration curves. (Camachoa, et al., 2013) also studied on interface friction in metal forming of industrial alloys including, steel, stainless steel, copper alloy, titanium alloy and nickel alloy. Ring compression test was used in order to determine friction calibration maps for different metal alloys that are typically used in industrial practice of metal forming. Furthermore, the differences and similarities in the behavior observed are evaluated for all materials. It was concluded that the necessity of using a friction calibration map for each material.

Considering the hypothesized relationship between interface frictions and materials friction calibration curve, the overall goal of this research is to investigate the frictional behavior and select suitable lubricant for cold working of AA 4032 by using ring compression test. Specifically, the effects of various surface roughness and lubricating conditions on interface frictions are to be investigated for their effects on metal flow. Through the use of a constant surface roughness variable of lubricating conditions was isolated for the purpose of investigating lubricant effects on the friction factor. A combination of ring compression experiments with finite element simulations is performed in order to analyze the effects of various surface roughness and lubricating conditions on the interface friction factor.

1.2 Research Motivation

Today, aluminum is a common material for a various range of applications such as building construction, automotive industry, aerospace industry and much more. (Stake & Staley, 1996) concluded that weight reduction can be achieved by using aluminum and its alloys. The use of aluminum alloys for truck and automobile engine blocks and cylinder heads, heat exchangers, transmission housings, engine parts and automobile wheels has risen steadily over the last decade with the principal aim to decrease the overall weight of the equipment's.

A better understanding of the material and the forming processes lead to usage in more critical application areas. Forgings offer a high strength to weight ratio, toughness, and resistance to impact and fatigue as summarized in the work of (Altan, et al., 1986). Therefore, the forging process is often used to produce components of aluminum with a defined and exact geometry at high value of structural integrity as well as moderate production costs. Today, aluminum alloys are used to manufacture the components which are likely to be exposed to high temperature such as turbine blades, heat exchangers, transmission housings, engine blocks and cylinder heads. They offer excellent creep resistance in the range of 350 to 450 ºK that is described by (Rao, et al., 1998). Moreover, aluminum and silicone alloying element has been chosen for the wide range of industrial applications as they are excellent corrosion and heat resistant.

From the aluminum alloy uses and applications point of view, investigation frictional behavior and selection of suitable lubricant for processing AA 4032 material is desired. Nowadays, Hibrat Manufacturing Industry, Addis Ababa, Ethiopia, manufactures different aluminum alloys through casting process, and finally received by other industries such as Bishoftu Automotive Industry to made different automotive components through forging process. Moreover, AA 4032 has gained wide applications in recent years due to its strength. It is characterized by an excess of silicone atoms, as indicated in Appendix II. This excess of solute atoms in its chemical compositions enhances its mechanical properties and make it competitive aluminum alloy when high strength is required beside light in weight.

1.3 Statement of Problem

During deformation, as the metal spreads over the compression die surface to increase its diameter, frictional forces will oppose the outward flow of metal. The problem is especially critical in cold forging of metal forming process which induces high contact pressure and new surface generation. Friction is an important parameter to study in metal forming processes since it affects metal flow in the die, forming load, strain distribution, tool life and surface quality of product. Most of the time, for reducing of the cost and time of manufacture, metal forming industries have been used un-recommended lubricant to reduce the friction during forging. Furthermore, they use similar friction factor for all metal alloys during the various metal forming process which is not realistic. However, the friction factor of the different metal alloys shows different behavior under different metal forming processes. Additionally, the investigation of friction behavior of aluminum 4032 alloy with respect to various lubricating conditions and surface roughness of work piece are yet to be clearly understood during cold forging process. Therefore, in this research an attempt was made to investigate the effect of various surface roughness and lubricating conditions on interface friction factor for aluminum 4032 alloy by using ring compression test. Moreover, the integration of ring compression test and finite element simulation were conducted to effectively evaluate frictional behavior of aluminum 4032 alloy. Nowadays, aluminum alloy and different non-ferrous material combinations are widely used for applications such as car component production, airplane industry and civil engineering, where light in weight material is required. Due to these wide applications, it is better to understand the frictional behavior of aluminum 4032 alloy under various surface roughness and lubricating conditions to explore the possibility of selecting suitable lubricant for aluminum 4032 alloy as a means to improve performance and quality in industry.

1.4 Research Questions

The following key research questions are addressed:

1. How does the surface roughness of metal affect the interface friction?
2. How friction affects the deformation load requirement, effective stress and strain induced?
3. Which lubricant is most suitable for aluminum AA 4032 alloy during cold forging process?
4. Is combined ring compression test and finite element simulations approach is a suitable method for evaluation of frictional behavior of light metals?

1.5 Objective of the Study

1.5.1 General Objective

The general objective of this research is to investigate the frictional behavior of aluminum AA4032 alloy using experimental and numerical approach.

1.5.2 Specific Objectives

- To experimentally study the effect of various surface roughness and lubricating conditions on interface friction factor.
- To evaluate the effects of interface friction on the deformation load requirement, effective stress and strain induced for various surface roughness and lubricating conditions.
- To determine the suitable lubricant for aluminum 4032 alloy during forging process.
- To develop a suitable methodology for evaluating frictional behavior of aluminum alloys.

1.6 Significance of Study

This research is expected to contribute to both fundamental metal working knowledge and forging industry practice. From a fundamental perspective, the research will help to provide additional insight regarding the relationship between friction, lubricant and surface roughness of work piece during cold forging. If a correlation can be drawn between friction, lubricant and surface roughness for metal flow, this will also contribute to development of a more comprehensive friction model for metal forging that accounts for surface geometry. Friction modeling improvements will advance die design by optimizing wear and heat patterns within the die leading to longer die life.

With respect to industry practice, this research can help to select the suitable lubricant for forging process of AA 4032 alloy. There is a relative motion between the work piece and the tooling setup during forming and due to this friction arises in the interface between the work piece and the tooling setup. Proper and adequate lubrication of a correct lubricant is essential to reduce this interface friction failing which there would be many ill-effects. It is not economically practicable or viable to test a large number of lubricants in the production shops, since any failure in lubrication may result in huge losses of money and time. Performance of the lubricants also cannot be predicted accurately. This again leads to wrong usage of lubricants and subsequently losses. Therefore, it is essential to conduct the friction measurement test and find the lubricity of the lubricants in a laboratory setup under actual production conditions.

1.7 Scope of Study

This research is limited to investigation of frictional behavior and selection of suitable lubricant for processing of AA 4032 alloy by using ring compression test. Ring compression tests is performed to quantify the effects of various surface roughness values and lubricating conditions on the friction factor during cold working conditions. The effects of interface friction on the deformation load requirement, effective stress and strain induced for various lubricating conditions and surface roughness are evaluated. Three different surface roughness of work piece namely, 1.5 µm, 2.5 µm and 3.5 µm are examined, to understand how various surface roughness affects the friction behavior. Also, three different types of lubricants namely, palm oil, grease, and emulsion oil are examined. To determine whether the various lubricating conditions influences the interface friction, the same work piece roughness are used. Finally, a commercial finite element simulations, DEFORM-3D is also used, in order to evaluate frictional behavior of AA 4032 alloy effectively.

1.8 Thesis Organization

- In chapter one, the general information consist of introduction, background and justification, research motivation, problem statement, objectives, scope of the research and organization of the thesis are presented. The research questions of this study are also stated.
- In chapter two, the literature on friction behavior of metals, and the techniques used to test the interface friction of metal forming processes are reviewed. In addition, the commonly used friction models for metal forming processes are also reviewed. Literature on finite element analysis of metal forming also reviewed.
- In chapter three, the used materials and experimental test procedure for this study discussed. Detailing the compression test apparatus and specimen preparation methodologies are also stated.
- In chapter four, the results and discussions that have been obtained through the experimental testing and finite element simulations are presented. Both results, both experiment and finite element simulation of ring compression test are analyzed. Simulations results are compared with the experimental results to evaluate the interface friction of AA 4032 properly.
- Chapter five summarizes the conclusions of this study, and the recommendations for future work are given in this chapter as well.

CHAPTER TWO

LITERATURE REVIEW

2.1. Introduction

In the past, significant work has been carried out in the field of metal forming to make the process highly competitive and efficient. Extensive researches have been done to understand the dynamics of metal forming. A detailed literature survey has been carried out to understand the effects of various parameters that affect the metal forming process in general and interface friction in particular.

In metal forming operations, process variables such as, work piece geometry, tooling setup, forming load, ram speed, forming temperature and material properties of the deforming body can all be measured by well-established techniques. Die geometries and change in work piece geometries can be accurately measured by conventional measuring instruments. Forming load can be measured by a load cell conveniently though various other methods are also employed. Material properties can be quantified by standardized tensile test, compressive test, impact test or torsion test under controlled conditions. However, interface friction, a process parameter between the tooling setup and the work piece, is difficult to understand and measure accurately either in theory or in actual conditions.

In this chapter, a brief description of aluminum and its alloys, frictional behavior of metals, determination of friction factor, a short review to friction test methods in bulk metal forming and related literature surveys, differences and similarities between those are presented. Finally, information on finite element simulation and a research gaps for investigation of frictional behavior are also presented.

2.2 Aluminum and its Alloys

There are wide ranges of aluminum alloys from low-strength aluminum alloys such as AA 1100 and AA 6061 to high strength aluminum alloys such as AA7075 in aluminum forging. Aluminum alloys are most often extruded in the form of aluminum bars initially, but in some cases, cast billets are also used for production. During the manufacturing process, a billet is produced which is characterized by a homogeneous structure completely free of pores and blow holes as presented by (Kevorkijan, 2001).

Aluminum alloys are mostly named and designated with its composition. The first of the four digits in the designation indicates the alloy group in terms of the major alloying elements as can be seen in Table 2.1. For example, if the amount of copper in aluminum alloy composition is high, it is called as 2XXX alloy group although if the amount of the zinc is high in aluminum alloy composition, alloy group is called as 7XXX, (Yoshimura & Tanaka, 2000).

Table 2. 1 Aluminum alloy groups and their major alloying elements

Alloy Groups	Major Alloying Elements
1XXX	Aluminum with 99.0 % minimum purity and higher
2XXX	Copper
3XXX	Manganese
4XXX	Silicone
5XXX	Magnesium
6XXX	Magnesium and Silicon
7XXX	Zinc
8XXX	Other elements
9XXX	Unused series

2.3 Frictional Behavior of Metals

(Wagoner & Chenot, 1996) described friction in a simple manner as surface resistance to the relative sliding or rolling motion while in metal forming operations it was defined as work piece-die surface resistance to metal flow. On the contrary to its simple definition, (Kalpakjian & Schmid, 2001) concluded that friction is very complex phenomenon in metal forming and includes several parameters that interact with one another such as; sliding speed, contact pressure, surface roughness, material properties, temperature and lubrication condition.

In metal forming process, the friction condition on the interface between the die and ring specimen can be described in two ways, one was friction coefficient factor, according to the Coulomb friction law; another was friction factor according shear friction law. In the Coulomb friction law, friction coefficient factor was defined in (Bay, 1987) as:

$$\mu = \frac{F}{N} = \left(\frac{F}{S} \Big/ \frac{N}{S} \right) = \frac{\tau}{\sigma} \quad (2.1)$$

While in the shear friction law, friction factor was defined as:

$$m = \frac{\tau}{\tau_0} \tag{2.2}$$

Shear friction factor was also referred to as constant shear friction factor; indicating that it was independent of interfacial stress as described by (Hartley, et al., 2007). According to the Von Mises criterion, the tensile and shear yield stresses are related in the uniaxial stress condition as follows, (Wanheim, et al., 1974).

$$\sigma_0 = \sqrt{3}\tau_0 \tag{2.3}$$

Thus,

$$m = \frac{\tau}{\tau_0} = \sqrt{3}\frac{\tau}{\sigma_0} \tag{2.4}$$

As it was discussed by (Avitzur, 1968), the average Coulomb friction coefficient factor can be calculated with measured shear friction factors using the following relation:

$$\mu = \frac{m}{\sqrt{3}}\left(\frac{\sigma_0}{P_{ave}}\right) \tag{2.5}$$

In the metal compression process, the die would interact with the specimen to provide the internal force for shape change. It is desired to have the shape change controllable. Therefore, the internal force that causes the unrecoverable deformation would be of interest. When the material of the structure is at its yield point, the normal stress is equal to the yield strength, thus the friction factor would be:

$$m = \sqrt{3}\mu \tag{2.6}$$

For materials that do not show strong strain hardening behavior, the axial stress would keep the level at the yield strength, after the axial stress reaches the yield point, then the friction factor would remain as $\sqrt{3}\mu$.

2.4 Methods of Evaluating Interface Friction in Bulk Metal Forming

2.4.1 Ring Compression Test

The ring compression test was developed by (Male & Cockcroft, 1965) and has been verified as a robust tool to measure friction between a work pieces and die surfaces. Because of this, the test has wide application to forging practice including, lubricant evaluations as conducted by (Kalpakjian & Schmid, 2001), the examination of surface roughness's on dies as explained by (Sahin, et al., 2007), and the relationship of flow stress and softening at different temperatures as discussed by (Douglas & Altan, 1975). In the ring test, a hollow metal cylinder having a fixed ratio of outer diameter: inner diameter: height, usually 6:3:2 is compressed. The resulting change in the height and inner diameters is then compared to a known set of curves to determine the interface friction as discussed by Male and Cockcroft.

Male and Cockcroft reference the work of (Schroeder & Webster, 1949) in the pressing of thin solid disks for their calibration curves. Webster and Schroder developed a model for the relationship between pressures, friction, and total part deformation using thin uniform disks instead of rings under cold forming conditions. Webster and Schroder overestimated the amount of deformation in their work. This is attributed to the ideal deformation that the researchers assumed in their mathematical model as compared to the actual bulging that took place in the experiment. Male and Cockcroft used the effects of part width and height explored by Webster and Schroder extensively to develop their calibration curves that are now used as a standard reference. In ring compression tests, the inner diameter of the ring may increase, decrease or remain constant, depending on the magnitude of friction at the die and work piece interfaces. For instance, under extremely low friction conditions, or when the friction between the work piece and tool is lower than a critical value, the material flows outwards, and both inner and outer diameters of the ring increase. If the friction at the contact interfaces is higher than a critical value, the material close to the inner diameter flows inwards, which decreases the inner diameter of the ring, and the remainder material flows outwards, which enlarges the outer diameter of the ring. This method is an indirect method to measure the interface friction, and it is the most widely applied method for determining contact conditions in bulk forming processes; therefore it is treated as the standard, universal method for determining of friction factor.

(Sofuoglu & Rasty, 1999) also utilized ring compression test to investigate the effect of material properties, strain-rate sensitivity, and barreling on the behavior of friction calibration curves. The compression tests were conducted to obtain the necessary material properties for the finite element analysis. A series of ring compression tests were then conducted in order to determine the magnitude of the friction coefficient. The experiments were first conducted for the modeling materials, namely, white and black plasticine and later on, for aluminum, copper, bronze, and brass. The experiments were then simulated via an elastic-plastic finite element code (ABAQUS). Contrary to the results available in the literature, where the same friction calibration curves are recommended for all types of materials and test conditions, the results of this investigation showed that friction calibration curves are indeed affected by the material properties and test conditions.

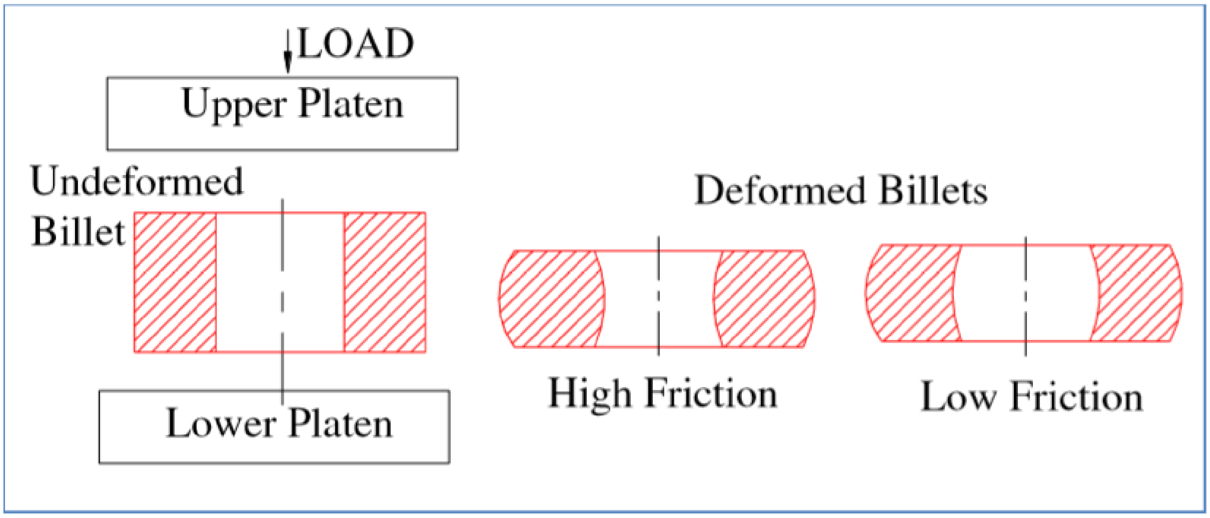

Figure 2. 1 Rings subjected to different friction conditions (Male & Cockcroft, 1965)

2.4.2 Cigar Test

Another test that is used to measure friction in forging applications is the so called cigar test. The name results from the fact that after small rectangular slabs are compressed, they closely resemble the shape of a cigar. In this test the change of width of the compressed specimen is used to calculate the interface friction between the parts and die. This test can be used to measure friction factor, as long as the initial specimen length is at least ten times larger than its width. Due to frictional restraint in the long axis, the specimen will preferentially deform along the direction of the shortest dimension. However, if friction is low enough along the long axis, the length or the longest dimension will also increase which makes it difficult to measure a friction factor using only the change in width. The use of a shorter ratio was however investigated by (Fricker & Wanheim, 1974), who used specimens where the length was much less than ten times the width, in order to evaluate lubricants at cold working temperatures. However, while they were able to accurately measure very low coefficients of frictions (i.e. coefficients less than 0.05), it should be noted that for higher values the ring compression test has been shown to be more accurate. This accuracy was achieved by using a ratio of the change of width and length, instead of just the width dimension. Low values of friction coefficients and factors are normally observed in cold forming. In hot forging, friction values are much higher, limiting use of this test with very short length/width ratios test and thus the ring compression test is more commonly used.

2.4.3 Cylinder Upsetting

Compression of cylindrical specimens parallel to the longitudinal axis, termed upsetting, has also been used to study friction in metal forming. In frictionless upsetting, deformation should proceed in a proportional manner and result in a compressed geometry that is free of any curvature or bulging. However, when friction is present, it restricts radial flow at the die interfaces and causes the material to preferentially flow in the mid-section of the part. The constrained flow adjacent to the top and bottom faces creates a bulging effect which is proportional to the degree of frictional restraint. (Schey, et al., 1982) attempted to use changes in the height and diameter of a cylinder as a means to predict a friction factor but promote caution based on a complex surface interaction which is termed stick-slip friction. Stick-slip friction occurs when the surface of a specimen moves relative to the dies, but as frictional forces increase, the specimen will start to adhere or stick causing the lateral metal flow to cease. As deformation continues and increased force is applied to the die, the part seemingly becomes un-stuck and resumes flowing. The cyclic nature of the process is caused by the friction regime alternating between static and dynamic friction. If performed using a lubricant, the upsetting test can be more reliable since the lubricant provides a film for the material to flow on, minimizing the stick-slip phenomena. Running the test dry creates issues besides stick-slip, including the need for a large press load to complete the test, as well as accelerated part chilling, since as contact pressures increase, heat transfer increases as well.

The upsetting test has also been compared against the ring compression test as a method to determine the friction factor for different lubricants. The calculation is performed by analyzing the deformation of cylindrical and ring specimens using identical conditions to find the actual friction factor encountered. The bulge radius of curvature has been found to have a good correlation to the actual values obtained by the ring compression test as the bulge diameter will decrease with interface friction.

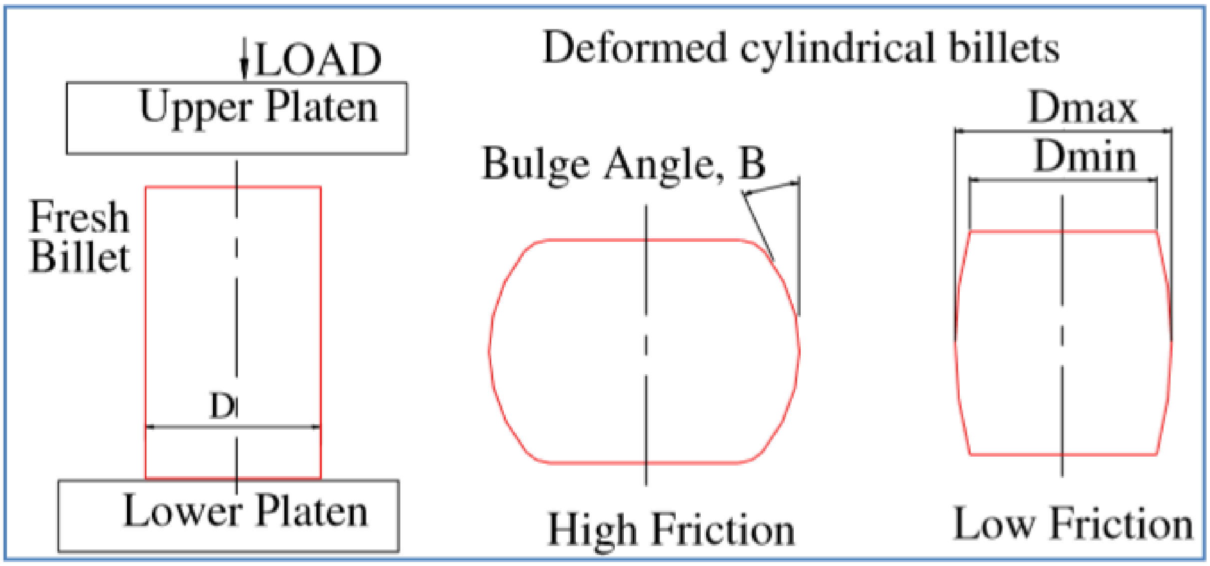

Figure 2.2 cylinder upsetting test (Schey, et al., 1982)

2.5 Effect of Lubricants on Friction

(Wogaso, et al., 2014) studied powder metallurgical Al-4%Cu preforms frictional behavior under different initial relative densities and lubricating conditions. A series of ring compression tests were carried out to obtain friction factor for a number of lubricating conditions, including zinc stearate, graphite, molybdenum disulfide powder, and unlubricated condition. Finite element simulations were also used to analyze materials deformation, densification, and geometric changes, and to derive the friction calibration curves. The friction factor has been determined for various initial relative densities and different lubricating conditions, and a proper lubricant for cold forging of powder metallurgical Al-4%Cu preforms was found. Studies show that the use of lubricants has reduced the friction. However, increase in the number of pores in the preforms leads to excessive friction. The finite element simulation results demonstrate a shift in the neutral plane distance from the axis of ring specimen, which occurred due to variations in the frictional conditions and initial relative densities.

One of the more comprehensive discussions of friction in metal forming was presented by (Schey, 1983). While, he presented a broad overview of the topic; there are several key points pertaining to hot forging and frictional effects that are worth noting. In relation to die topography and friction, Schey discussed that has considered on identifying optimal lubricants or treatments to reduce friction. He reviewed the use of liquid and solid lubricants, as well as surface treatments such as nitriding, that can be applied to die surfaces to promote metal flow. However, most of the findings are very dependent on process conditions. He has also noted that liquid lubricants have the best performance in both cold and hot forming.

(Forcellese, et al., 1994) studied the frictional conditions of AA 6082 in cold metal forming, performed by the double cup extrusion method. Four lubricants were used in this investigation of multipurpose extreme pressure grease with small particles of molybdenum disulphide, poly-tetrafluorethylene spray coating, mineral oil and alcohol. They found that the double cup extrusion is strongly influenced by the friction shear factor. Friction factor ranging from 0.01 to 0.25 were determined for the lubricants investigated. It was found that the load required for the double cup extrusion is lower than that for the forward and backward extrusions.

(Tan, et al., 1998) investigated and analyzed coefficient of friction carried out with alternative to ring-compression test applied three different ring geometries, namely, concave, rectangular and convex shaped ring cross-section. AA6082 was used in the experiments, in both annealed and work-hardened conditions with soap and molybdenum disulphide were used as lubricants. It is found that the friction is influenced by the strain hardening of materials, but in a complicated manner, it is due to the influence on the normal pressure. Further investigation is necessary to determine the parameters influencing the friction.

(Ryo & Kozo, 2004) studied measurement of friction in cold upsetting with mist lubrication. The coefficient of friction during upsetting under semi-dry conditions was measured using the ring compression test. A small amount of mist lubricant was sprayed onto the mirror surfaces of cemented tungsten carbide tools, and pure aluminum specimens are compressed by the tools. It was found that spraying a small amount of lubricant reduces the friction effectively.

(Bonab, et al., 2015) analyzed the hot working behavior and friction conditions in the hot forging process of the 6082 aluminum alloy. The ring compression test was used to determine the shear friction coefficient in hot working processes, and the pressure test of cylindrical specimens was utilized to specify the hot working behavior of AA 6082 alloy. Graphite, teflon and mica sheets were chosen as lubricants. Friction calibration curves are plotted using the finite element simulation to compare these results with the results obtained from the tests. Shear coefficients were obtained for every lubrication case. The results demonstrate that the best lubrication case of the hot working of AA 6082 alloy was achieved when the shear friction coefficient of 0.32 was used, whereas the value of 0.69 is obtained in the case when no lubricant was used.

2.6 Effects of Surface Roughness on Friction

One of the basic premises of friction is that apparently polished surfaces present imperfections when seen on a microscopic scale. (Sahin, et al., 2007) have found these imperfections are known as roughness, representing the coarseness of the material surface.

(Becker, et al., 2003) conducted a study that had both an experimental and finite element analysis component where they attempted to use the surface roughness of a die to estimate the friction factor in cold forming. Surface roughness is normally measured with a profile-meter and provides a measurement that averages asperity height over a fixed length. They assumed a constant amplitude and period of a sinusoidal waveform to create an average roughness which can be compared to a profile-meter measurement. Using various amplitudes and periods, the researchers calculated various die surface roughness. A two-dimensional finite element model was then used calculate friction factor based on the sinusoidal waveform die texture. The calculated values were then verified experimentally using aluminum rings having a 6:3:2 ratios. The ring tests were performed at room temperature under dry conditions using dies with various surface roughness. The surface roughness were measured before the test and used within the model. The deformed ring dimensions were then compared to the calibration curves to obtain a friction factor. The model to predict the friction factor based on the surface roughness closely followed the experimentally determined value. As friction factor was increased by way of increasing the amplitude or period of the sinusoidal approximation, the resulting ring inner diameter had decreased in size, indicating the friction factor had increased.

(Rasp & Wichern, 2002) studied flat drawing, rolling and plain strain upsetting to analyze surface roughness and lay with respect to friction factor using aluminum work pieces on dies. Their study considered on asymmetric friction upsetting which uses plane strain deformation to simulate conditions occurring in a roll gap. The surface of the aluminum work piece was roughened on opposite faces by different processes that included polishing, chemical etching, and grinding with emery paper. Upsetting was varied parallel and perpendicular to the direction of the long axis of the aluminum, producing a texture that lay could be orientated to the dies. The test was run at room temperature both with and without lubricant. Based on the results from the study, they concluded that having the lay perpendicular to the rolling direction helped reduce friction factor when using lubricant. However, no correlation was found between friction factor and the work piece lay.

2.7 Finite Element Simulation in Friction Evaluations

The finite element analysis technique was first developed for solving complex elasticity problems and structural analysis problem in civil and aeronautical engineering; however, it has been applied to problems such as thermal, electromagnetism and fluid dynamics discussed in (Zienkiewicz, 1971). It is a numerical technique for finding approximate solutions to differential equations. Finite element analysis is achieved by dividing up a continuum into small elements that can be solved in relation to each other, replacing the continuous problem by a discontinuous element network. Especially for static problems, the finite element analysis can provide precise simulation of the physical experiment. Nowadays, it is used to simulate the physical experiment in order to save the expensive investment in the physical trials.

(Stahlmann, et al., 2012) used finite element analysis simulation to investigate how friction factor in a wire drawing process changes the resulting surface topography of the drawn part. The investigation focused on a multi-stand cold drawing process and the evolution of the surface roughness of a wire as it was reduced using a series of progressively smaller dies. The researchers broke down each drawing stand into multiple steps which were modeled in finite element simulation. They broke down the process in order to capture as much of the physical mechanics at work and to increase the model resolution. The primary variables that were varied included contact normal pressures, die angles and lubricant properties. A separate calculation block outside of the main finite element analysis solver was used that increased the number of elements on the surface nodes. The solver then proceeded with calculations based on the increased resolution to further the accuracy of the nodes on the surface and their respective deformation based on the variables listed above. The resolved nodes were then reintroduced to the finite element analysis solver, the model re-meshed and the calculation cycled until the error was acceptable. The calculation cycle was then tested against a manganese-chromium alloy slug in a barrel compression and sliding test where a cylindrical specimen was forced through a die at various fixed loads. The resulting geometry was then used to examine friction of the die. Overall, the finite element analysis methodology produced good correlation to the actual data. While the study was not considered surface roughness's of work piece for forging application. Generally, many commercial tools have made the finite element analysis easier to be carried out in industry with reliable solutions.

A study by (Li, et al., 2010) used the bulge radius from cylindrical steel specimens to establish if large strain rates had an effect on the friction factor in hot forging. Steel cylinders were heated to temperatures between 1472^{o}F and 2192^{o}F and then upset to true trains ranging from 0.2 to 1.6. A carbon sheet was placed between the work piece and dies to act as a lubricant as well as an insulator. Mica sheets were also used to provide additional insulation since unheated dies were used. To further minimize die chilling, the experiments were conducted using induction-heating coils to help maintain the work piece temperature. The study was also conducted in a vacuum to minimize scale formation on the work piece. The DEFORM software code was used to back calculate the friction factor based on the bulge radius obtained from experimentation. Based on the results, they found that friction factor was not constant during large strain rate deformation but showed an increase with strain. The researchers also found that the friction factor did not demonstrate a strong correlation to the bulge radius when cylinders were upset to high strain values. While the researchers did find a way to calculate an instantaneous friction factor, the large temperature difference between the work piece and the dies caused significant die chilling, even with the insulators in place. The experiment only varied work piece temperature instead of die temperature or surface conditions, which would also be expected to have an effect on friction. While the researchers did demonstrate good agreement between the computer model and the experiment, the results are difficult to use directly in order to improve die design.

(Equbal, et al., 2016) studied on lubrication behavior of 35C8 steel using ring compression test and finite element simulation. The friction coefficients of different lubricating conditions such as, graphite in hydraulic oil, graphite in furnace oil, DF 150 (graphite, water-based) die lubricant and dry or without any lubrication were obtained from the ring compression test for the commercial medium carbon steel. The geometry of the ring compression test specimen has been prepared in the ratio of 6:3:2. A Finite element simulation has been conducted to validate the results and to evaluate material deformation, geometric changes and load-displacement. The simulation results presented an excellent agreement with the experimental results.

(Robinson, et al., 2004) also presents a study of the ring compression test using physical modelling experiments and finite element simulation. Using commercially available modelling clay, material stress–strain relationships were obtained from compression tests of solid cylindrical specimens. A series of ring compression tests were carried out to obtain friction coefficients for a number of lubricants including, vaseline, zinc stearate and talcum powder. Finite element simulations were used to derive the friction calibration curves and to evaluate material deformation, geometric changes and load-displacement results. Friction coefficient values of the tested lubricants are in agreement with the results obtained by other researchers. Further investigation was necessary to determine the effects of material properties, test conditions and use of calibration curves on the ring compression test. It was suggested that the combined use of physical modelling experiment and finite element simulation provides a simple and effective means in the study of frictional mechanisms for bulk material deformation.

(Kochumman & Sarathchandradas, 2014) investigate the effect of barreling on the behavior of friction calibration curves. The concept of friction calibration map to determine different frictional conditions between interfaces of die and billet in the upsetting process was presented. The maps are generated based on the finite element simulation studies. A series of ring compression tests were then conducted to obtain the friction calibration curve. According to the Male and Cockcroft the standard geometry (6:3:2) is modelled with outer diameter 30 mm, inner diameter 15 mm and height 10 mm. The simulation was first conducted for the modelling steel AISI 1010 material, and were simulated using non-linear analysis finite element code ANSYS. For different height reduction and friction coefficients was provided for simulation, the profile changes for inner surface node are investigated and friction calibration curve was obtained. Ring compression test was carried out experimentally and the results are compared with the numerical results and validated.

(Menezes, et al., 2006) presented the effect of friction on metal forming by conducting compression tests of cylindrical Al-Mg alloy using finite element method technique. Three kinds of compression tests were performed. For the first test, a constant coefficient of friction (i.e., 0.65) was employed at both upper die-work piece and lower die-work piece interfaces. For the second and third tests, the coefficient of friction between the upper die and work-piece interface was same as that of previous test. However, at the lower die-work piece interface, two different coefficient of friction values, namely 0.65 and 0.35, were employed at different locations (i.e., each halves and each quarters of the cylindrical work piece for the second and third tests, respectively) in the tests. Simulation results showed that a difference in metal flow occurs near the interfaces owing to the difference in coefficient of friction. It was concluded that the variations in coefficient of friction between the dies and work-piece directly affect the stress distribution and shape of the work piece. This would directly affect the microstructure of the material being processed.

(Rahul, et al., 2012) studied on the development of new design of specimens for friction determination in metal forming. The main objective of their research was to find alternate specimens for friction determination, and develop their friction calibration curve. Geometry of specimen was assumed as circle in circle, triangle in circle and square in circle. Finite element simulation was carried out using these alternative specimens and friction calibration curves are generated. Result of these curves were compared with ring compression test. The result of this investigation shows that such alternative specimens may play important role in friction determination in absence of ring specimen. It was observed that the geometry of those specimens which consist any geometrical shape inside circle give very close friction values.

2.8 Applications of Aluminum Alloys

Demand for aluminum forging products especially in automotive and aerospace industry has been increased in recent years due to their lightness, strength and formability. Aluminum forging products are used in automotive and aerospace industry for the necessity to make modern vehicles lighter, safer and more environmental friendly. The automotive industry is one of the major users of aluminum forged parts since low-fuel-consumption cars have been demanded for the economy in recent years as discussed in (Henning, 2007).

Stress analysis of pistons made up of two different materials was discussed in the work of (Tamrakar & Mittal, 2013). The finite element analysis was performed to analyze the various results, and compare the results of stress analysis of piston made up of two different materials. The materials chosen for this analysis are steel and alloy of AA 4032. The results can be used to choose the suitable material for manufacturing of pistons. AA 4032 has the advantage of high thermal conductivity and high thermal expansion coefficient due to which the maximum temperature on the crown is less for AA 4032, but for steel it was on the higher side as it has less thermal expansion coefficient and less thermal conductivity than the aluminum alloy. The stress parameters do not have much difference among them but the temperature parameters have a large difference. The maximum temperature on AA 4032 piston was much less than on the steel piston, so in spite of having little larger value of stress, AA 4032 piston must be chosen for as it gives less temperature on the piston crown.

The aluminum parts are generally used in the car automotive components, the wheels and the suspension in modern cars as indicated in the work of (Behrens, et al., 2007). The suspension components are the most important aluminum forging parts in modern cars. For example, many of suspension components need better-quality and reliable properties such as high strength and toughness. Aluminum forging is a good alternative for such suspension parts with weight reduction up to 40%. According to (Mondolfo, 1976), aluminum forgings provide several advantages over the other types of metals as follows;

- Aluminum alloys are ductile, in high strength with low weight and have a good corrosion resistance.
- In aluminum forging, the grain structure can be arranged to correspond to the main loading direction leading to high strength and fatigue properties.
- Aluminum alloys do not develop scale during heating.
- Aluminum alloys can be forged into a variety of shapes by open die forging, close die forging and ring rolling.

2.9 Summary

Table 2. 2 Summary of literature review

	Author name, year of publication	Title of the research	Objectives	Main process parameters	Method/ technique of analysis	Main findings achieved
1	Sofuoglu and Rasty (1999)	Determination of friction coefficient by employing the ring compression test	Effect of material properties, strain-rate sensitivity, and barreling on the behavior of friction calibration curves.	white plasticine and black plasticine	Ring compression test and FEM	The use of generalized friction calibration curves, regardless of the material type and test conditions, must be avoided.
2	Equbal et al. (2016)	Study on lubrication behavior of 35C8 steel using ring compression test and finite element simulation	To study the friction coefficients of different lubricating conditions for the medium carbon (35C8) steel.	Different lubricating conditions including, graphite in hydraulic oil, graphite in furnace oil, DF 150 and without any lubrication	Ring compression test and FEM	A high coefficient of friction giving a greater value for percentage reduction in internal diameter than a lower one, for the same amount of deformation. Hydraulic oil + graphite lubrication condition is recommended

						for free forging whereas DF-150 is preferable for deep drawing and close die forging operations.
3	Wogaso et al. (2014)	Friction factor evaluation using experimental and finite element methods for Al-4%Cu preforms	To study the frictional behavior of powder metallurgical Al-4%Cu preforms using experiment and FE simulation	Different initial relative densities and lubricating conditions (zinc stearate, graphite, molybdenum disulfide powder, and unlubricated condition.)	Ring compression test and FEM	Zinc stearate is found to be proper lubricant for successful transformation of P/M Al-4%Cu preforms to the final desired part. The use of lubricants has reduced the friction.
4	Robinson et al. (2004)	Study on ring compression test using physical modeling and FE simulation	To investigate the frictional behavior based on physical modeling experiments and FE simulation.	Different lubricants including, vaseline, zinc stearate, talc powder and three different mixture ratios of vaseline	Ring compression test and FEM	Concluded that the combined use of physical modeling experiments and the FE method provides an effective means in the study of frictional behavior.

				and zinc stearate.		
5	Ryo, M. and Kozo, O. (2004)	Measurement of friction in cold upsetting with mist lubrication	To investigate the coefficient of friction under semi-dry conditions in order to realize dry and semi-dry metal forming processes.	Various Weight of lubricant and Ratio of lubricated area	Ring compression test	The lower the viscosity of a lubricant is, the lower the friction is during forming under slight lubrication, and it is difficult to spray a lubricant of high viscosity. The mist spraying system for metal cutting is effective in realizing semi-dry metal forming.
6	Kochumman and Sarathchandradas (2014)	Friction calibration in die metallic interface and stress analysis of steel [AISI 1010] employing ring compression test under specified lubrication	To investigate the effect of barreling on the behavior of friction calibration curves	Barreling under different lubricating conditions	Ring compression test and FEM	The friction curve is more useful for analyzing the material behavior on forging process and selecting the lubricant for the process. The stress analyses were useful to analyze the material flow and profile variations for different lubrication.

7	Rahul et al.(2012)	Development of new design of specimens for friction determination in metal forming	To find alternate specimens for friction determination, and develop their friction calibration curve.	Different geometry of specimen (as circle in circle, triangle in circle and square in circle)	Compression test and FEM	It was observed that the geometry of specimens which consist of any geometrical shape inside circle, give very close friction value.
8	Camacho et al. (2013)	Investigations on friction factors in metal forming of industrial alloys	To determine friction calibration maps for different metal alloys	Different metal alloys	Ring compression test and FEM	The study show that the necessity of using individual friction factors maps for every kind of material to be formed in both industrial and laboratory testing applications. The use of a general map for all materials is not recommended.
9	Bonab et al. (2015)	A study on hot working and frictional behavior	To find the calibration curves of the 6082	Various temperature rate and the strain rates	Ring compression test and FEM	The results show that the best lubricant for the hot forging of 6082 aluminum

		of 6082 aluminum alloy during hot forming using pressure tests and finite element simulation	aluminum alloy using different lubricants (graphite, teflon and mica sheets)			alloy is teflon with the shear friction coefficient of 0.32, and at the temperature of 450^{o}C.
10	Menezes et al. (2006)	Influence of friction during forming metal processes	To investigate the effect of friction on metal forming by conducting compression tests of cylindrical Al-Mg alloy	Three kinds of compression tests at various coefficient.	Ring compression test and FEM	Higher the value of coefficient of friction at the interface more will be the constraint to plastic flow of the material and thus less will be the flow of material.

2.10 Gaps Identified in the Literature Review

The literature on the determination of the interface friction factor by various methods, friction evaluation methods in bulk metal forming, influence of the lubricant and surface roughness on interface friction and finite element simulation were reviewed in this chapter. However, the availability of literature studies related to the evaluation of frictional behavior using ring compression test with various surface roughness of work piece and lubricating conditions for AA 4032 alloy process are limited. In addition, in recent time aluminum and its alloys have been broadly applied in various fields (car production, airplane industry and civil engineering) due to the fact that aluminum has smaller density than steel, good resistance to corrosion and good mechanical and recycling properties as described by (Mondolfo, 1976). Thus, it is quite significant to study the frictional behavior of aluminum 4032 alloy using experimental and finite element simulation for different initial relative surface roughness finish and lubricating conditions.

CHAPTER THREE

MATERIALS AND EXPERIMENTAL METHODS

3.1 Introduction

This chapter presents the materials and experimental methodologies used to investigate the frictional behavior and selection of suitable lubricant for aluminum AA 4032 alloy material. Ring compression test was conducted, in order to investigate the effects of different lubricating conditions and influence of surface roughness on interface friction. Descriptions of the procedures used to perform ring compression testing, including the preparation of the experimental equipment and specimens, are presented in the following sections. A finite element simulation was also conducted using the commercially available DEFORM-3D software code to visualize local material flow in the vicinity of the die and work piece interface during the ring compression test.

3.2 Research Methodology

A combination of ring compression experiments with finite element simulations was performed in order to analyze the effects of various surface roughness and lubricating conditions on the interface friction factor, and the procedure followed was outlined in Figure 3.1. The procedure developed to examine frictional behavior of AA 4032 alloy, and selection of suitable lubricant for AA 4032 as closely as industrial forging possible.

The ring specimens were prepared by machining the aluminum AA 4032 alloy to standard ring compression specification of outer diameter: inner diameter: height ratio of 6:3:2 (24:12:8 mm). The surface roughness of each ring was prepared as described in Table 3.3, in order to analysis the effects of various surface roughness on the interface friction during dry forging conditions. Suitable surface roughness of work piece was selected, in order to evaluate the effects various lubricating conditions on the interface friction factor. Then, experimentally investigating the effect of various lubricating conditions on interface friction was take place. Selection of the suitable lubricant with lower friction factor for AA 4032 according to the relationship between the change in internal diameter and height dimensions of the ring specimens for various lubricating conditions can be obtained. Also, ring compression test and finite element simulation results were integrated to evaluate friction behavior of AA 4032 material effectively.

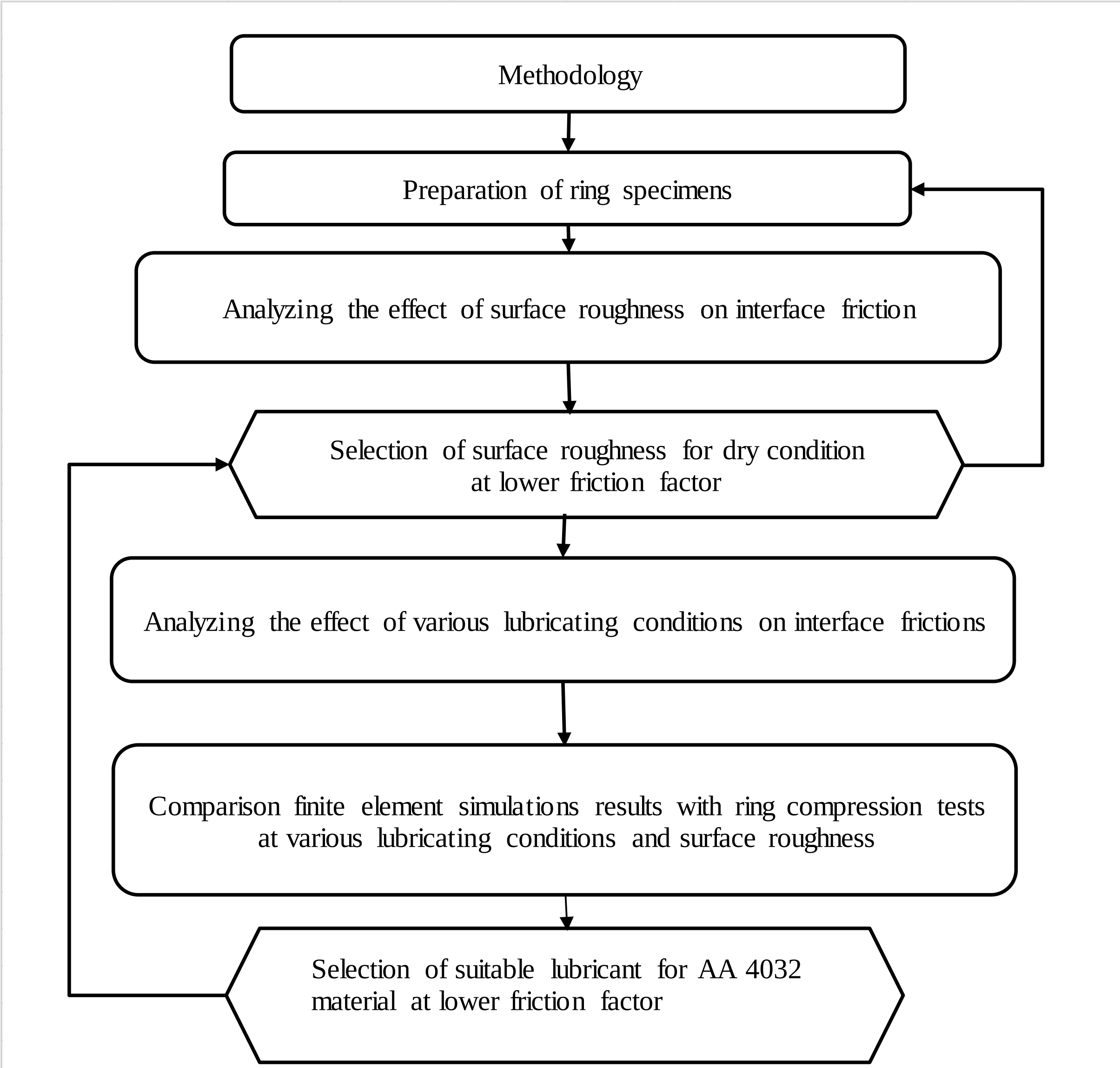

Figure 3. 1 Flow chart of the research methodology

3.3 Materials and Equipment Used for the Study

For this research, aluminum AA 4032 alloy was used for investigation. Today, aluminum is a common material for a various range of applications such as building construction, automotive industry, aerospace industry and much more. It is known that weight reduction can be achieved by using aluminum and its alloys. The chemical composition of the aluminum AA 4032 alloy was determined and presented in Table 3.1. Other elements are also available in the composition, but only in small amounts.

Table 3. 1 Chemical composition of AA4032 specimen

Al	Si	Fe	Cu	Mn	Mg	Zn	Ni	Cr	Pb	Sn	Element
81.3	11.51	1.12	1.65	0.31	0.31	1.42	1.77	0.062	0.13	0.14	Percentage

3.3.1 Selected Lubricant for the Study

Nowadays, environmental issues are of great importance. Lately, lubricants are formulated from heavily compounded chemically active minerals and frequently different types of additives are used that are not environmentally friendly as stated by (Cisson, et al., 1996), and their production process produces some environmentally hazardous chemical components. However, the scientific world is now looking for alternative lubricants that are more environmentally friendly.

Consequently, there was considerable motivation to find an alternative lubrication method, especially for cold forging soft aluminum alloys. Since the aluminum ring test was characterized extremely low surface expansion and the hardness of the specimen that were made from AA 4032 was medium, according to (Bay, 1994), commonly used vegetable oils and shop grease were selected as lubricants for the test.

Therefore, in this research, experiment was done in order to select a suitable lubricant as well as pollution-free for processing of AA 4032 alloy during cold forging processes. The tests were carried out using lubricants, vegetable oil-based (palm oil), grease and emulsion oil. In the ring compression test, the performance of these lubricants was evaluated by using a hydraulic pressing machine at room temperature.

All ring compression tests performed in this research are by using a hydraulic press machine (Model Toni Technik-2031), shown in Figure 3.2. The hydraulic press machine was available in Mechanical Test Laboratory of Ethiopian Standards Agency. To achieve a controlled surface roughness of die during compression tests, AISI H-13 dies having rectangular shape were used. AISI H-13 tool steel was the platen stock as it is widely used as a cold forging die material due to its hardenability, hot hardness, and fatigue resistance. Its dimensions was 400 mm length, 350 mm width, 40 mm thick. Additionally, equipment used in this research were listed in the below Table 3.2.

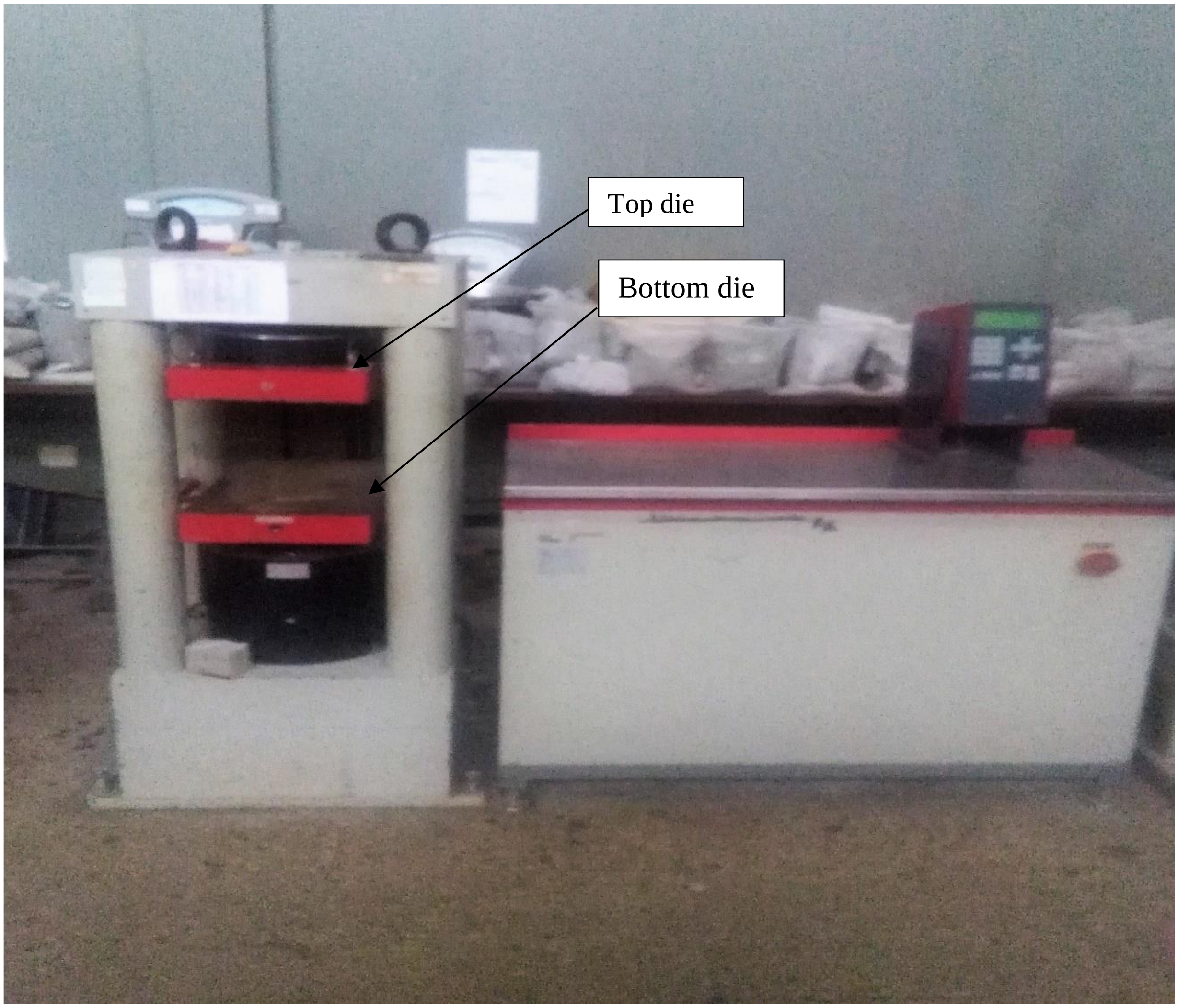

Figure 3. 2 Photograph of hydraulic press machine

Table 3. 2 Equipment used in the research

S.No	Equipment	Purpose
1	Hydraulic pressing machine	Perform compression test
2	Lathe machine	Machine AA 4032 material to required dimensions
3	Surface grinder	Grinding work piece to required roughness
4	Hacksaw	Cut AA 4032 to required dimensions
5	Digital Vernier caliper	Measure the work piece dimensions.

3.3.2 Preparation of Ring Specimens

The ring compression specimens were prepared by machining the bar made of AA 4032 alloy to standard ring compression specification of 6:3:2, which mean that the outer diameter was 24 mm, the inner diameter 12 mm and the height 8 mm. A 6:3:2 ratios was selected for the study since it minimizes the strain rate sensitivity of the aluminum as reported by (Dutton, et al., 1999) who found that it resulted in a balance between measurable deformation and friction factor variations caused by a material's strain rate sensitivity. Grinding and polishing were the two commonly used methods for surface preparation of ring specimens.

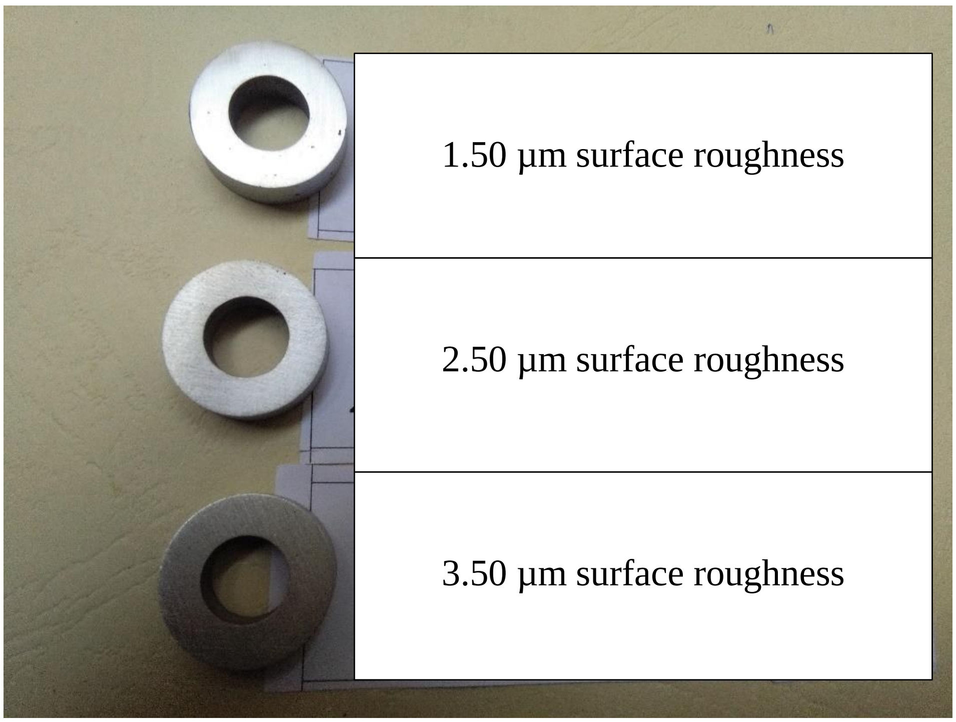

Figure 3. 3 Photograph of ring specimens before deformation

3.3.3 Preparation of Surface Roughness for Ring Specimen

There are some literatures focused the substrate surface roughness before texturing. All of them show that one need serious consideration of the surface roughness of the substrate. (Wiklund, et al., 2008) studied frictional mechanisms in mixed lubricated regime in metal forming and concluded that frictional response showed a correlation to the surface topography, such as the amplitude parameter and texture aspect ratio parameter. When predicting the frictional response of surfaces with multi-component distributions, the standard deviation of the distribution above the mean line was more suitable. The frictional response in mixed lubricated regime is dominated by the original surface topography besides oil viscosity, sliding velocity, and pressure, which were held constant in their experiments. The correlation between coefficient of friction with respect to the average surface roughness is positive linear. In addition, (Menezes, et al., 2006) show for the randomly polished steel forging die the coefficient of friction is lower than other machining marks. (Hu & Dean, 2000) studied the relation between friction and surface topography using various lubricants and found that a random smoother surface could retain more lubricant and thus reduce friction.

Based on the pioneer’s research work, and also considering roughness effect on the final results, surface roughness of specimens were intentionally hand polished to ensure the machining marks are randomly. In order to investigate the effect of surface roughness on interface friction factor, roughness of work piece corresponding to 1.50 µm, 2.50 µm and 3.50 µm were used. All measurement of surface roughness data can be found in Appendix I in Table C. To get accurate results, roughness test was repeated two times for all parameter conditions. Roughness of 1.50 µm (termed low surface roughness) was selected as it was typical of the work piece finishes employed in industry. Additionally, medium and larger roughness values of 2.50 µm and 3.50 µm (termed as medium and higher surface roughness respectively) were employed and intended to simulate work piece surfaces.

Before carrying out experiments on the various selected lubricants, it was important to prepare surface roughness for the selected material at dry conditions. Carrying out the surface roughness analysis at dry condition, so that the quantitative relationship between friction factor and surface roughness properties was obtained at the prepared roughness. After this step was done, quantitative relations between friction factor and various lubricating condition properties were also obtained for all selected lubricants. A comprehensive list of surface roughness and various lubricating conditions used in this investigation are shown in Table 3.3 below.

Table 3. 3 Numbers of ring specimen tested and its parameters

Specimen geometry (mm)	Lubricating condition	Work piece roughness (µm)	Numbers of specimen tested
OD:ID:H 24:12:8	Dry	1.50	3
		2.50	3
		3.50	3
	Palm oil	Selected at lower values of friction factor during dry condition.	3
	Grease		3
	Emulsion oil		3

A standard flat grinder and different grit size emery papers were used in order to achieve accurate surface roughness of work piece. The surface of the specimens was polished using different waterproof abrasive paper. Emery paper followed by 60, 120, 240, 320, 360 and 380 grit size were used to make repeated passes across the ring surface. Using repeated passes at various emery paper sizes; it was possible to create a consistent required surface roughness. Ring specimens having surface roughness of 1.50 µm were machined using a standard surface grinder. Surface grinding was commonly employed in the manufacturing of commercial die surfaces, making it an appropriate selection for this investigation. All grinding passes were limited to a single direction as this allowed a uniform surface roughness to be achieved. In order to reduce grinding surface profile that was marked on the surface of work piece after machining, waterproof abrasive paper of 380 grit size was used. In order to obtain surfaces roughness values of 2.50 µm, emery paper followed by 60, 120, 240, 320 and 360 grit size were also used in this study. Similarly, to achieve the 3.50 µm surface, emery paper with 60,120, and 240 grit sizes were used again.

Roughness values for all specimens were checked after machining. The surface roughness of the test specimen was measured with a surface roughness tester (SRT-6210 model) type instrument found in the material laboratory shop of Addis Ababa Institute Technology University. This instrument was compatible with standards of ISO, and it was widely used in production site to measure surface roughness of various machinery-processed parts, calculate corresponding parameters according to selected measuring conditions and clearly display all measurement parameters. When measuring the roughness of a surface, the sensor was placed on the work piece surface, and then uniformly slides along the surface by driving the mechanism inside the tester. The sensor gets the surface roughness by the sharp built-in probe. This roughness causes displacement of the probe which results in change of inductive amount of induction coils so as to generate analogue signal, which was in proportion to the surface roughness at output end of phase-sensitive rectifier. The exclusive digital signal processor processes and calculates, and then displayed measurement results on screen.

Figure 3. 4 Surface roughness tester and ring specimen setup

3.4 Procedure for Ring Compression Tests

The compression apparatus for testing of interface friction between die and work piece was hydraulic pressing machine with maximum force of 3000 KN. The ring compression test was carried out between two parallel flat mirror finished open dies of hydraulic press with a ram speed of 0.25 mm/s. The non-related parameters such as, the die surface roughness, and the environment temperature and humidity, were all kept at constant values. All ring specimens were cleaned before tests. A summary of the conditions used to investigate the friction factor for each surface roughness and lubricating condition were listed in Table 3.3 above. To verify the consistency of the results, three replications were performed under each parameter conditions. The tests were performed on eighteen specimens totally, where nine specimens were used to investigate the effect of surface roughness on interface friction factor at dry condition, and nine specimens were used again to investigate the effect of the various lubricating conditions on interface friction factor. The test procedure is given as below.

i. The tooling die setup was cleaned and polished by means of dry cloth before use.
ii. The ring specimen was also polished by brushes to ensure that it was free from burrs before the experiment.
iii. Set the final stroke of the press ram. The die setup and the ring specimen were copiously applied with the selected lubricant or surface roughness before the starting of the experiment.
iv. During investigation of various lubricant effect on friction factor, both work piece and die surface were lubricated with selected lubricants. Lubricant was applied manually on both work piece and die surfaces.
v. Put the ring specimen on the bottom die. Since the ring compression tests are axis-symmetric, the specimen should be concentric to the ram. This will be done by putting the sample into formed grid line that concentrically guides the sample.
vi. Set the ram speed as 0.25 millimeter/second and start the test.
vii. Remove the ring specimen and cloth cleaning
viii. Measure and record inner diameter, outer diameter and height of compressed specimen. The digital vernier caliper was used for measuring the heights of the ring specimen and the diameters of the ring. The procedure was repeated with increment of deformation load until fracture was detected on ring specimen.

The height reduction and inner diameter change of ring specimens with respect to various surface and lubricating conditions on can be compared with that of (Male & Cockcroft, 1965) theoretical friction conditions. During the ring compression test the outside diameter of the specimen expands outward. The inside diameter however, either expands outwards or contracts inwards, depending on the frictional conditions that exist at the die-work piece interface. For instance, under extremely low friction conditions, or when the friction between the work piece and tool is lower than a critical value, the material flows outwards, and both inner and outer diameters of the ring increase. If the friction at the contact interfaces was higher than a critical value, the material close to the inner diameter flows inwards, which decreases the inner diameter of the ring, and the remainder material flows outwards, which enlarges the outer diameter of the ring.

3.4.1 Measurement of Specimen Dimensions

Accuracy of the measurement of specimen dimensions before and after the test has a great impact on test results. The dimensions of ring specimen before and after compression were checked using a digital caliper. Due to the inherent variability in experimental data collected under cold forging conditions, replications were performed to obtain an average value. Therefore, to measure the inner diameter of the specimen more accurately, an average value was taken from three repeated measurements of compressed ring. The height reduction percentage was also calculated from the average of three measurements.

3.4.2 Determination of Material Flow Curve

In ring compression process, the specimen was under a uniaxial stress-strain state ideally. The calculation method of the stress and strain was important, especially for large strains in the plastic deformation. After the ring compression test was performed the value of engineering stress and strain, true stress and strain, strain hardening exponent and strength coefficient were determined based on the output data from hydraulic pressing machine. From compression test, the value of the progress of load and reduction in height was used to calculate the engineering strain and stress. Since, the engineering strain-stress and the true strain-stress can be easily converted, the investigation of the compression flow curve for AA 4032 material often was carried out in two steps. First, the engineering strain and engineering stress were determined from equation (3.1) and equation (3.2) respectively. Second, convert the engineering strain and stress to true strain and stress by using equation (3.3) and equation (3.4) respectively. The original height was taken from original height of the ring specimen before deformation.

$$\text{Engineering strain, e} = \frac{H_o - H_f}{H_o} = \frac{\Delta H}{H_o} \qquad (3.1)$$

$$\text{Engineering stress, S} = \frac{F}{A_o} \qquad (3.2)$$

The engineering stress-strain curve does not give a true indication of the deformation characteristics of a material because it is based entirely on the original dimensions of the specimen and these dimensions change continuously during the test. In metal working processes, the work piece undergoes appreciable change in cross sectional area. Thus, measures of stress and strain which were based on the instantaneous dimensions are needed as presented by (Altan & Boulger, 1973).

$$\sigma_t = \frac{\mathrm{F_i}}{\mathrm{A_i}} = \mathrm{S}(1 + \mathrm{e}) \qquad (3.3)$$

The axial true strain were expressed as given below,

$$\varepsilon_t = \ln\ (H_o/H_f) = \ln(1 + e) \qquad (3.4)$$

Metal forming, such as forging process, involves large strains and plastic deformation. In engineering practice, the period of elastic deformation is often neglected and the corresponding true stress after the yield point was named as flow stress for the large strain situation. Flow curve can be obtained by plotting true stress values against equivalent true strain values. When ring specimens remain isotropic, the material properties are direction-independent and the effective stresses for plastic deformation can be described by Ludwik's equation flow rule on the basis of (Hill, 1985). Thus, only the influence of friction on ring flow is recognized.

$$\sigma_e = \mathrm{K}(\varepsilon_e)^n \qquad (3.5)$$

The strain hardening and strength coefficient were determined by taking the values of the true strain and true stress that represent the plastic flow of the material. Then, true stress and true strain were converted into natural logarithm form of true strain versus true stress, and curve was plotted. By fitting this equation to whole range of flow data, strain hardening exponent and strength coefficient values can be determined for various roughness and lubricating conditions. Therefore, in order to find strain hardening and strength coefficient from plotted graph, equation (3.5) can be written as follows, as indicated in the work of (Narayanasamy, et al., 2007).

$$\ln\ (\sigma_e) = \ln\ (K) + n \ln\ (\varepsilon_t) \qquad (3.6)$$

Which was a straight line on an x-y plot. This line can represent by the following equation

$$y = mx + b \tag{3.7}$$

From equation (3.6) and equation (3.7) the following variables and constants can be defined:

$$y = \ln\ (\sigma_e) \tag{3.8}$$

$$x = \ln\ (\varepsilon_t) \tag{3.9}$$

$$m = n \tag{3.10}$$

$$b = \ln\ (K) \rightarrow K = e^b \tag{3.11}$$

Several workability tests are available to study the deformation behavior under the combined stress and strain conditions usually found in bulk deformation process. One of the compression test on cylindrical specimens has been presented by (Kobayashi, 1970) for the study of deformation behavior under combined stresses. During compression of a cylinder the lateral free surface barrels and fractures form at the barrel. The barreled surface results in the development of a tensile stress in the circumferential direction and a decrease in the magnitude of the axial stress below the average compressive stress in the material. Thus, a variety of stress and strain states can be generated in the equatorial regions of the ring specimens, providing a convenient test for deformation and fracture studies. The deformation behavior obtained from ring compression test to a fracture detected deformation is worth studying to determine the flow pattern. The equation (3.12) will enable us to calculate the effective strains on the geometric center of the bulge surface, and are identical to the equations derived by (Kudo & Aoi, 1967).

$$Effective\ strain = \frac{2}{\sqrt{3}} \sqrt{\left(\varepsilon_x - \varepsilon_y\right)^2 + (\varepsilon_y - \varepsilon_z)^2 + (\varepsilon_z - \varepsilon_x)^2} \tag{3.12}$$

Where, the incompressibility condition $\varepsilon_x + \varepsilon_y + \varepsilon_z = 0$ has been used. For an isotropic material axial and circumferential strain were evaluated at the geometric mid-sectional of the specimens. Axial and circumferential strain values were calculated from the height and outer diameter measurements according to $\varepsilon_z = \ln\left(H_f/H_o\right)$ and $\varepsilon_x = \varepsilon_y = \ln\left(OD_f/OD_o\right)$, respectively. The effective strain obtained by this method allowed estimates of the effective stress from the stress-strain power law relationship discussed in equation (3.5). The fit of power relationships such as that given by equation (3.5) is good enough within limited ranges of strain, since this equation tend to overestimate the stress at high strains.

3.5 Finite Element Simulation in Friction study

Finite element analysis of ring compression test was carried out using rigid-plastic formation. Modeling and analysis of metal forming process have been specialized application, and only a limited range of finite element software was capable of conducting the analysis. Hence, the selection of software is one of the dominant aspects of metal forming process analysis. (Oh, et al., 1991) validated the finite element program DEFORM for its use in metal forming analysis. It is capable of handling several different types of materials such as rigid plastic, elastic plastic and powder materials. Simulation of bulk forming processes with finite element method was a powerful tool for analyzing the metal forming processes.

The finite element modeling of ring compression test carried out using DEFORM 3D software is illustrated in Figure 3.5 for typical example. The geometry of the model matched the experiments. An axisymmetric formulation of the work piece was considered during modeling; hence 3D modeling in Figure 3.5 represents only one half of the ring specimen simulation.

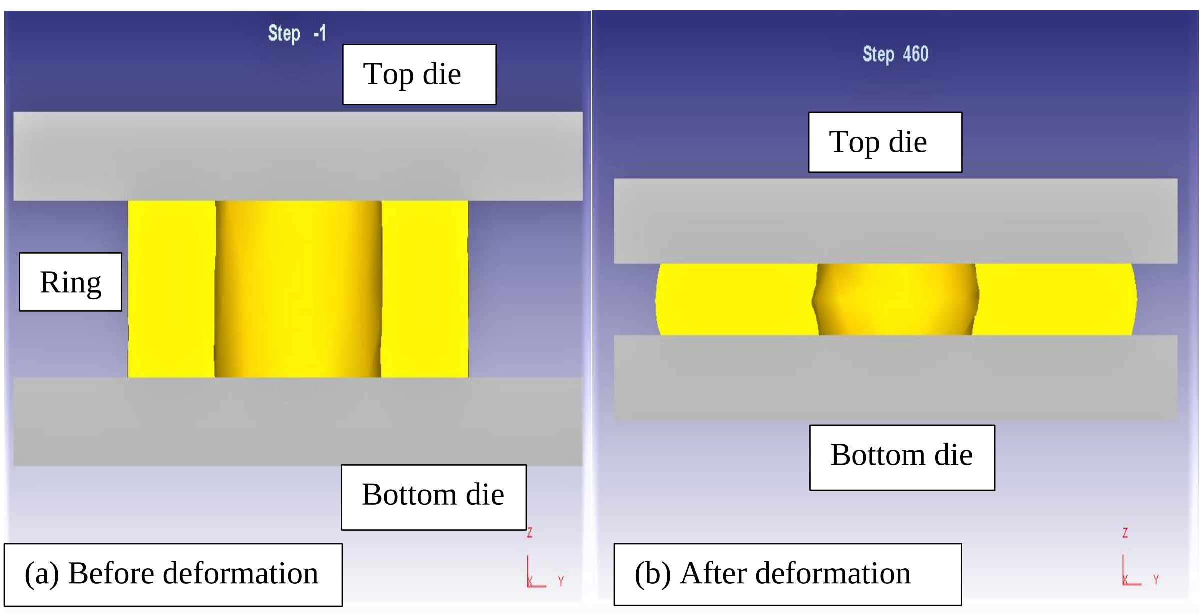

Figure 3. 5 Finite element method modeling of ring compression test

The sizes of ring specimens were same as the ones used in experiments. In the methodology of finite element simulations, as suggested by the researchers (Babu Rao, et al., 2009) the tetrahedral element size which reduces the number of iteration had been chosen and the specimen geometry was neither too meshed nor coarse meshed, such that long computational time and accuracy with unnecessary precision was minimized. Therefore, a tetrahedral nodded with elements of two thousand were used to mesh the ring geometry.

DEFORM 3D is capable of auto-remeshing for large deformation process, which is most suitable for forging simulations. Auto remeshing can be triggered by a number of options such as, maximum stroke increment in millimeters, maximum time increment in seconds, maximum step increment, or interference depth. In addition to these four keywords, remeshing is automatically initiated when the mesh is not usable. The first three options are self-explanatory, the interference depth criterion controls the initiation of remesh based on the interference between the slave object and master object presented in (Ohio, 2016). The automatic meshing and remeshing procedure improves the processes of simulation at a considerable level. Once the optimum mesh density is determined at every point in the domain to be meshed, automatic mesh generator automatically constructs a three-node tetrahedral element mesh system.

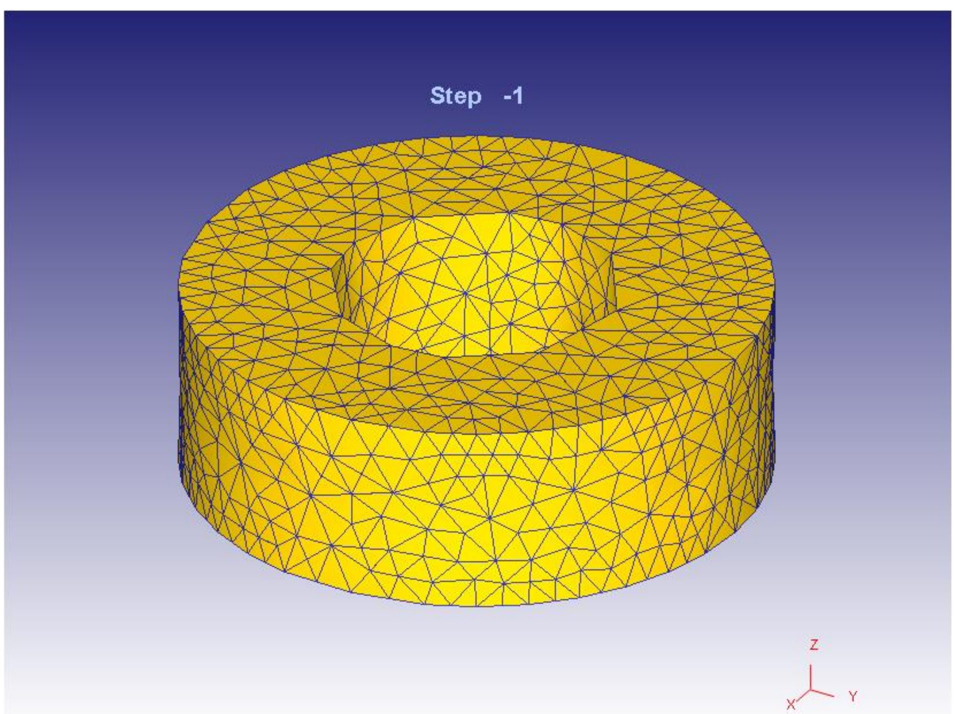

Figure 3. 6 Mesh of the 3D ring specimen

In ring compression test, material plasticity was dominate the deformation. Similarly in DEFORM 3D, the selected material was simplified to fully plastic, and the power law was accommodated with isotropic flow rule where the strength coefficient and strain hardening controls the flow of deformation. The true stress-true strain curves of AA 4032 were generated from the ring compression test results for various roughness and lubricating conditions. The true strain and true stress curves generated were then converted to natural logarithm to determine strength coefficient and strain hardening value. The average strength coefficient and strain hardening value were taken, and used to generate flow stress equation of AA 4032 alloy. The generated flow stress equation is entered into the DEFORM 3D software as input data.

AISI H-13 alloy tool steel was used as the compression die material for finite element simulations, as it was widely used as a die material in metal forming operations and retains several favorable forging tool characteristics including; high hardenability, hot hardness, and fatigue and wear resistance. To maintain a consistent surface finish and minimize surface wear, each die underwent a hardening heat treatment process presented by (Diehl, 2015), achieving a Rockwell hardness between 50 and 55. As heating H-13 tool steel in air results in excessive oxidation, the hardening heat treatment was conducted in an ammonia atmosphere furnace. Two dies, top die and bottom die, were used in the simulations. The dies were set as rigid and ram speed was 0.25 mm/sec which was same as the hydraulic press used in experiment. The geometry of meshed ring with quarter of the cross section before deformation and after deformation shown in Figure 3.7.

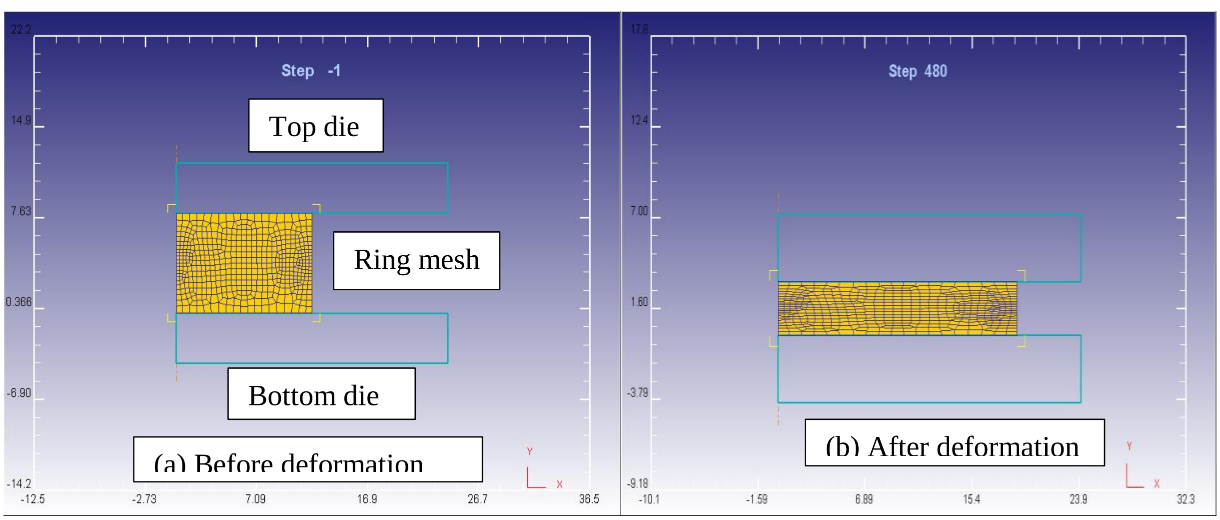

Figure 3. 7 Finite element simulation of ring compression test

A friction model is one of the key input boundary conditions in finite element simulations. Among the various friction models, which one is of higher accuracy is still unknown and controversial. However, (Fereshteh-Saniee, et al., 2004) studied on friction modeling for the physical simulation of the bulk metal forming processes. Coulomb and constant friction model are the two most commonly used mathematical models for friction quantification in metal forming process. Coulomb model is mainly used in processes with low pressures, whereas constant friction model is adequate for processes where high effective strains and pressures prevail. (DePierrie & Gurney, 1974) also presented that the constant friction factor is more realistic than the Coulomb coefficient of friction, in describing and quantifying the shear stresses in bulk forming processes. Constant friction model assumes that friction stress is constant, and it only depends on the shear flow stress. For example, for perfect lubrication ($m = 0$) friction stress is null, whereas for sticking conditions ($m = 1$), friction stress equals the shear flow stress. Therefore, in the finite element simulation, constant friction model was used for various surface roughness and lubricating conditions since its simplicity and seemingly indicating the material feature of plastic deformation.

3.5.1 Determination Procedure of Friction Factor

First attempt was made to determine the friction factor for various surface roughness and lubricating conditions by measuring the change in the inner diameter and reduction in height of the ring specimens. The properties of AA 4032 material was determined by using compression test for different surface roughness and lubricating conditions, respectively.

In order to evaluate the friction factor between the interface of the die and ring specimen, the friction calibration curve was standardized into plots that represent the deformation in the ring as it was compressed. The friction calibration curves were derived by using finite element method software (DEFORM 3D) by incorporating the properties of material as input. As shown in Figure 3.5, an axis-symmetric model was created in DEFORM 3D which is a commercial software and a product of Scientific Forming Technologies Corporation. The sizes of ring samples are same as the ones used in experiments. Series of simulations were run with same setup but different friction factors between die and ring specimen. Friction factors were varied between 0 and 1. The height reduction and inner diameter changes at each step were measured, as indicated in Figure 3.8 for typical example.

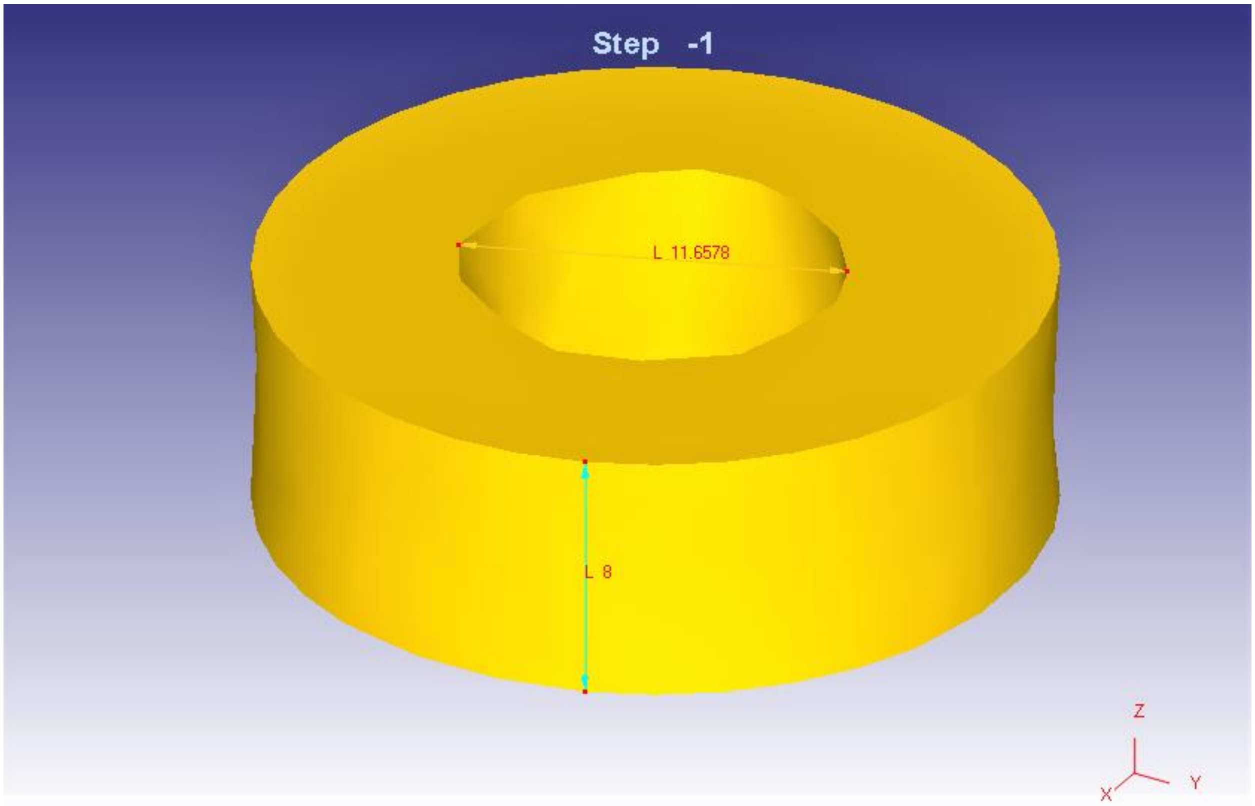
Step -1
L 11.6578
L 8
Z
Y
X

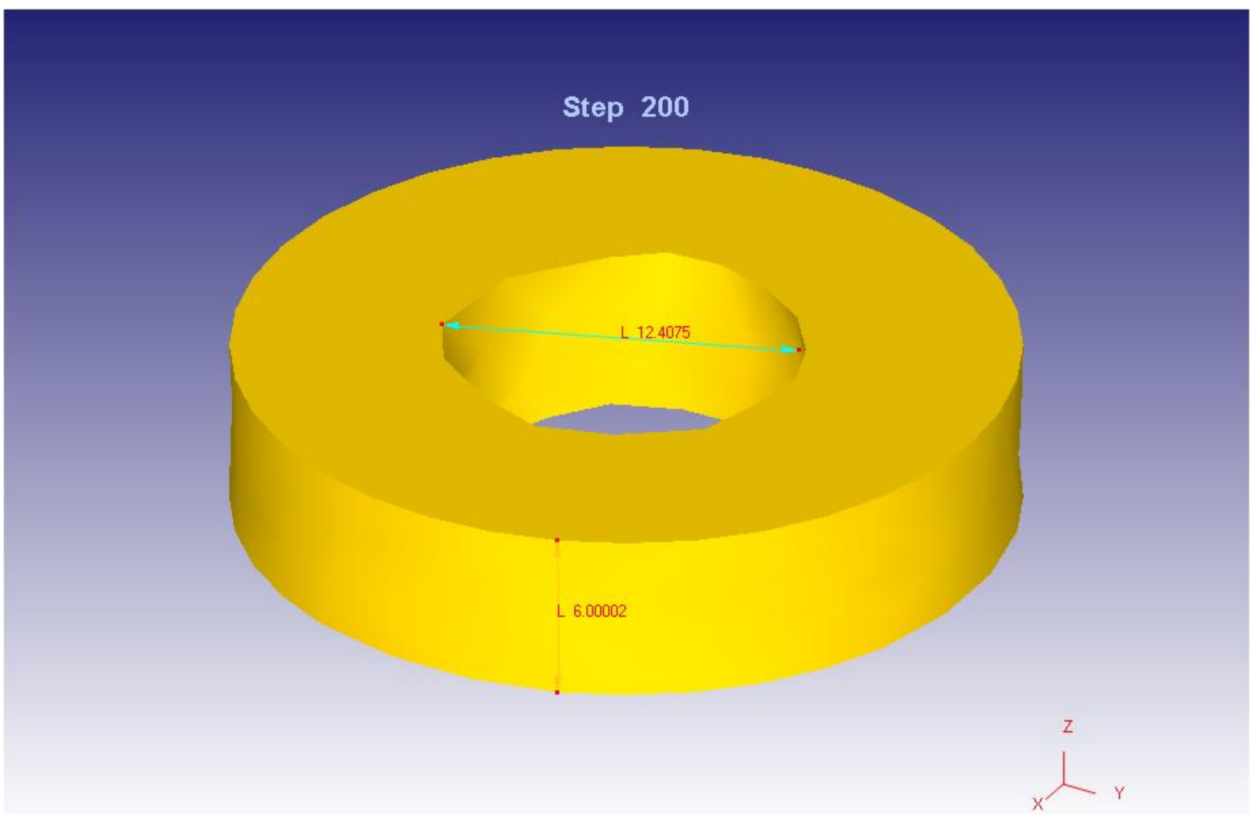
Step 200
L 12.4075
L 6.00002
Z
Y
X

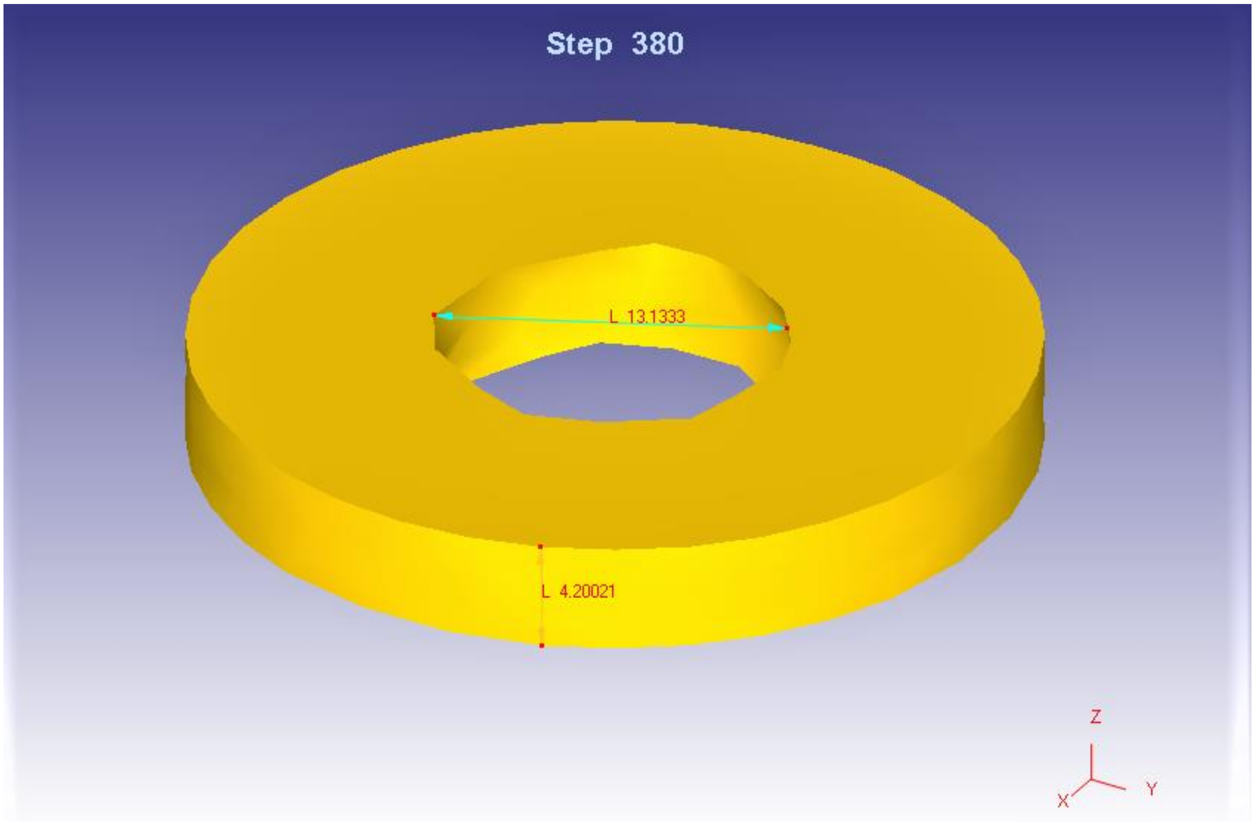

Figure 3. 8 Height and inner diameter measurement procedure using FEM simulations

After recording the data of height reduction and inner diameter change and calculating its reduction rate, one can generate a (Male & Cockcroft, 1965) friction calibration curves in which each curve represents a distinct value of friction factor. The friction factor can be obtained simply by plotting percentage of height reduction and inner diameter change of ring specimen, and made to fit against Male and Cockcroft friction calibration curves.

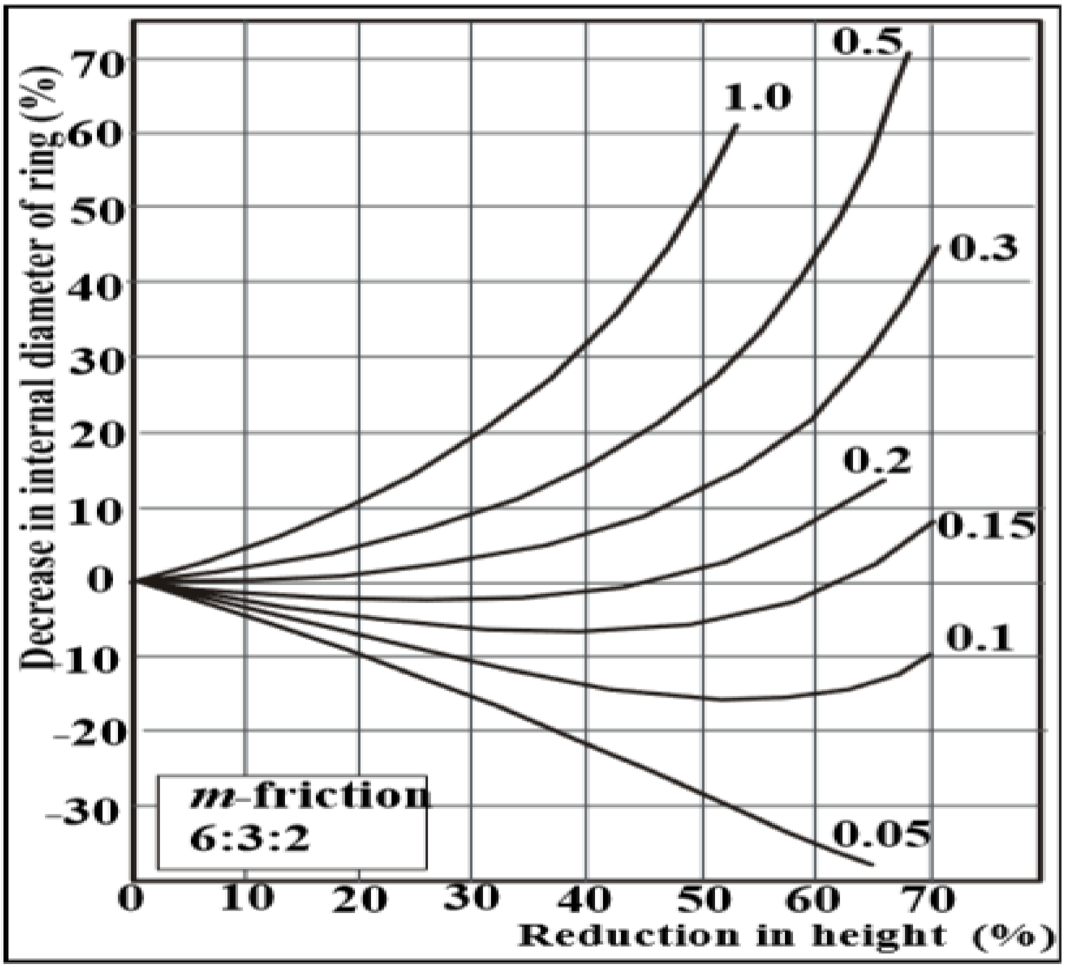

Figure 3. 9 Typical Male and Cockcroft friction calibration curve (Male & Cockcroft, 1965)

CHAPTER FOUR
RESULTS AND DISCUSSION

4.1 Introduction

This chapter presents the experimental results and finite element simulations obtained from ring compression tests which were conducted under various surface roughness and lubricating conditions. Tests were performed with 50 KN deformation load increment up to fracture detected for each AA 4032 ring specimen. As the first step, the effects of specimen's surface roughness on the friction factor during dry conditions were separately presented and discussed. By using the surface roughness at lower friction factor, the effects of various lubricating conditions on the friction factor was performed. Thereafter, the suitable lubricant for AA 4032 alloy was obtained. The finite element simulation results were compared with experimental results in terms of effective strain and effective stress.

4.2 Results and Discussions of Ring Compression Test

4.2.1 Determination of Material properties

Table 4.1 shows the average results of ring geometry measurement namely, outer diameter, inner diameter, and height of the ring specimen which were recorded before and after deformation for different surface roughness and lubricating conditions. Also, the measurements of the height reduction and inner diameter change percentage of the ring specimen for various surface roughness and lubricating conditions are given. To get accurate results, each experiment was repeated three times for all experimental conditions. All repeated test data can be found in Appendix I. In order to determine the compression flow curves for AA 4032 material, load-height reduction data obtained from ring compression test were used.

Table 4. 1 Mean value of experimental data for AA 4032 ring compression test

Ring specimen with 1.5 µm surface roughness							
Load (KN)	0.00	50.00	100.00	150.00	200.00	250.00	329.00
Outer diameter (mm)	24.01	24.15	24.40	24.97	25.90	27.51	30.52
Inner diameter (mm)	12.01	12.00	11.90	11.74	11.32	10.63	9.68
Height (mm)	8.01	7.88	7.64	7.13	6.38	5.38	4.13
%ID reduction	0.00	0.14	0.95	2.27	5.75	11.56	19.39

%H reduction	0.00	1.60	4.67	10.99	20.35	32.89	48.38
Ring specimen with 2.5 µm surface roughness							
Load (KN)	0.00	50.00	100.00	150.00	200.00	250.00	327.67
Outer diameter (mm)	24.02	24.13	24.36	24.91	25.80	27.37	30.21
Inner diameter (mm)	12.03	12.00	11.89	11.70	11.26	10.59	9.49
Height (mm)	8.01	7.92	7.67	7.17	6.43	5.44	4.22
%ID reduction	0.00	0.27	1.15	2.76	6.42	11.97	21.16
%H reduction	0.00	1.21	4.22	10.46	19.71	32.06	47.39
Ring specimen with 3.5 µm surface roughness							
Load (KN)	0.00	50.00	100.00	150.00	200.00	250.00	326.00
Outer diameter (mm)	24.04	24.12	24.34	24.86	25.74	27.26	30.00
Inner diameter (mm)	12.03	11.99	11.87	11.67	11.23	10.53	9.31
Height (mm)	8.01	7.94	7.71	7.22	6.49	5.50	4.28
%ID reduction	0.00	0.40	1.32	3.03	6.70	12.51	22.60
%H reduction	0.00	0.96	3.84	9.90	19.07	31.34	46.62
Ring specimens lubricated with palm oil							
Load (KN)	0.00	50.00	100.00	150.00	200.00	250.00	335.33
Outer diameter (mm)	24.02	24.21	24.54	25.21	26.31	28.13	31.49
Inner diameter (mm)	12.02	12.02	12.01	11.94	11.74	11.26	10.46
Height (mm)	8.01	7.83	7.55	7.02	6.24	5.21	3.94
%ID reduction	0.00	0.03	0.09	0.65	2.35	6.37	13.01
%H reduction	0.00	2.18	5.69	12.31	22.06	34.97	50.78
Ring specimens lubricated with grease							
Load (KN)	0.00	50.00	100.00	150.00	200.00	250.00	331.67
Outer diameter (mm)	24.02	24.20	24.50	25.14	26.18	27.92	31.16
Inner diameter (mm)	12.00	11.99	11.94	11.88	11.62	11.10	10.41
Height (mm)	8.01	7.85	7.58	7.06	6.30	5.28	4.02
%ID reduction	0.00	0.15	0.50	1.04	3.18	7.54	13.26
%H reduction	0.00	2.02	5.40	11.83	21.39	34.06	49.82

Ring specimens lubricated with emulsion oil							
Load (KN)	0.00	50.00	100.00	150.00	200.00	250.00	330.33
Outer diameter (mm)	24.01	24.17	24.43	25.05	26.01	27.69	30.82
Inner diameter (mm)	12.01	12.00	11.90	11.79	11.39	10.76	9.93
Height (mm)	8.01	7.86	7.61	7.09	6.33	5.32	4.07
%ID reduction	0.00	0.13	0.92	1.90	5.22	10.41	17.34
%H reduction	0.00	1.73	5.48	11.49	20.98	33.59	49.20

Figure 4.1 shows the photographs of deformed ring specimens at fracture detected deformation load during compression testing with various surface roughness and lubricating conditions. At fracture detected deformation, it was observed that the contraction of inner diameter was increased with increase in the surface roughness, whereas, height reduction was decreased with increase in the roughness. This was due to increase roughness (asperity peaks) on the work piece which restricts the metal flow at the die-work piece interfaces. Also, for various lubricating conditions the inner diameters of ring specimen lubricated with grease and emulsions were more contract than the inner diameter of ring specimen lubricated with palm oil. These observation were also in agreement with findings gained by (Male & Cockcroft, 1965).

Figure 4. 1 Photographs of deformed ring specimens at fracture detected deformation load

Load-height reduction data shown in Table 4.1, can easily be converted to engineering strain-stress data with the help of equations (3.1) and (3.2) respectively. Engineering strain-stress data gives the true strain-stress data with the help of equations (3.3), and (3.4) respectively. The engineering strain-stress curves of AA4032 alloy are generated from the ring compression test with different surface roughness and lubricating conditions, and are illustrated in Figure 4.2. In the engineering strain-stress curve of ring compression test for AA 4032 alloy, there was change in height reduction with respect to the various surface roughness and lubricating conditions. Considering a various lubricating conditions, at fracture detected deformation load, the induced strains were varies for constant surface roughness of specimens. When palm oil was used, higher reduction in the height was obtained. As a result, the induced strains were increases.

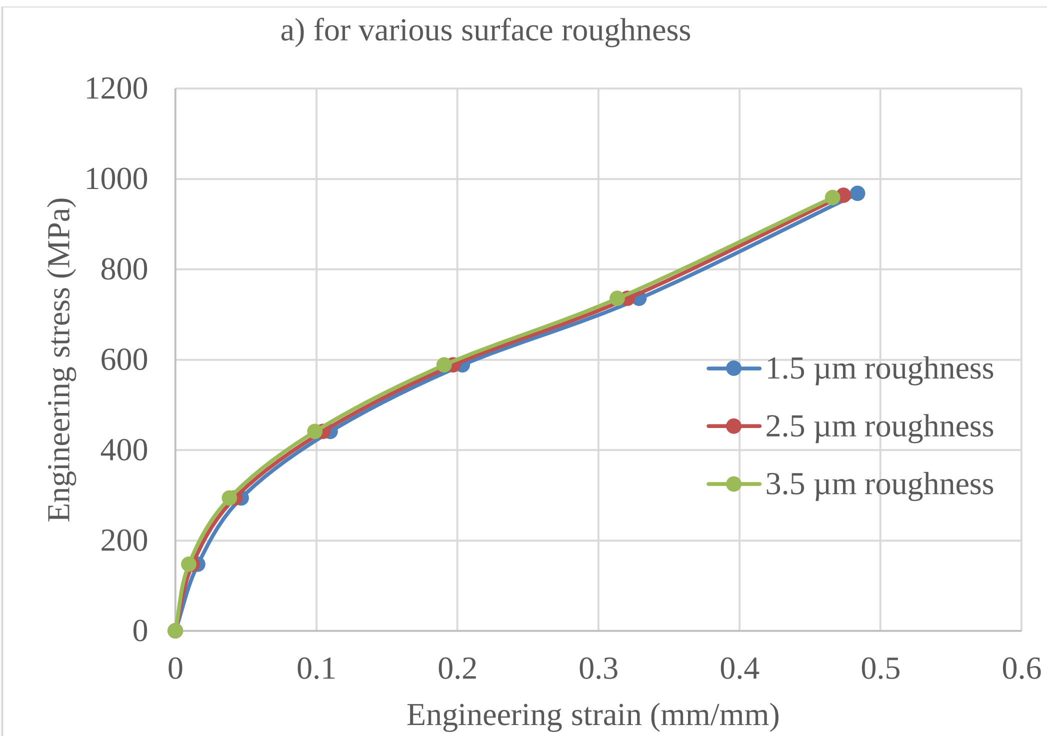

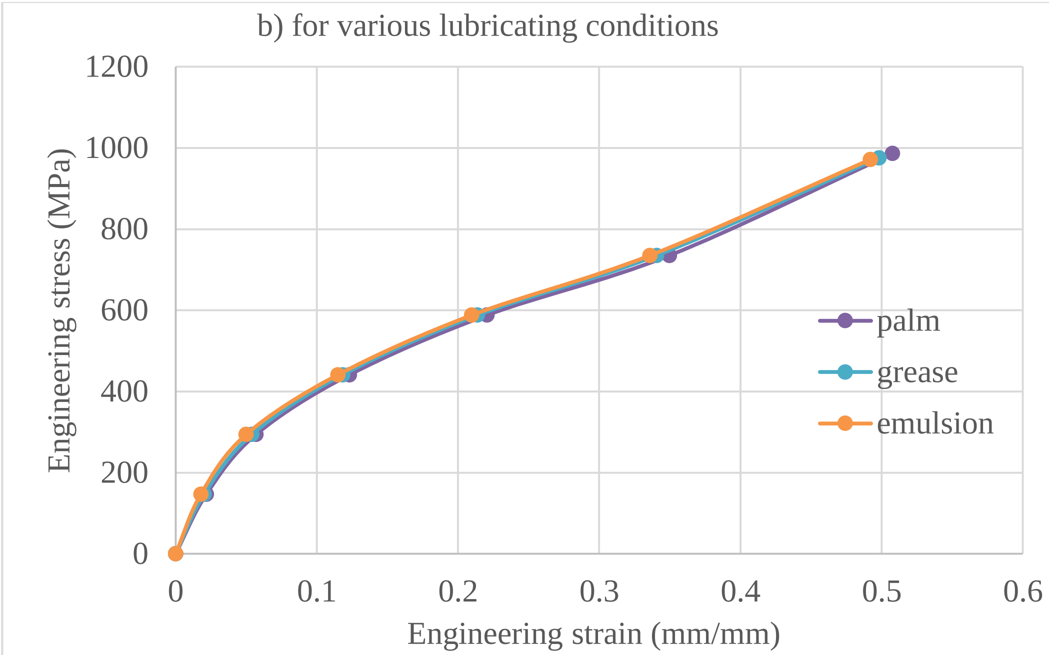

Figure 4. 2 Engineering stress-strain curve of AA 4032 obtained from ring compression test

Figure 4.3 shows the determination of strain hardening and strength coefficient from the whole compression flow data for various surface roughness and lubricating conditions respectively. The strain hardening and strength coefficient were determined from natural logarithm value of the true strain versus true stress, and curve was plotted. The strain hardening exponent may be defined by the slope of equation (3.7). In this way the values of strength coefficient can also be determined from equation (3.11) for all surface roughness of the work piece and different lubricating conditions.

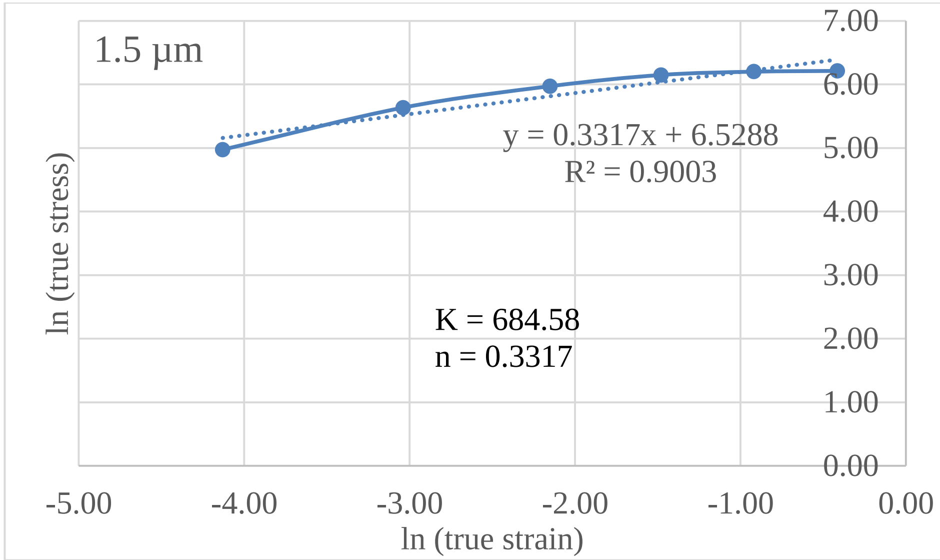
1.5 µm
y = 0.3317x + 6.5288
R² = 0.9003
K = 684.58
n = 0.3317
ln (true stress)
ln (true strain)
7.00
6.00
5.00
4.00
3.00
2.00
1.00
0.00
-5.00
-4.00
-3.00
-2.00
-1.00
0.00

(a)

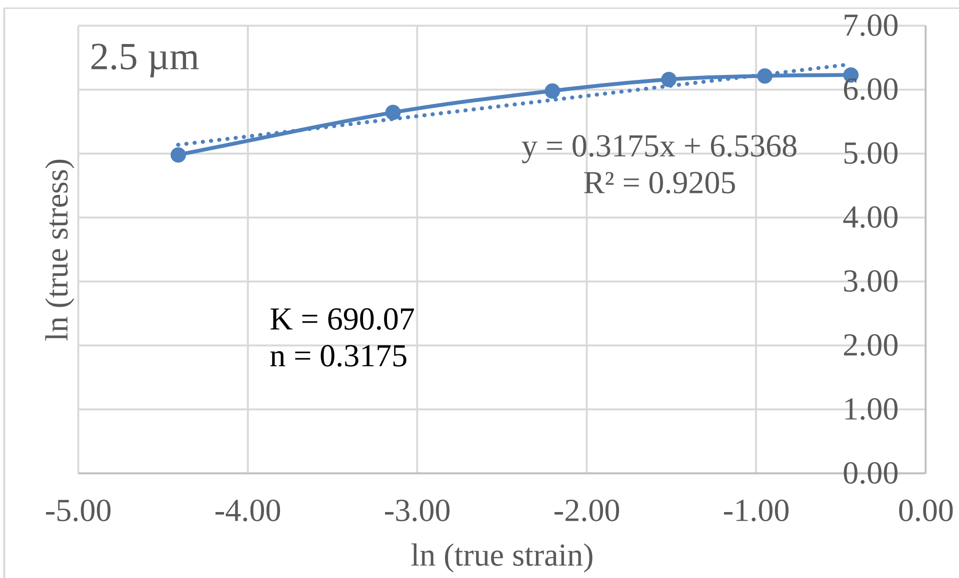
2.5 µm
y = 0.3175x + 6.5368
R² = 0.9205
K = 690.07
n = 0.3175
ln (true stress)
ln (true strain)
7.00
6.00
5.00
4.00
3.00
2.00
1.00
0.00
-5.00
-4.00
-3.00
-2.00
-1.00
0.00

(b)

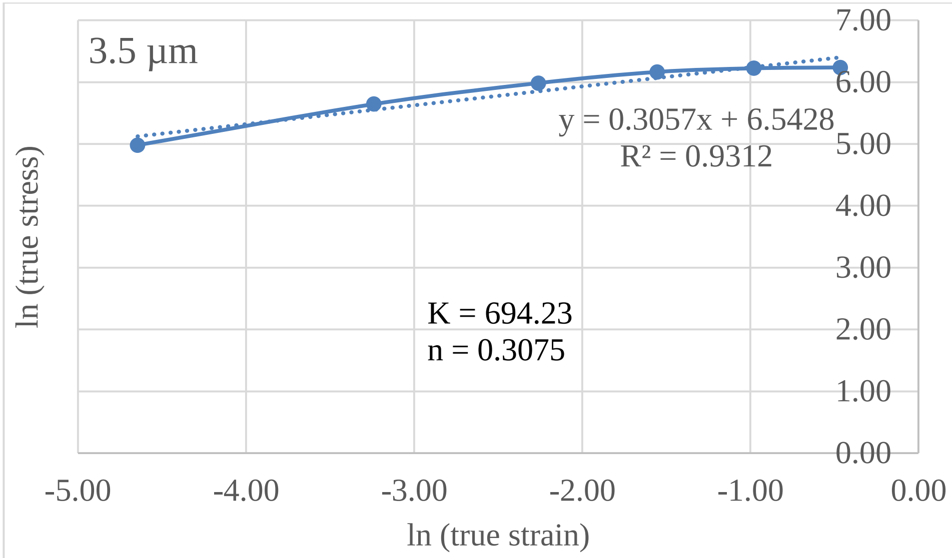
3.5 µm
7.00
6.00
5.00
4.00
3.00
2.00
1.00
0.00
y = 0.3057x + 6.5428
R² = 0.9312
K = 694.23
n = 0.3075
ln (true stress)
-5.00
-4.00
-3.00
-2.00
-1.00
0.00
ln (true strain)

(c)

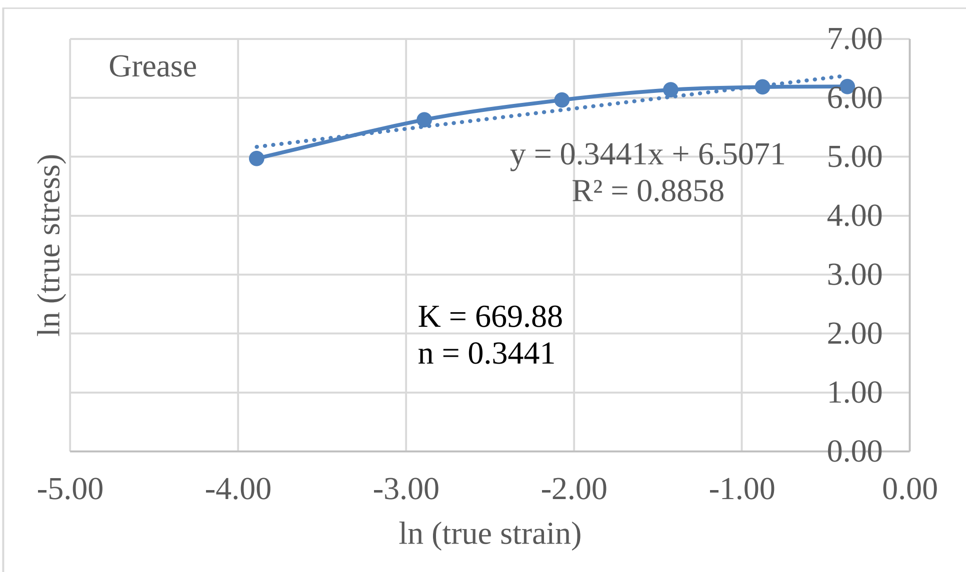
Grease
7.00
6.00
5.00
4.00
3.00
2.00
1.00
0.00
y = 0.3441x + 6.5071
R² = 0.8858
K = 669.88
n = 0.3441
ln (true stress)
-5.00
-4.00
-3.00
-2.00
-1.00
0.00
ln (true strain)

(d)

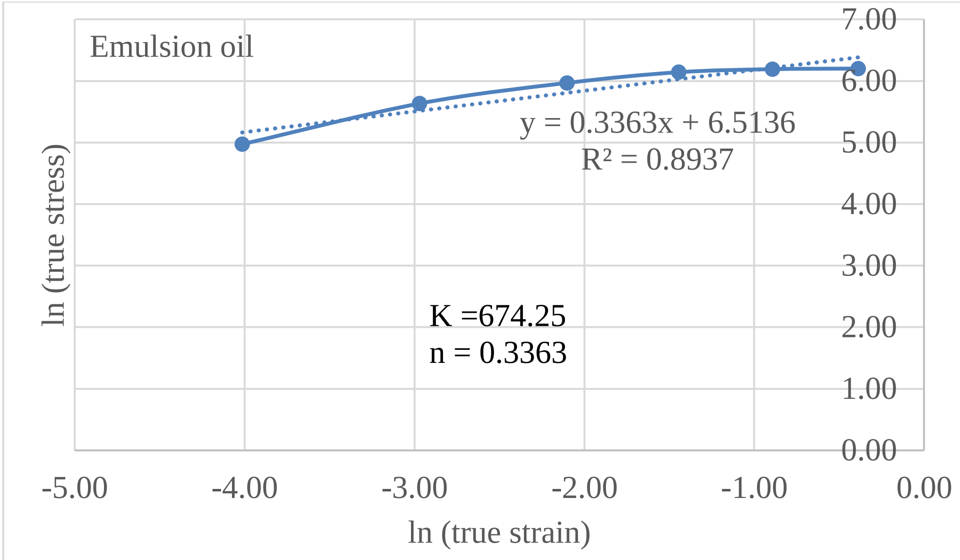

(e)

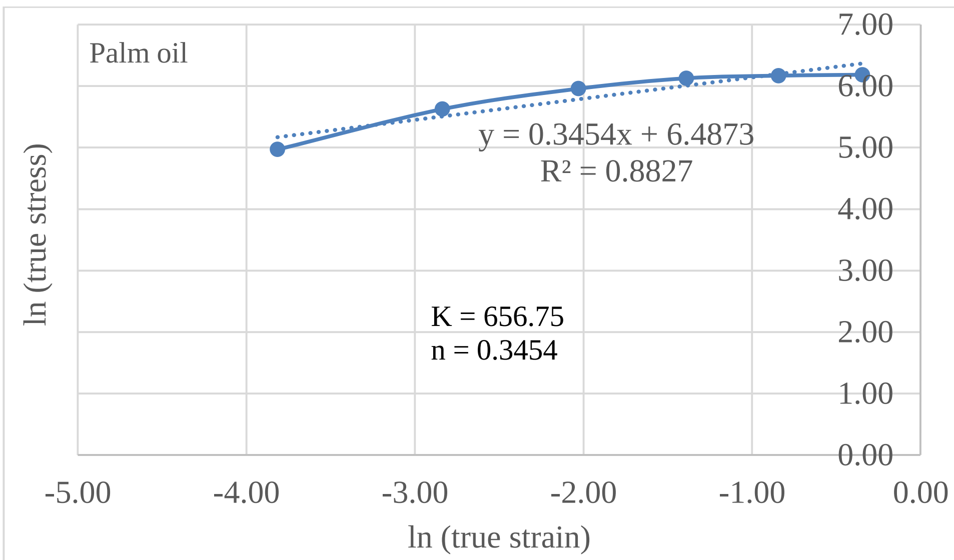

(f)

Figure 4. 3 Determination of n and k from the whole compression flow data

The general flow stress equation was obtained by fitting the properties of material, specifically, strain hardening exponent and strength coefficient. The ring compression test was done at the same chemical composition and room temperature for various surface roughness and lubricating conditions. Therefore, the general strain hardening exponent and strength coefficient values for AA 4032 was obtained by taking the average values. The flow-stress equation thus obtained is given as $\sigma = 678\ \varepsilon^{0.33}$ for various surface roughness and lubricating conditions. This flow-stress equation was treated to be material property, and used as input for finite element simulations.

This strain hardening and strength coefficient determination is also in agreement with findings gained by (Fereshteh-Saniee & Fatehi-Sichani, 2006). The strength coefficient and strain hardening exponent parameters are used widely to assess behavior in both uniaxial tension and compression at room temperature. These constants have been used to relate properties in metal forming. The strength coefficient gives the flow stress at unit strain and it is the measure of elastic spring-back. The strain hardening exponent is an important in metal forming. It signifies the strain hardening or work hardening characteristic of a material, that is, the higher the value of strain hardening exponent, higher is the rate at which the material work hardens. A material with high value of strain hardening exponent is preferred for process, which involves plastic deformation. The larger the strain hardening exponent value, the more the material can deform before instability.

Table 4.2 shows the calculated effective strains and stresses at each deformation load during compression testing with various surface roughness and lubricating conditions. Determination of the effective strain on each deformation load increment for various surface roughness and lubricating conditions were made from equation (3.12). The effective strain obtained by this method allowed to estimates of the effective stress from the strain-stress power law relationship described in equation (3.5). The finally obtained effective strain and stresses for AA 4032 alloy under various surface roughness and lubricating conditions are illustrated in Table 4.2.

Table 4. 2 Determination of effective strains and stresses

1.5 µm surface roughness						
Load	Engineering strain	Engineering stress	True strain	Flow stress	Effective stress	Effective strain
0.00	0.00	0.00	0.00	0.00	0.00	0.00
50	0.02	147.06	0.02	173.51	192.99	0.02
100	0.05	294.12	0.05	248.73	282.22	0.07
150	0.11	441.18	0.12	333.47	380.12	0.17
200	0.20	588.24	0.23	416.07	481.46	0.35

250	0.33	735.29	0.40	500.77	588.27	0.65
329	0.48	967.65	0.66	591.75	706.30	1.13
2.5 µm surface roughness						
Load	Engineering strain	Engineering stress	True strain	Flow stress	Effective stress	Effective strain
0.00	0.00	0.00	0.00	0.00	0.00	0.00
50	0.01	147.06	0.01	158.12	183.72	0.02
100	0.04	294.12	0.04	240.20	276.56	0.07
150	0.10	441.18	0.11	327.76	377.01	0.17
200	0.20	588.24	0.22	411.16	478.29	0.35
250	0.32	735.29	0.39	495.63	583.38	0.63
327.67	0.47	963.73	0.64	586.04	701.04	1.11
3.5 µm surface roughness						
Load	Engineering strain	Engineering stress	True strain	Flow stress	Effective stress	Effective strain
0.00	0.00	0.00	0.00	0.00	0.00	0.00
50	0.01	147.06	0.01	143.78	176.66	0.02
100	0.04	294.12	0.04	229.85	269.42	0.06
150	0.10	441.18	0.10	318.75	369.91	0.16
200	0.19	588.24	0.21	403.73	472.11	0.34
250	0.31	735.29	0.38	489.23	578.24	0.62
326	0.46	958.82	0.63	580.58	697.34	1.09
Grease						
Load	Engineering strain	Engineering stress	True strain	Flow stress	Effective stress	Effective strain
0.00	0.00	0.00	0.00	0.00	0.00	0.00
50	0.02	147.06	0.02	187.86	209.04	0.03
100	0.05	294.12	0.06	261.10	291.86	0.08
150	0.12	441.18	0.13	342.25	384.78	0.18
200	0.21	588.24	0.24	423.84	484.13	0.36
250	0.34	735.29	0.42	507.98	591.07	0.66
331.67	0.50	975.49	0.69	599.96	711.64	1.16

Emulsion oil						
Load	Engineering strain	Engineering stress	True strain	Flow stress	Effective stress	Effective strain
0.00	0.00	0.00	0.00	0.00	0.00	0.00
50	0.02	147.06	0.02	180.29	199.94	0.02
100	0.05	294.12	0.05	254.37	287.61	0.07
150	0.11	441.18	0.12	338.74	384.25	0.18
200	0.21	588.24	0.24	420.81	485.47	0.36
250	0.34	735.29	0.41	505.09	591.69	0.66
330.33	0.49	971.57	0.68	596.43	710.47	1.15
Palm oil						
Load	Engineering strain	Engineering stress	True strain	Flow stress	Effective stress	Effective strain
0.00	0.00	0.00	0.00	0.00	0.00	0.00
50	0.02	147.06	0.02	192.48	210.93	0.03
100	0.06	294.12	0.06	265.83	293.29	0.08
150	0.12	441.18	0.13	347.07	388.26	0.18
200	0.22	588.24	0.25	428.77	487.78	0.37
250	0.35	735.29	0.43	513.52	596.08	0.68
335.33	0.51	986.27	0.71	605.45	719.24	1.19

4.3 Effects of Surface Roughness on Friction Factor

Figure 4.4 shows friction factors obtained from ring compression tests conducted at dry condition under the specimen surface roughness of 1.50 µm, 2.50 µm and 3.50 µm. As discussed in chapter three, specimens were polished with various emery paper to create a various asperity peaks on the ring surface. The friction factor was determined by plotting reduction in height and inner diameter change of the ring specimen, and made to fit against (Male & Cockcroft, 1965) friction calibration curves. Therefore, the friction factors at the 1.50 µm, 2.50 µm and 3.50 µm die-work piece interfaces are supposed to be 0.50, 0.53, and 0.55 respectively. The greatest friction factor value was observed on the 3.50 µm specimen surface roughness used. This increase in friction factor was a result of the increased asperity contact at the die-work piece interface when higher roughness specimens are used. As the surface roughness of the test specimen is increased, a similar rise in the magnitude of the surface asperities occurs. This rise in asperity peaks leads to restricts the metal flow at the die-work piece interfaces. As a result, the interfacial friction factor between the die and specimen increases. In addition, it was observed that the contraction of inner diameter was increased with increase in the surface roughness, whereas, reduction in height was decreased with increase in the roughness.

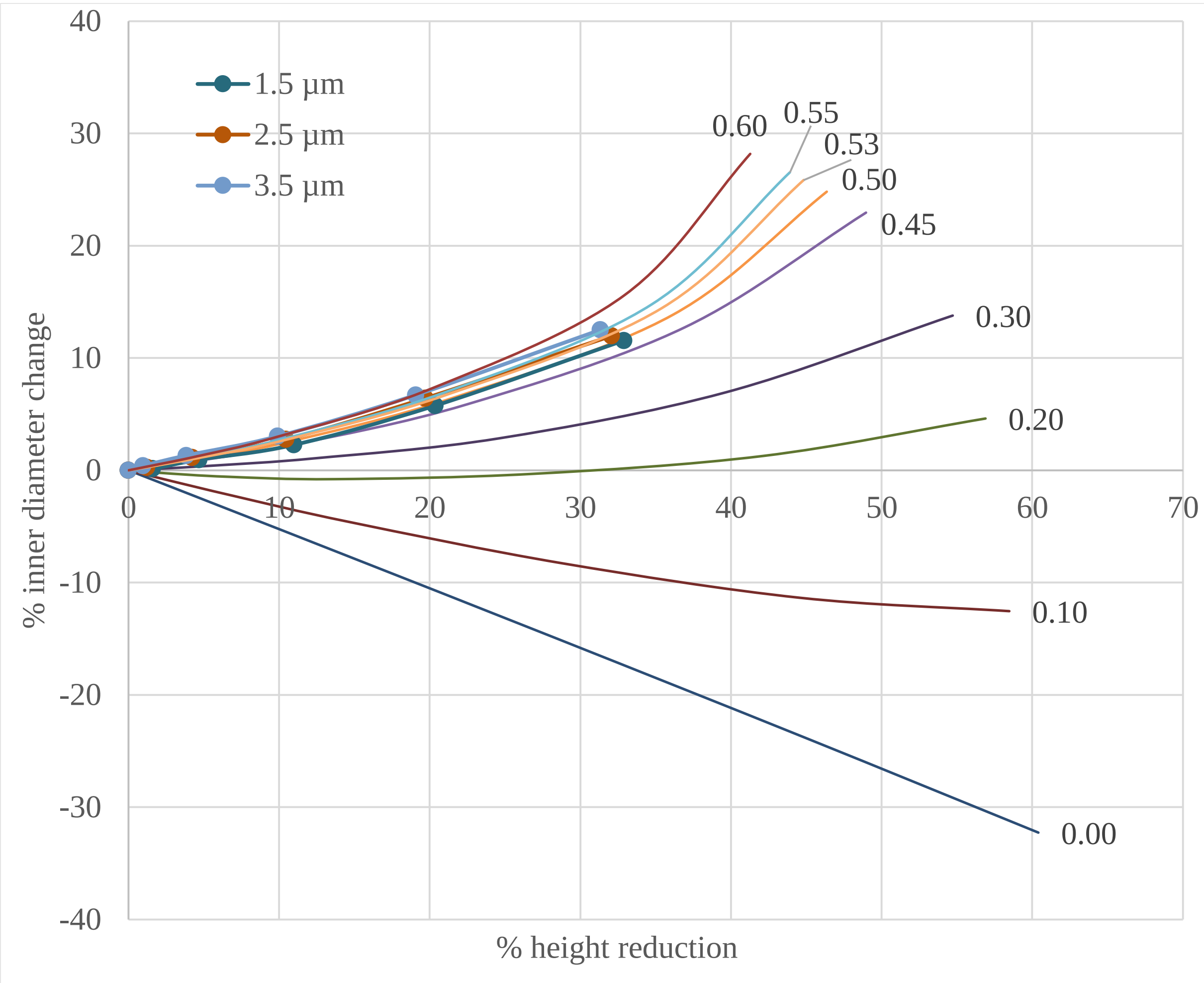

Figure 4. 4 Friction calibration curve of experimental results for various surface roughness

4.3.1 Effects of Friction Factor on Deformation Load Requirement

Figure 4.5 shows the effects of friction factor on the deformation load requirements for AA 4032 alloy during ring compression testing with surface roughness of 1.5 µm, 2.5 µm and 3.5 µm. At fracture detected, the average deformation load requirement for ring specimens are to be 329 KN, 327.67 KN and 326 KN with respect to specimen's surface roughness, as indicated in Table 4.1. To verify whether the relationship between deformation load and specimen's surface roughness was further influenced by friction factor, separate histogram was used. It was found that the required deformation load increased with decreasing the surface roughness of specimen. This is due to decrease in asperity peaks of the material which allows the metal flow between the die-work piece interfaces with high deformation rate.

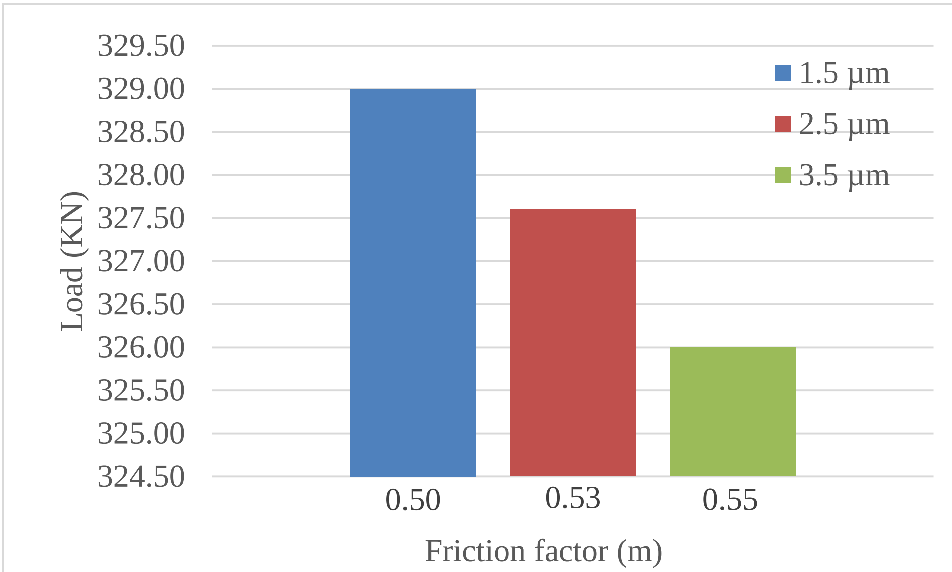

Figure 4. 5 Effects of friction factor on the deformation load at final height reduction

4.3.2 Effects of Friction Factor on Effective Strain

As a result of the relationships identified between friction factor and specimen's surface roughness observed for all, it was clear that metal flow was influenced by surface roughness of specimens. Hence, induced strain characterizes the metal flow between die-work pieces. Specifically, the induced strain was obtained from the geometry measurements for each specimen's surface roughness. To verify whether the relationship between induced strain and friction factor was further influenced by specimen roughness, separate histogram was used. The results obtained at each surface roughness are presented separately allowing for the influence of friction factor on induced strains to be investigated. Therefore, the increase in induced strain observed with respect to smoother surface roughness indicates that more metal flow was occurring between die-work pieces, while metal flow in the rougher surface was reduced. The relationship between specimen surface roughness and the induced strains was presented in Table 4.2. The relationship between friction factor and induced strains at fracture detected deformation load with respect to surface roughness is displayed in Figure 4.6.

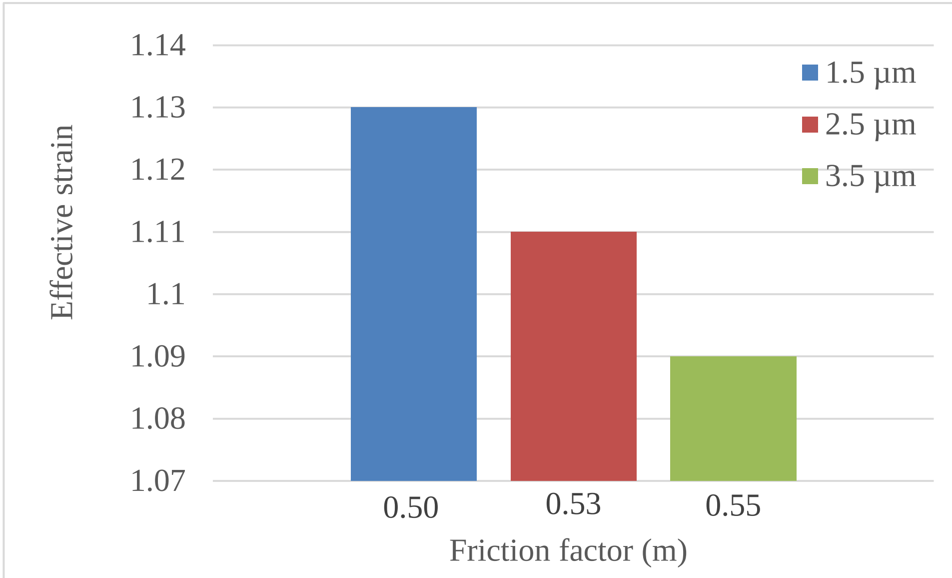

Figure 4. 6 Effects of friction factor on effective strain at final height reduction

Upon comparisons between the friction factor and induced strains shown in Figure 4.6, it can be seen that friction factor was increased with decreasing induced strains, while specimen surface roughness increases. When the 3.5 µm surface roughness specimen was used, a higher friction factor was noted for the low strain induced. As the specimen's surface roughness was decreased to the lower values, the friction factor appeared to decrease, while strain results appeared to continue increasing. Based upon these results, at various surface roughness the induced strain was influenced by friction factor.

4.3.3 Effects of Friction Factor on Effective Stress

Figure 4.7 shows the effects of friction factor on the effective stress for AA 4032 alloy during ring compression testing with various surface roughness. During deformation, specimens with smoother surface roughness undergo more deformation. This is due to increase in reduction of the material with the strain induced which allows the metal flow at the tool-work piece interfaces. From the Table 4.2, it was evident that effective stress increases with the increasing of the induced strain for the given surface roughness. As a result, the interfacial friction between the die and specimen decreased.

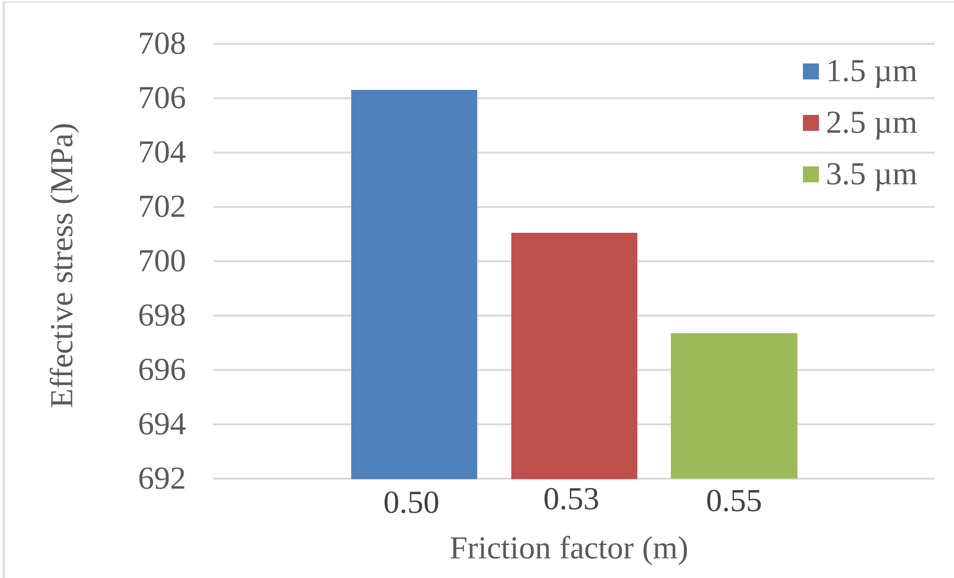

Figure 4. 7 Effects of friction factor on effective stress at final height reduction

Using the above concepts, effects of surface roughness on interface friction, the 1.5 µm surface roughness of AA 4032 alloy appear to be suitable roughness for dry condition, as it results in a more metal flow between die-work pieces without fracture detected.

4.4 Effects of Lubricant on the Friction Factor

Figure 4.8 shows effect of lubricants on interface friction factor when constant surface roughness of 1.5 µm specimens used. As shown in Figure 4.8, the friction factors for the palm oil, grease and emulsion lubricants are found to be 0.30, 0.35 and 0.45 respectively. Further investigation was warranted, some correlation between friction factor and lubricant is evident from the experimental data. Therefore, metal flow can be easily quantified through a measurement of true strain from the reduction in height of the compressed specimens, and used as a means to compare the effects of lubricant on material flow. From Table 4.1, variation in height reduction with respect to various lubricating conditions was observed during ring compression test. Reductions in height was used to determine the true strains. When various lubricants were used, all strains were increased as compared to dry conditions which means the material had increased flow between dies.

It was also observed in the Figure 4.8 that true strain increases with decrease in friction factor at different lubricating conditions. While, using palm oil as lubricant, the maximum true strain 0.71 was attained which could be observed from Table 4.2. Similarly, when grease and emulsion oil are used as lubricants it was found that maximum true strain decreases to 0.69 and 0.68, respectively. Among selected lubricants palm oil has extremely low friction factor. The reason was decrease in sticking nature of the material with the tool at the interfaces when palm oil used. Moreover, the inner diameters of ring specimen lubricated with grease and emulsions were more contract than the inner diameter of ring specimen lubricated with palm oil. Contraction of the inner diameter was increased with increase in the friction factor whereas, inner diameter expansion was increased with decreasing in the friction factor, as indicated in Table 4.1.

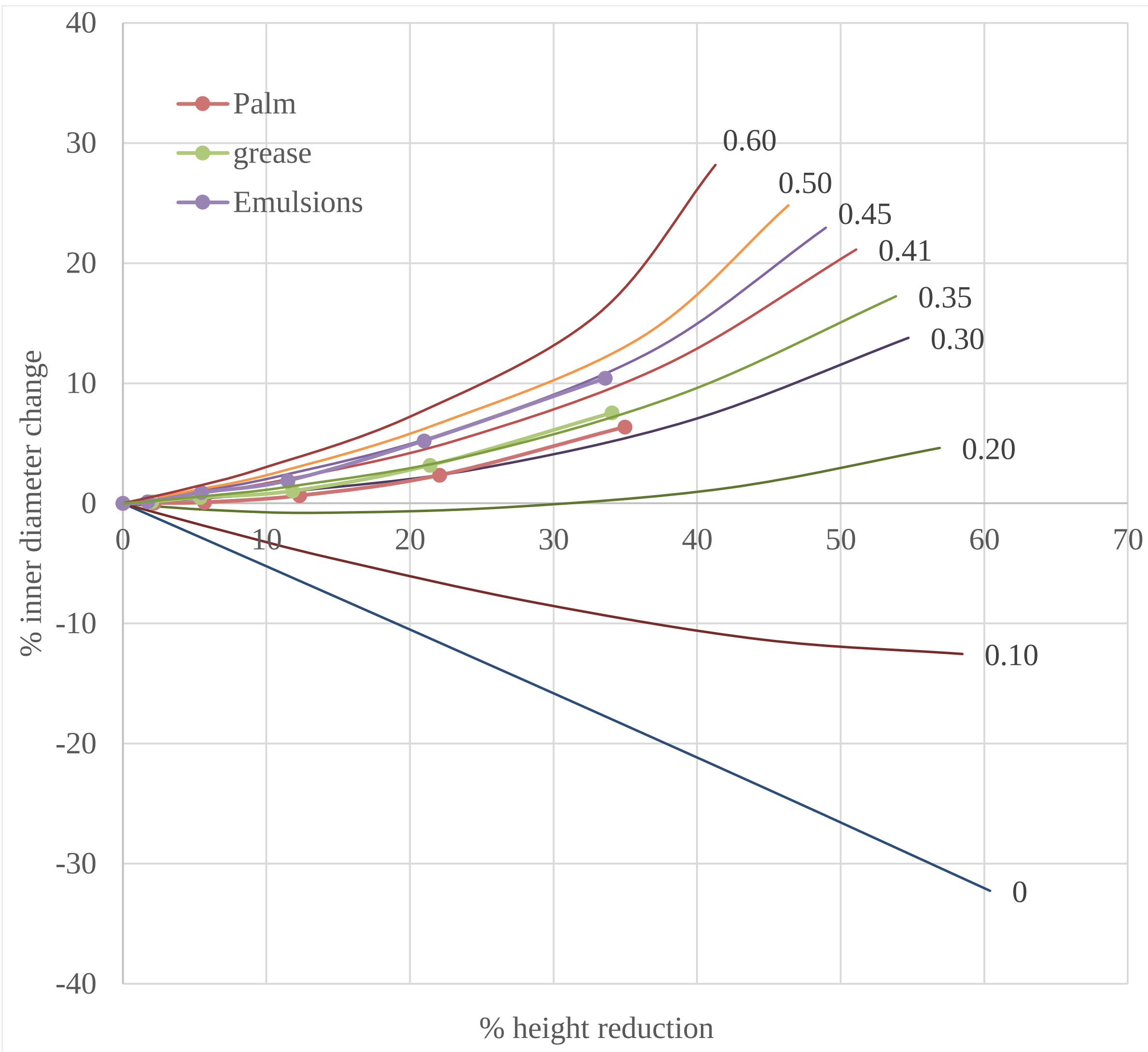

Figure 4. 8 Friction calibration curve for various lubricating conditions

4.4.1 Effects of Friction Factor on Deformation Load Requirement

Figure 4.9 shows the effects of friction factor on the deformation load requirements for AA 4032 alloy during ring compression testing with lubricating conditions of palm oil, grease and emulsion oil. In order to quantify the influence of friction factor on the deformation load, final deformation loads with respect to various lubricating conditions were considered at fracture detected. To verify whether the relationship between deformation load and various lubricating condition was further influenced by friction factor, separate histogram was also used. At fracture detected, the average deformation load requirement for ring specimens are to be 335.33 KN, 331.67 KN and 330.33 KN with respect to lubricating conditions, as indicated in Table 4.1. Comparing selected lubricants with respect to final deformation load, one can find that the required deformation load for palm oil lubricant was high. This was due to palm oil provides high capability to reduce the asperity peaks and more metal flow than grease and emulsion during deformation. Higher height reduction percentage was obtained with palm oil which can form film to achieve pretty low friction factor.

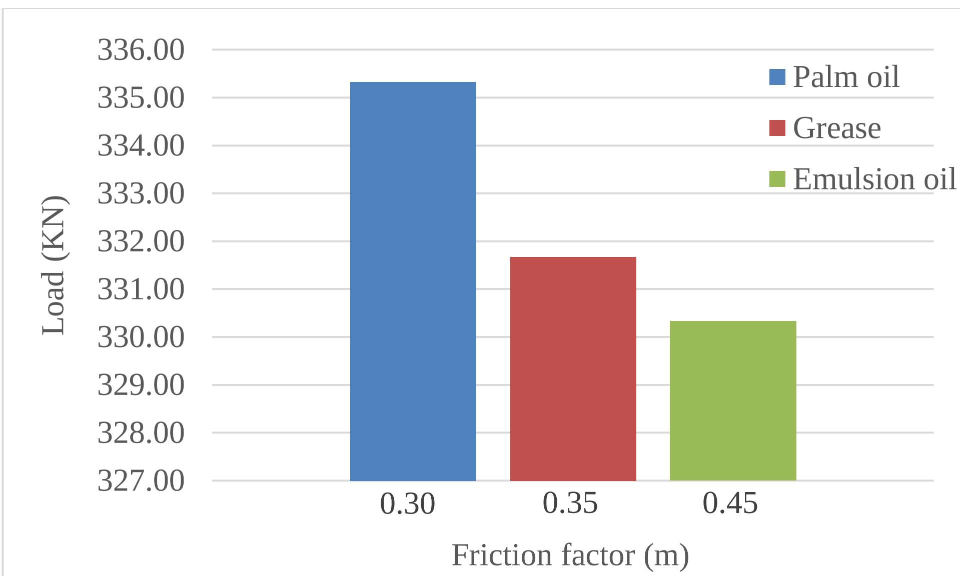

Figure 4. 9 Effects of friction factor on the deformation load at final height reduction

4.4.2 Effects of Friction Factor on Effective Strain

Figure 4.10 below shows the effects of friction factor on the induced strain for AA 4032 alloy during ring compression testing with lubricating conditions of palm oil, grease and emulsion oil. In order to quantify the influence of friction factor on the induced strain, final stage of true strains with respect to various lubricating conditions were considered, as indicated in Table

4.2. The results obtained at each lubricating conditions are presented separately, and allowing for the influence of friction factor on induced strains to be investigated.

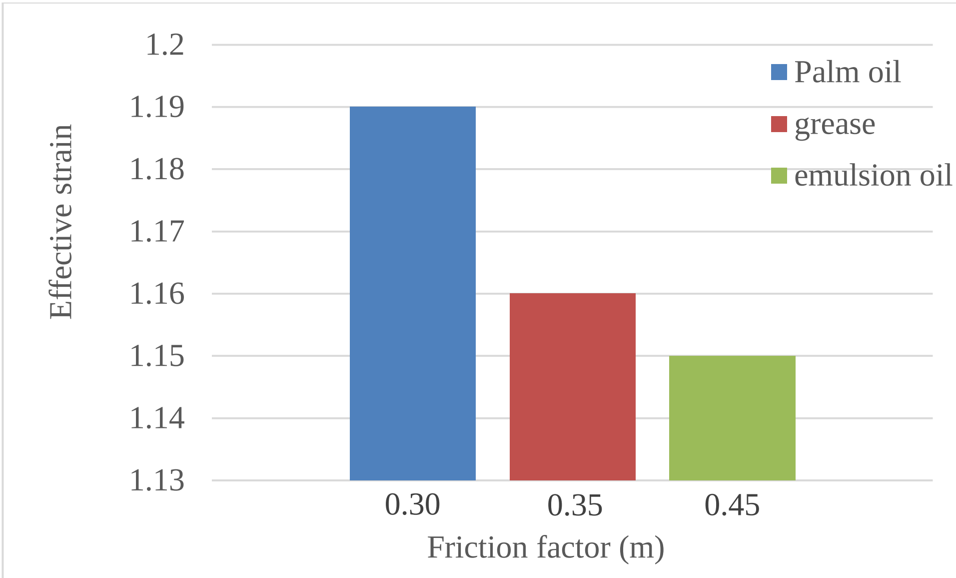

Figure 4. 10 Effects of friction factor on induced strain at final height reduction

Upon comparisons between the friction factor and induced strains shown in Figure 4.10, it can be seen that induced strains was decreased with increasing friction factor. When the emulsion oil was used, a higher friction factor was noted for the low strain induced. Moreover, when palm oil was used the friction factor appeared to decrease, while strain results appeared to continue increasing. Based upon these results, at various lubricating conditions the induced strain was influenced by friction factor.

4.4.3 Effects of Friction Factor on Effective Stress

The effective stresses were continuously increased with increasing in induced strain for all lubricating conditions, as indicated in Table 4.2. This comparison was made at each reductions of ring height. However, considering a various lubricating conditions at fracture detected deformation load, it was observed that the height reduction percentage increases with deformation load increased, as shown in Table 4.1. For lower height reduction percentage, the deformation load was lower because, lower metal flow and suddenly fracture was detected. This discussion illustrates that, in a ring compression test the deformation load and height reduction percentages were sensitive to interface friction. Moreover, the reduction in height was the sensitive parameter, and therefore it was used to evaluate the effective stress.

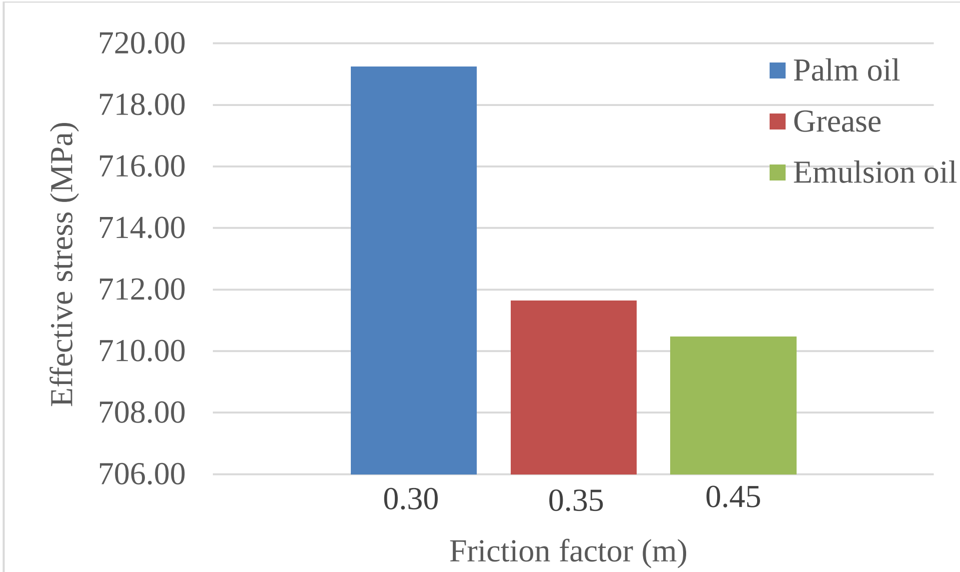

Figure 4. 11 Effects of friction factor on effective stress at final height reduction

From comparisons between the friction factor and effective stress shown in Figure 4.11, it can be seen that effective stress was increased with decreasing friction factor. When the emulsion oil was used a higher friction factor and minimum effective stress were noted. While, when palm oil was used lower friction factor and effective stress results appeared to continue increasing. Based upon these results, at various lubricating conditions the effective stress was influenced by friction factor.

4.5 FEM Simulation of Friction Behavior

4.5.1 FEM load requirements with respect to friction factor

The load requirement for deformation obtained from finite element simulations are illustrated in Figure 4.12 for various surface roughness. To verify the relationship between friction factor and surface roughness further solid work piece were simulated between two rigid die. The friction factor values obtained from the ring compression test (for 1.5 µm surface roughness 0.50, for 2.5 µm surface roughness 0.53 and for 3.5 µm surface roughness 0.55) were used for simulation. It was clearly evident that the load required for deformation increases with decrease in the friction factor for all the cases of surface roughness.

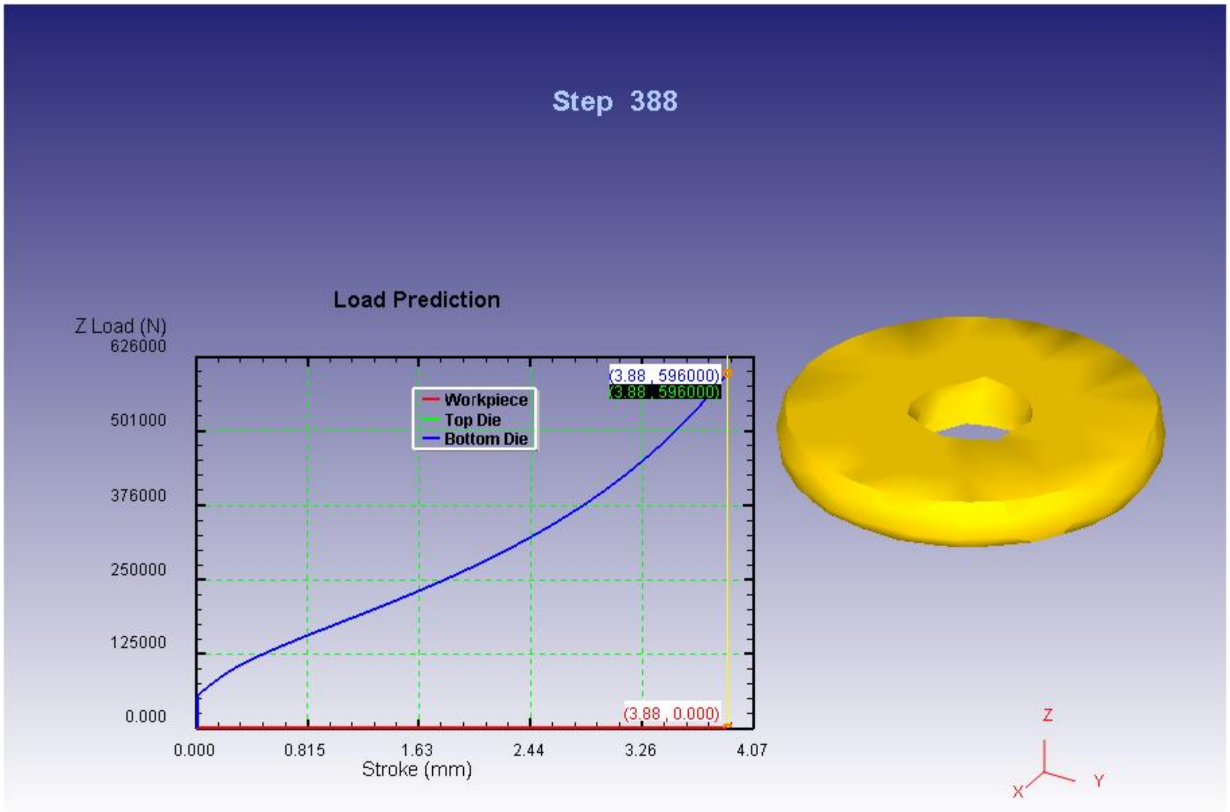
Step 388
Load Prediction
Z Load (N)
626000
501000
376000
250000
125000
0.000
0.000
0.815
1.63
2.44
3.26
4.07
Stroke (mm)
Workpiece
Top Die
Bottom Die
(3.88 , 596000)
(3.88 , 596000)
(3.88 , 0.000)
Z
Y
X

a) 1.5 μm

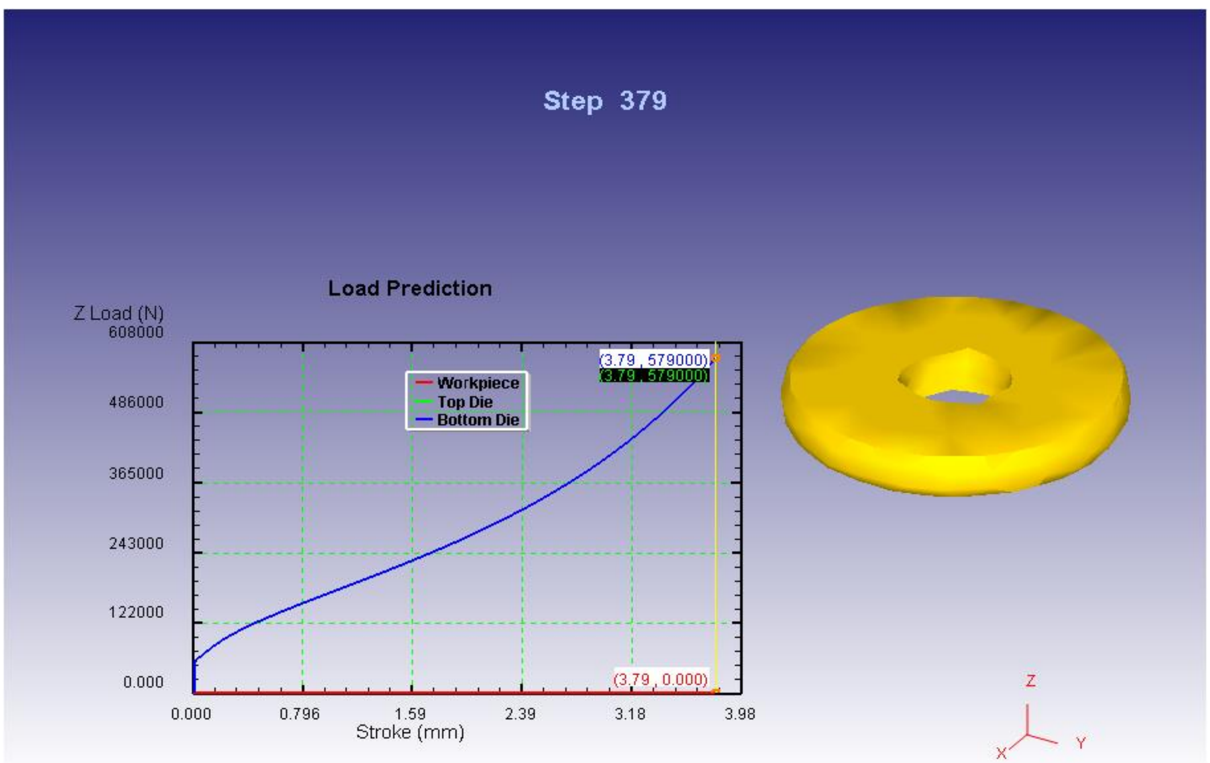
Step 379
Load Prediction
Z Load (N)
608000
486000
365000
243000
122000
0.000
0.000
0.796
1.59
2.39
3.18
3.98
Stroke (mm)
Workpiece
Top Die
Bottom Die
(3.79 , 579000)
(3.79 , 579000)
(3.79 , 0.000)
Z
Y
X

b) 2.5 μm

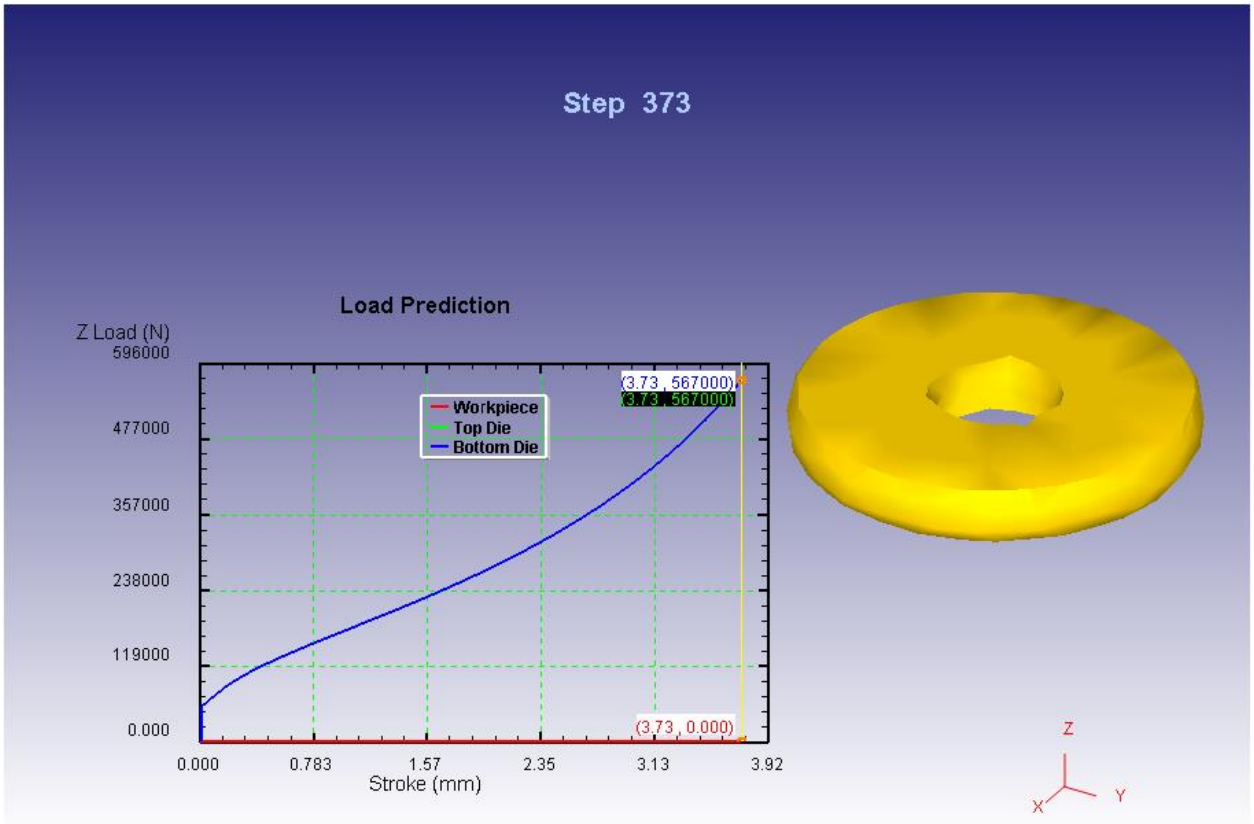

c) 3.5 µm

Figure 4. 12 FEM load requirements for various surface roughness

Figure 4.13 shows the effects of friction factor on the deformation load requirement for various lubricating conditions by using finite element simulations. The friction factor values obtained from the ring compression test (for palm oil 0.30, grease 0.35 and for emulsion oil 0.45) were used for simulation. The deformation load requirement is increasing when the friction factor decreases. It was observed that when lower friction factor was used, the reduction in height results appeared to higher deformation rate without fracture detected. It means that the higher deformation was obtained when palm oil was used between die-work pieces.

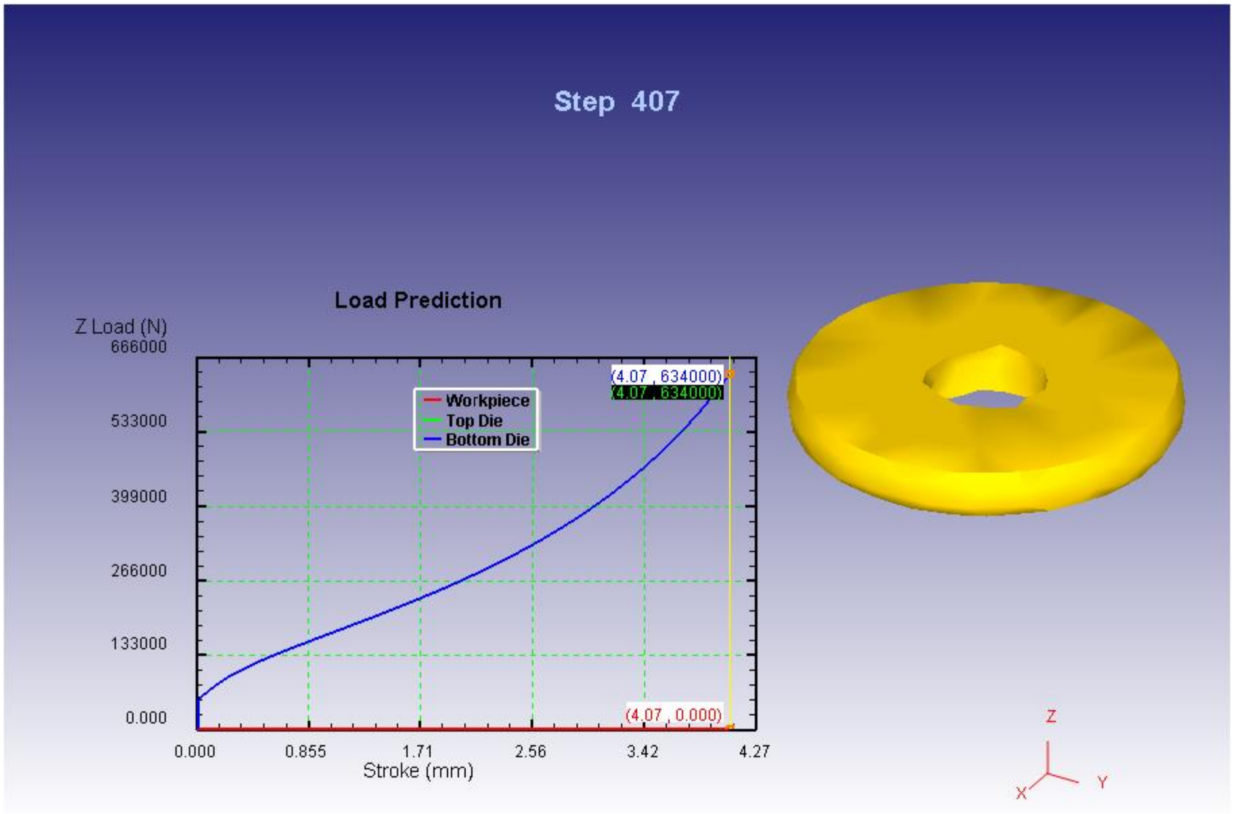

a) Palm oil

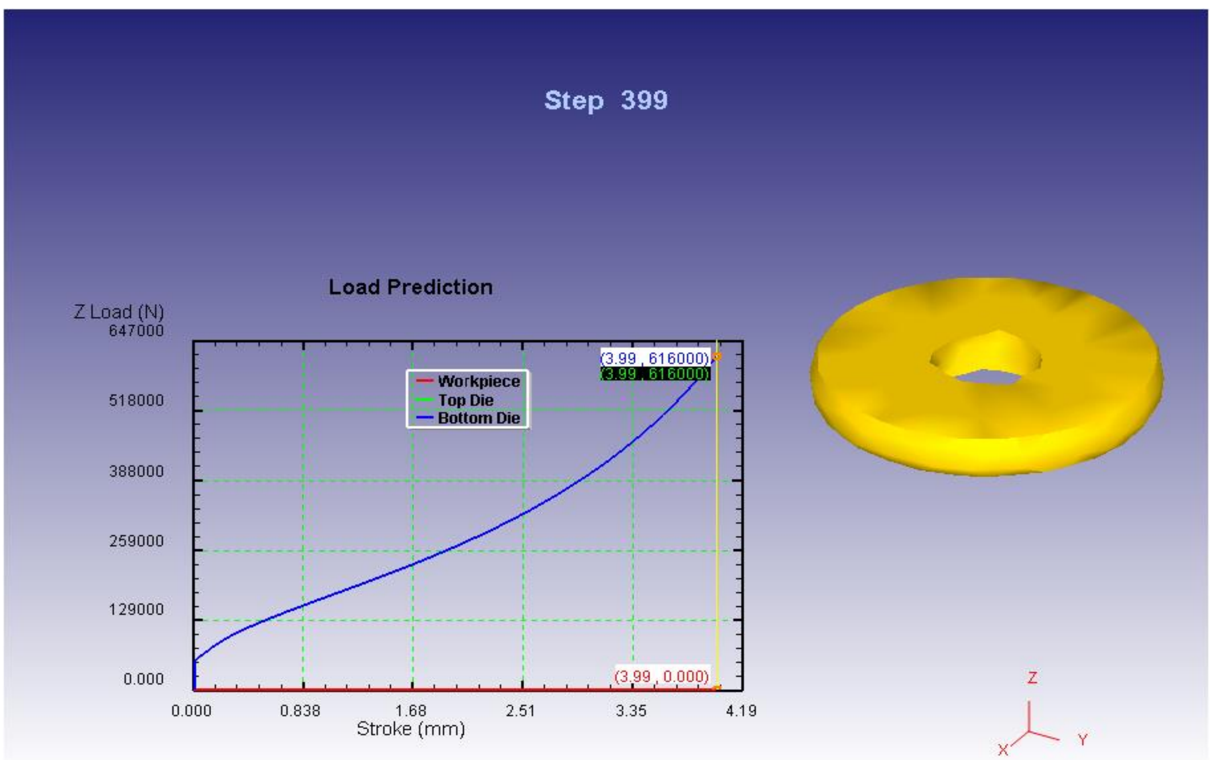

b) Grease

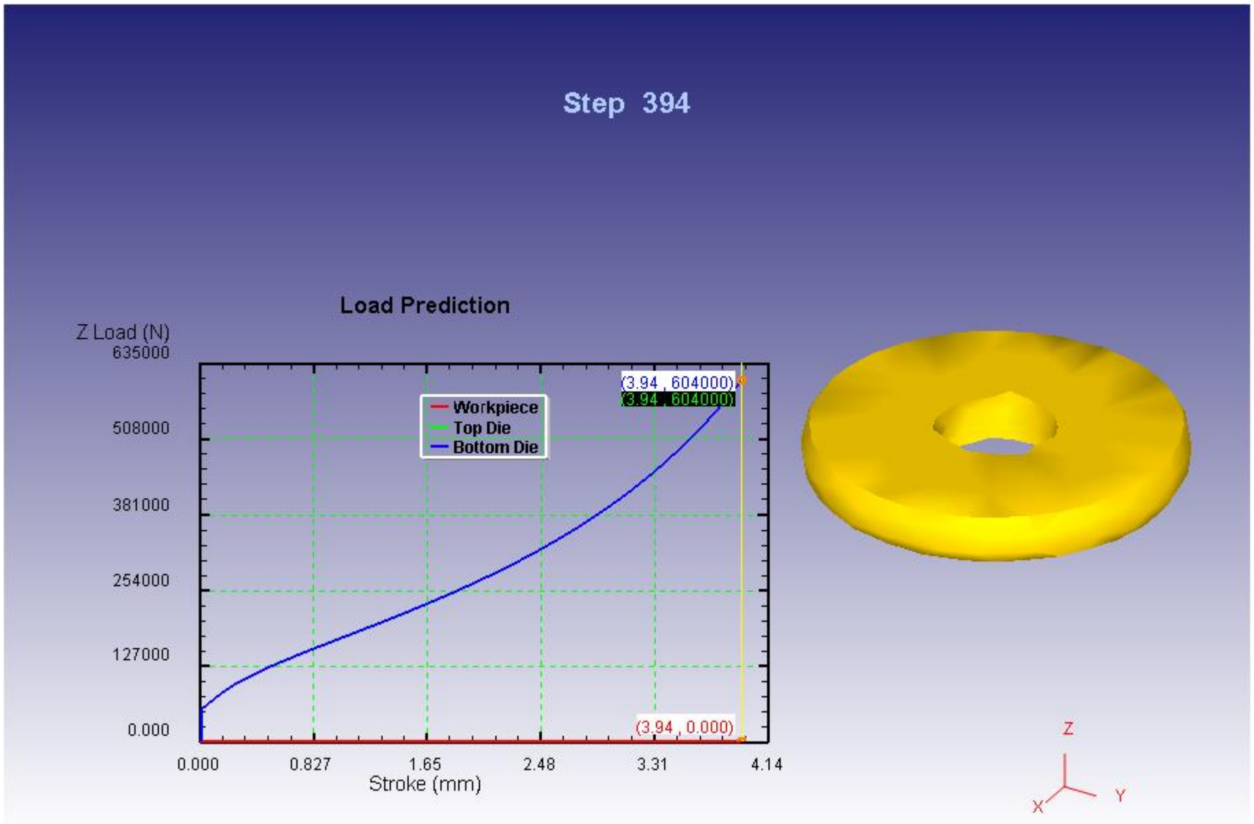

c) Emulsion oil

Figure 4. 13 FEM load requirements for various lubricating conditions

4.5.2 FEM Effective Strain with respect to Friction Factor

Variation in effective strain with respect to friction factor was analyzed for different roughness and lubricating conditions using FEM software (DEFORM 3D), and illustrated in Figure 4.14 and Figure 4.15, respectively. The effective strain are continuously decreasing with increase in the friction factor for selected surface roughness. This is due to a smaller surface roughness reduces the number of large asperities. Material has to move over to be able to flow, thus increasing the amount of strain.

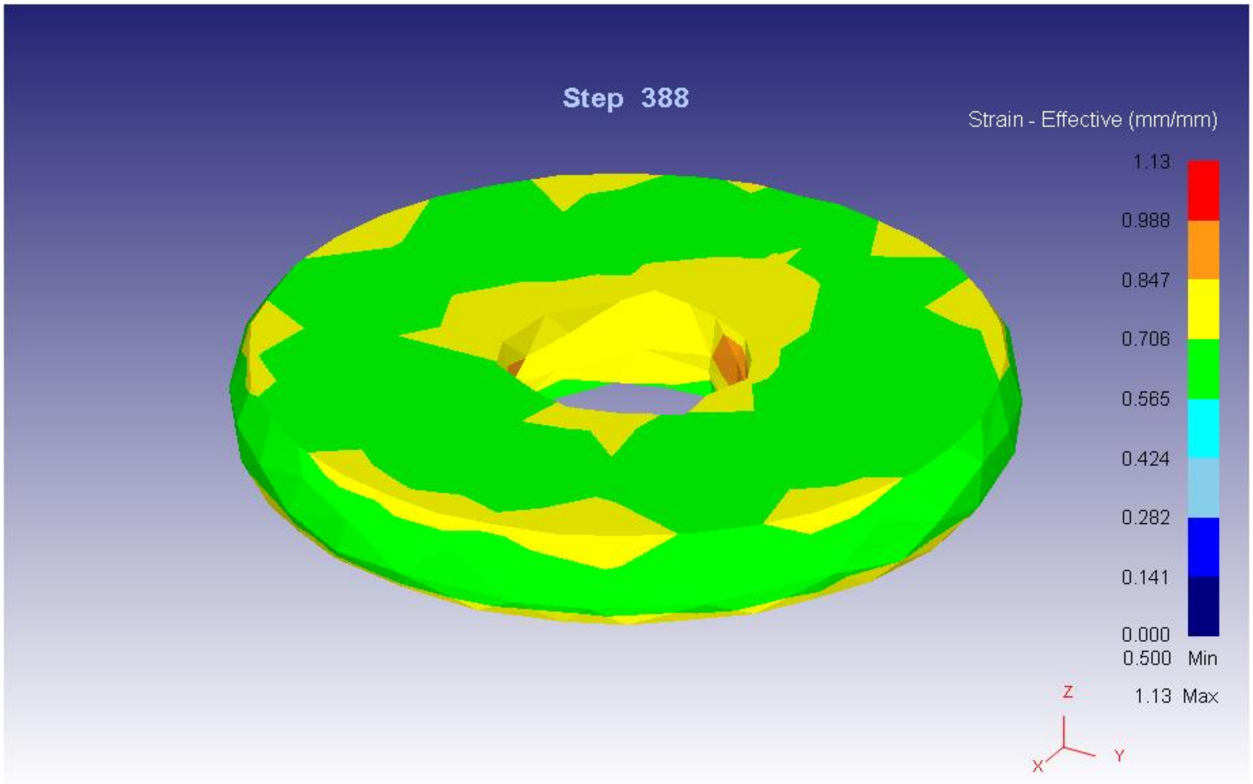
Step 388
Strain - Effective (mm/mm)
1.13
0.988
0.847
0.706
0.565
0.424
0.282
0.141
0.000
0.500 Min
1.13 Max
Z
X
Y

a) 1.5 µm

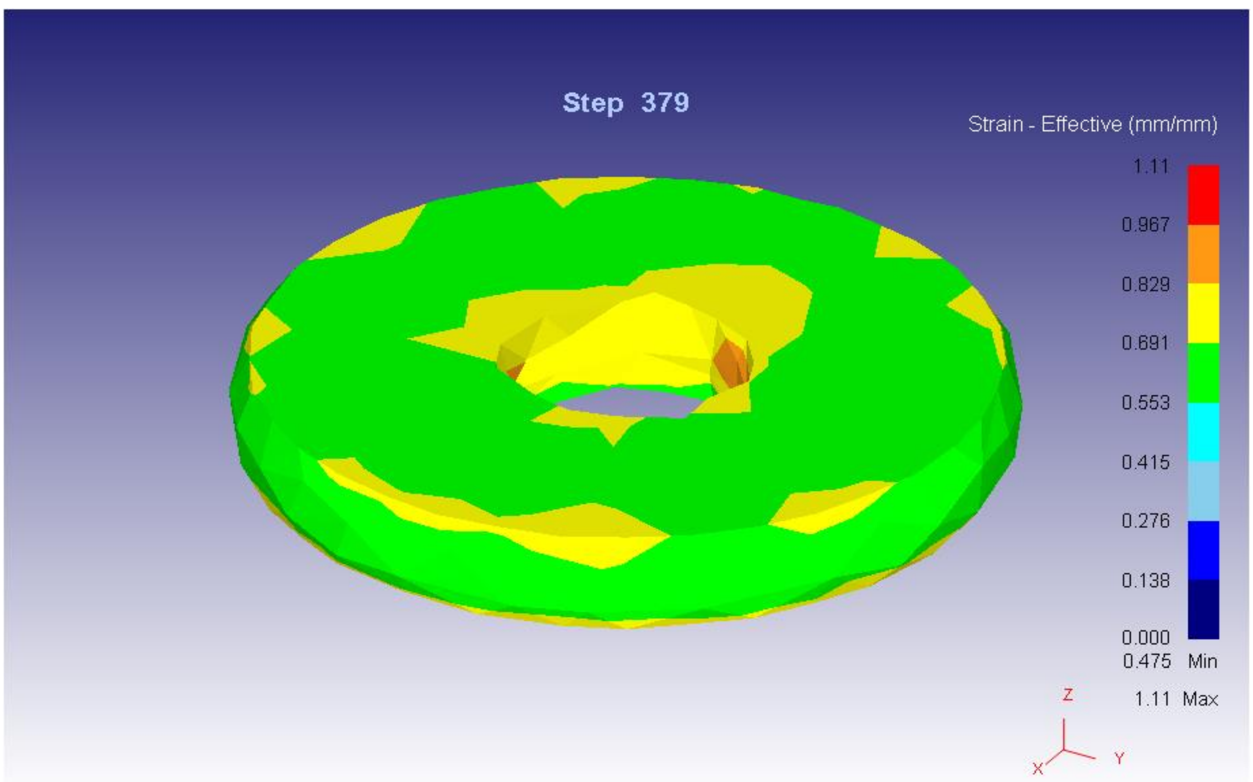
Step 379
Strain - Effective (mm/mm)
1.11
0.967
0.829
0.691
0.553
0.415
0.276
0.138
0.000
0.475 Min
1.11 Max
Z
X
Y

b) 2.5 µm

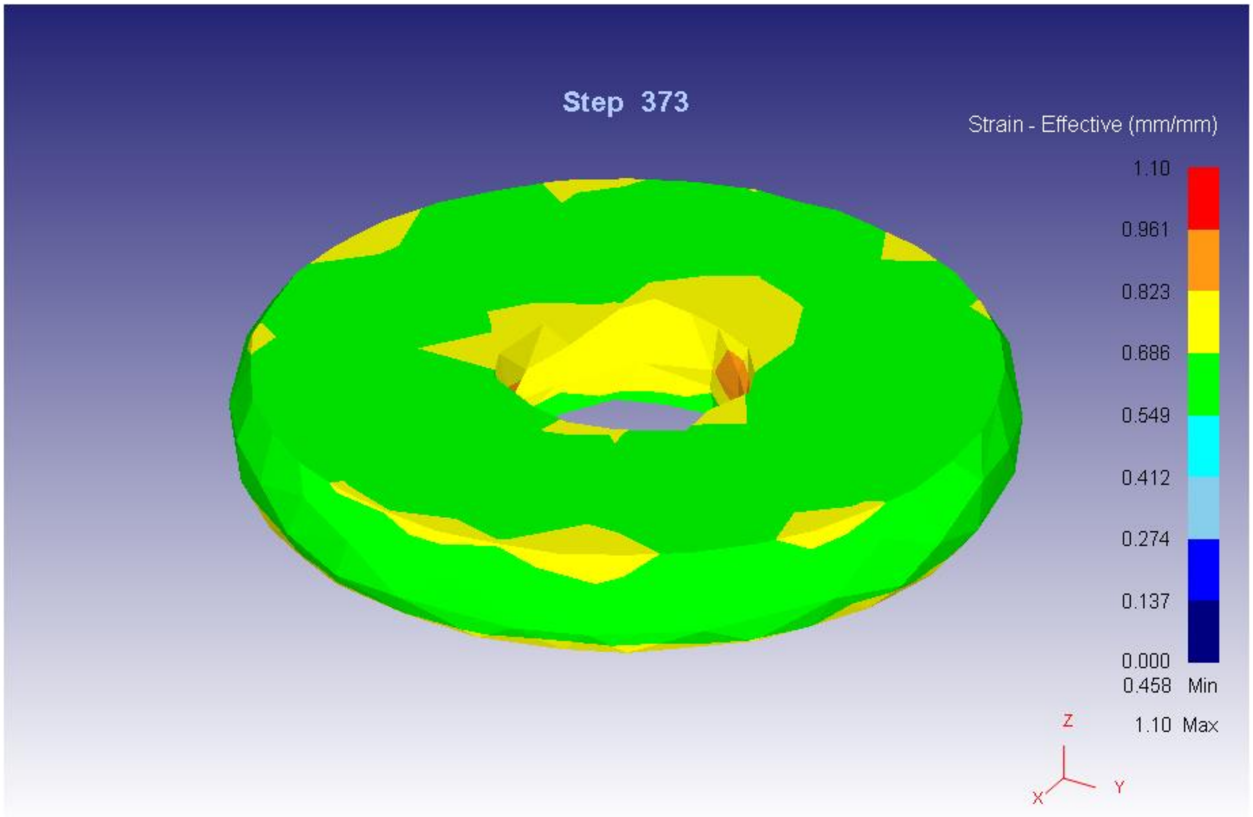

c) 3.5 µm

Figure 4. 14 FEM effective strain for various surface roughness

Figure 4.15 shows that how the effective strain for samples made of AA 4032 varies with the friction factor for different lubricating conditions. The friction factor values obtained from the ring compression tests were used for simulation. The reduction in height was increases when lubricants are used. It was observed that when lower friction factor was used, the reduction in height results appeared to higher deformation rate. It means that the higher deformation was obtained when palm oil was used between die-work pieces.

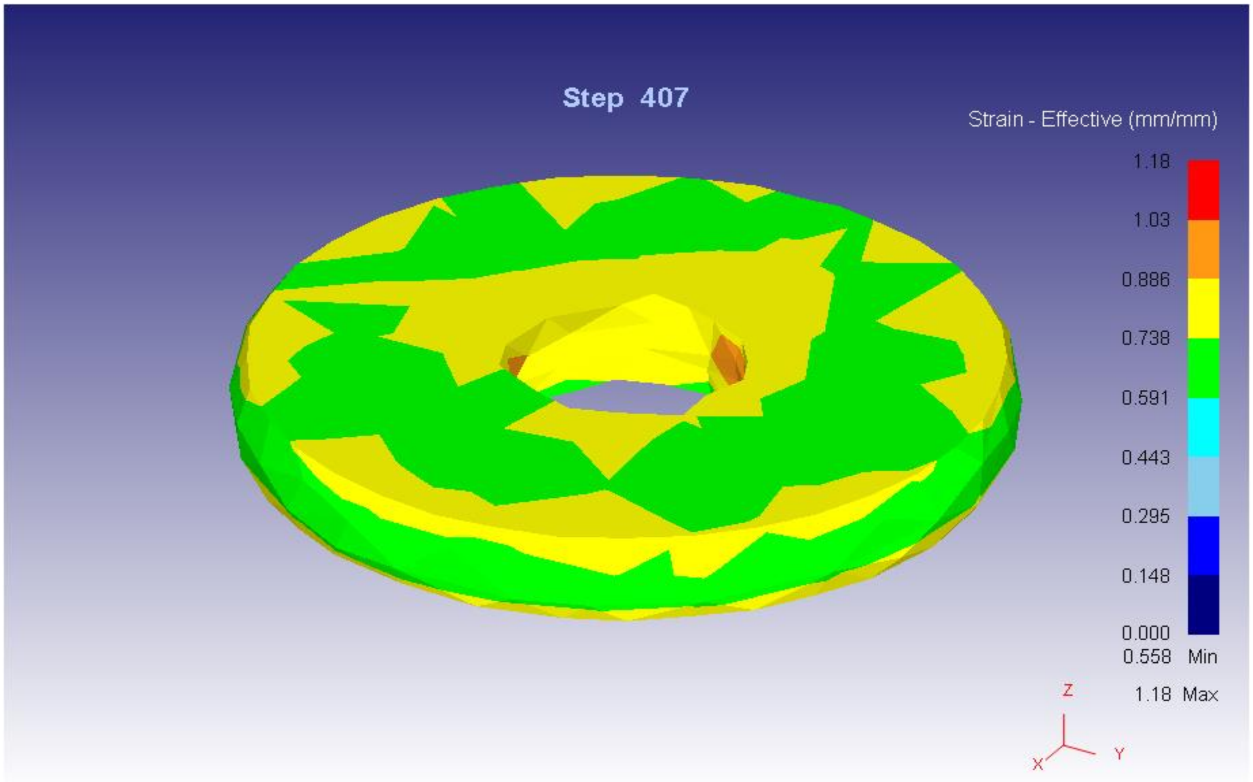

a) Palm oil

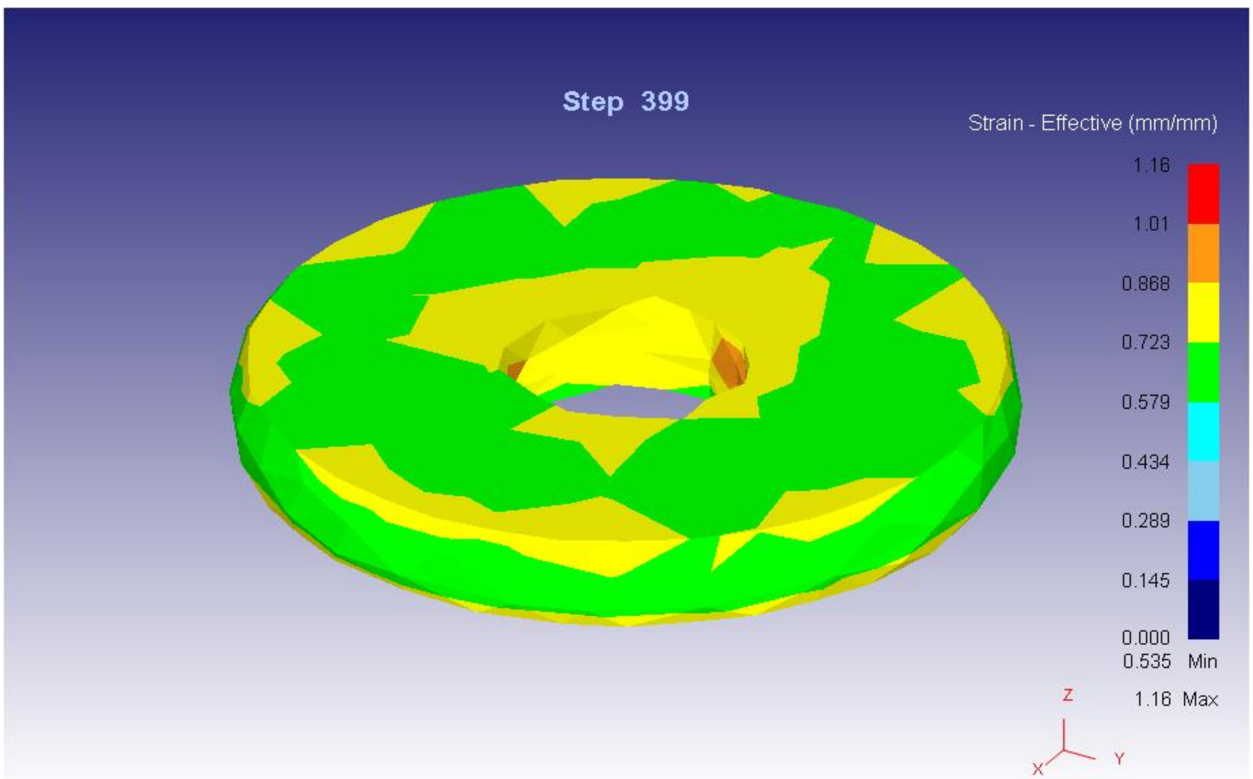

b) Grease

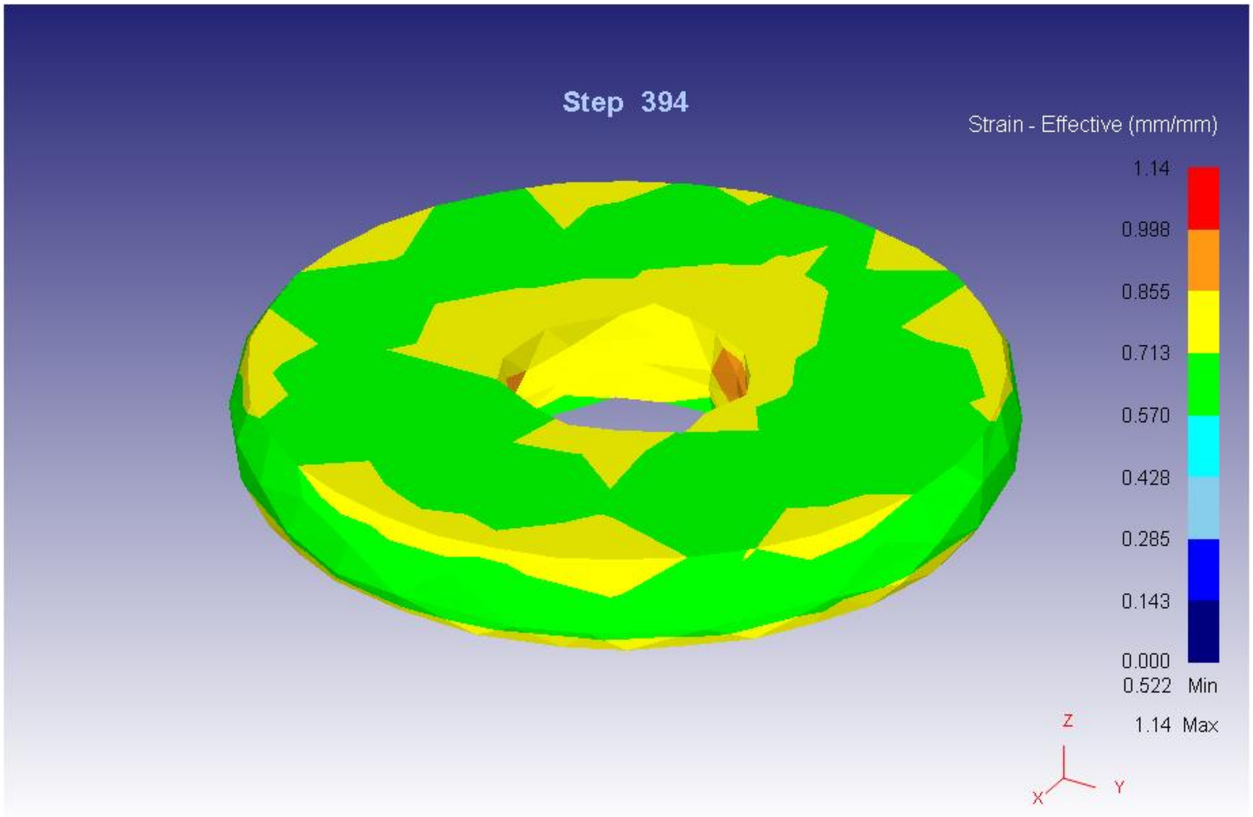

c) Emulsion oil

Figure 4. 15 FEM effective strain for various lubricating conditions

4.5.3 FEM Effective Stress with Respect to Friction Factor

Figure 4.16 shows the effects of friction factor on the effective stress by using finite element simulation for various surface roughness. The distribution of effective stress obtained through DEFORM 3D software was compared with friction factor. Further, it was observed that the effective stress decreases with increase in friction factor. On other hand, it means that the effective stress increases with decrease in specimen's surface roughness.

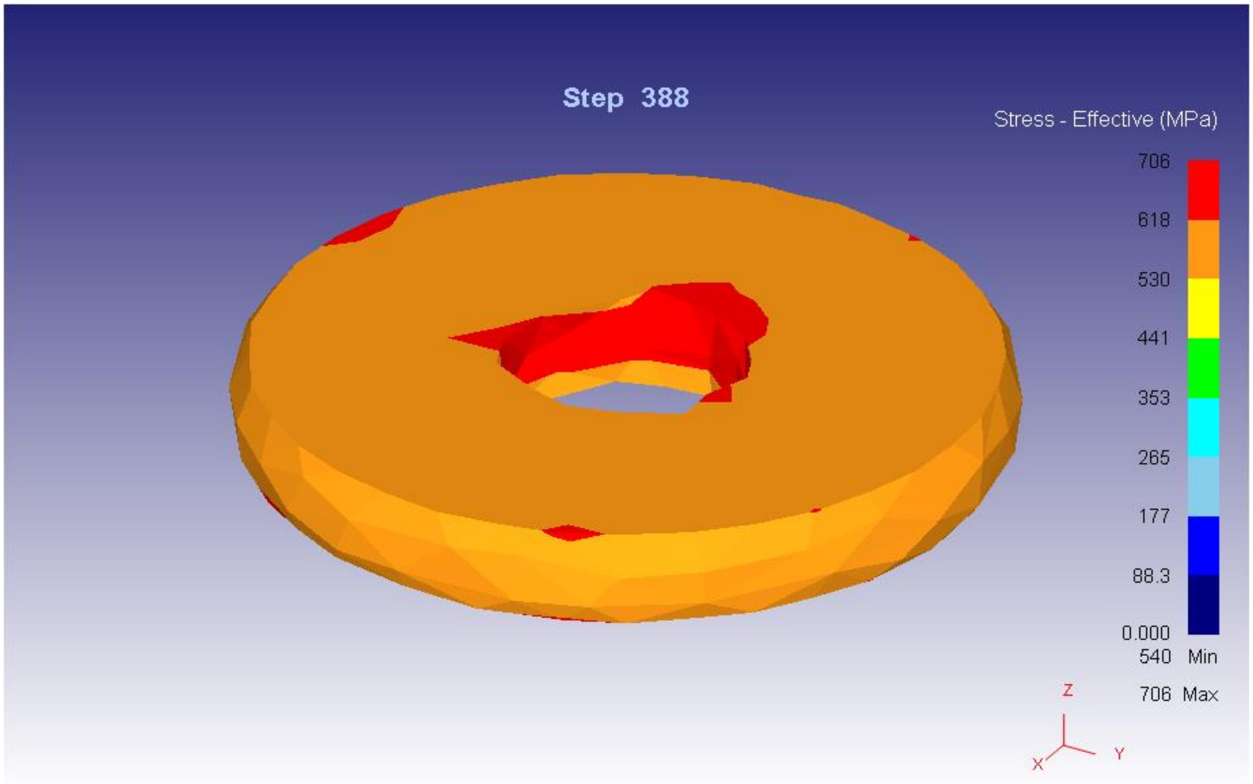
Step 388
Stress - Effective (MPa)
706
618
530
441
353
265
177
88.3
0.000
540 Min
706 Max
Z
X
Y

a) 1.5 μm

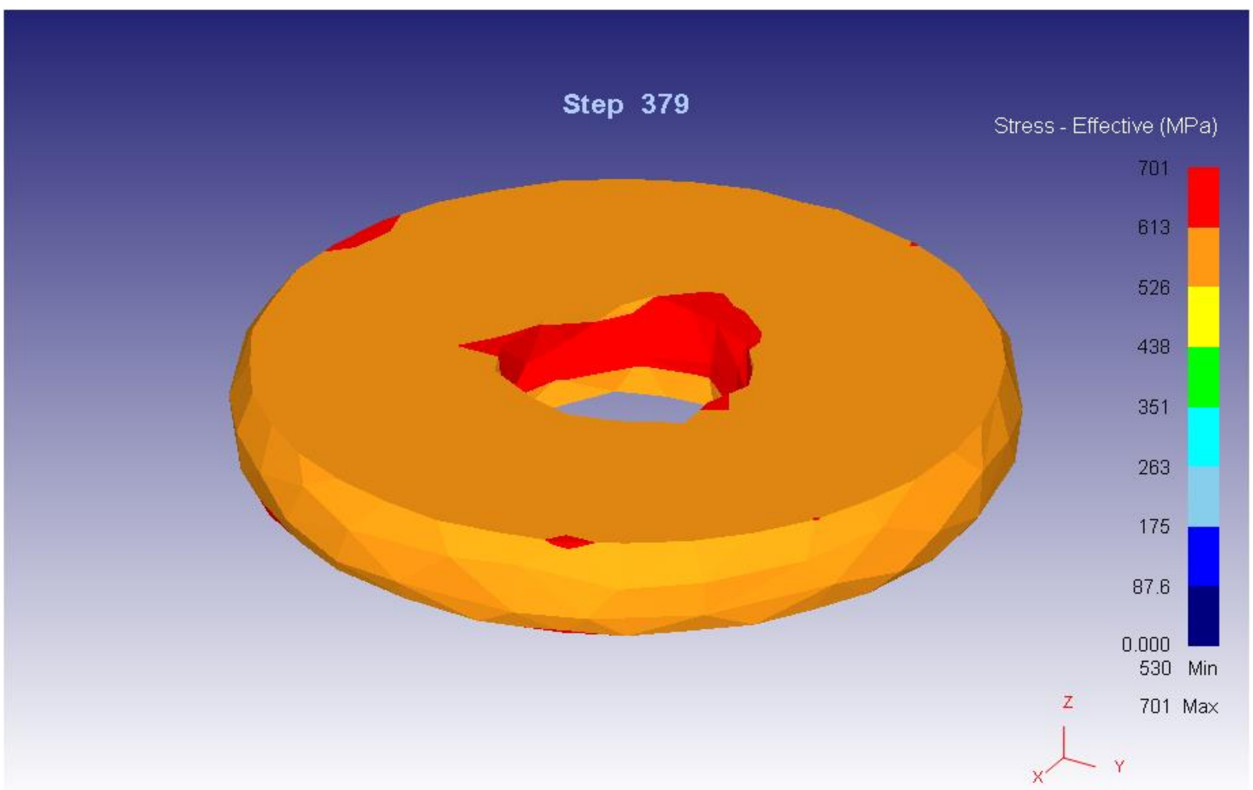
Step 379
Stress - Effective (MPa)
701
613
526
438
351
263
175
87.6
0.000
530 Min
701 Max
Z
X
Y

b) 2.5 μm

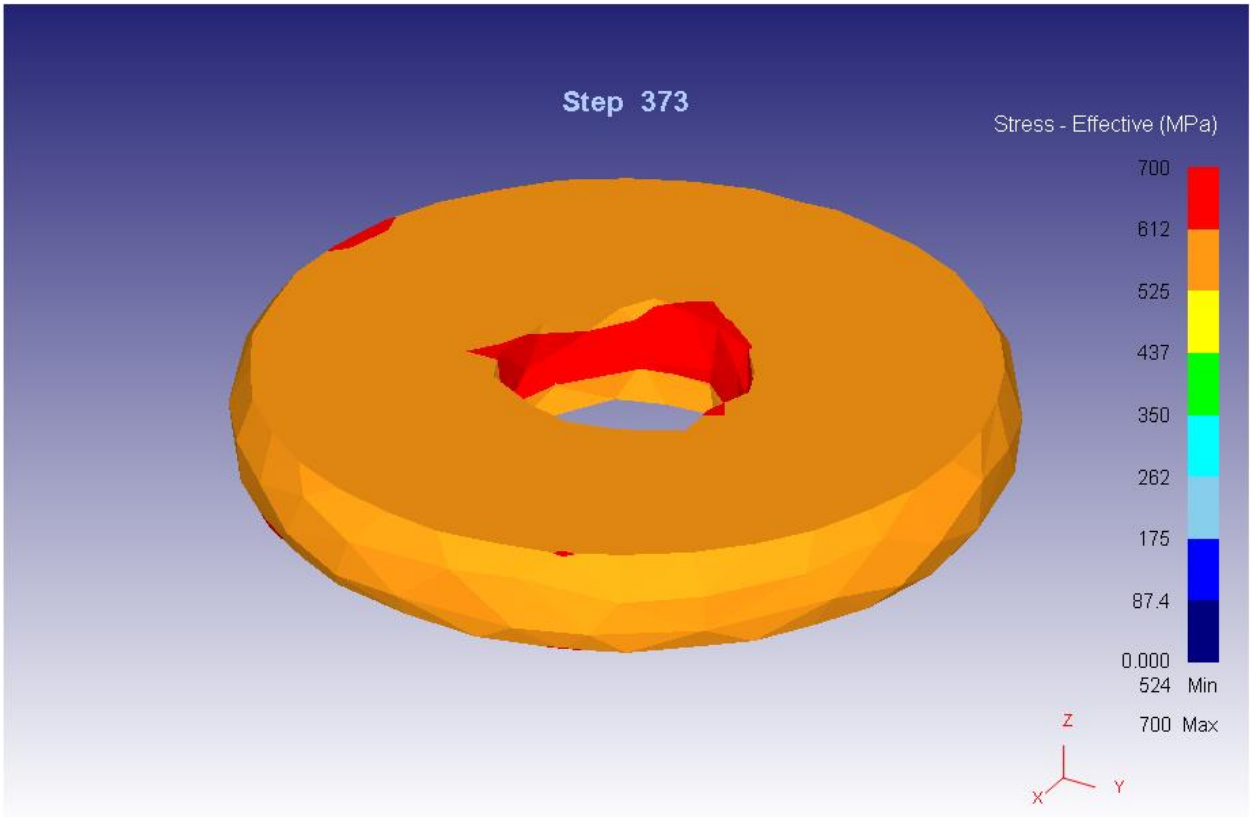

c) 3.5 µm

Figure 4. 16 FEM effective stress for various surface roughness

Figure 4.17 clearly shows that the effects of interface friction factor on effective stress by using finite element simulation for various lubricating conditions. In order to verify the relationship between effective stress and interface friction further with simulation, friction factor obtained at various lubricating conditions were used as in input for simulations. The effective stresses were continuously decreasing with increase in the friction factor for the selected lubricants.

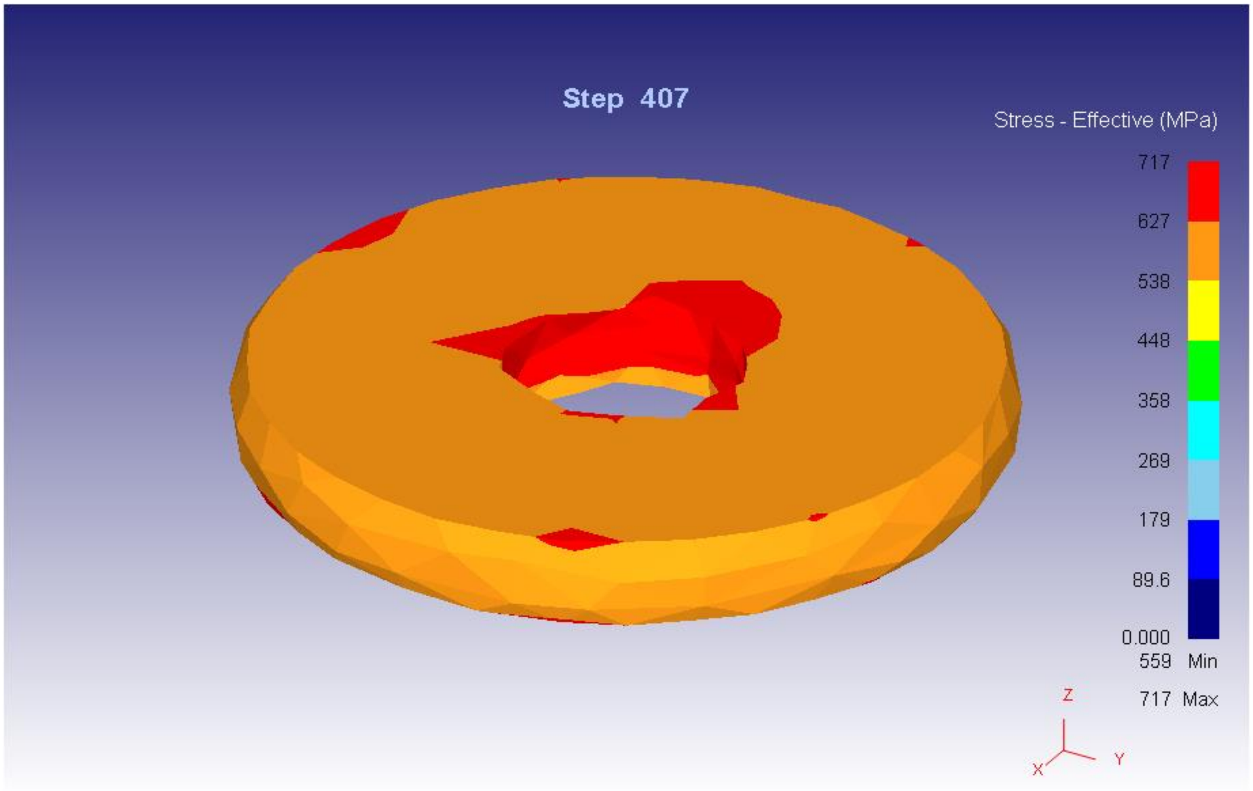

a) Palm oil

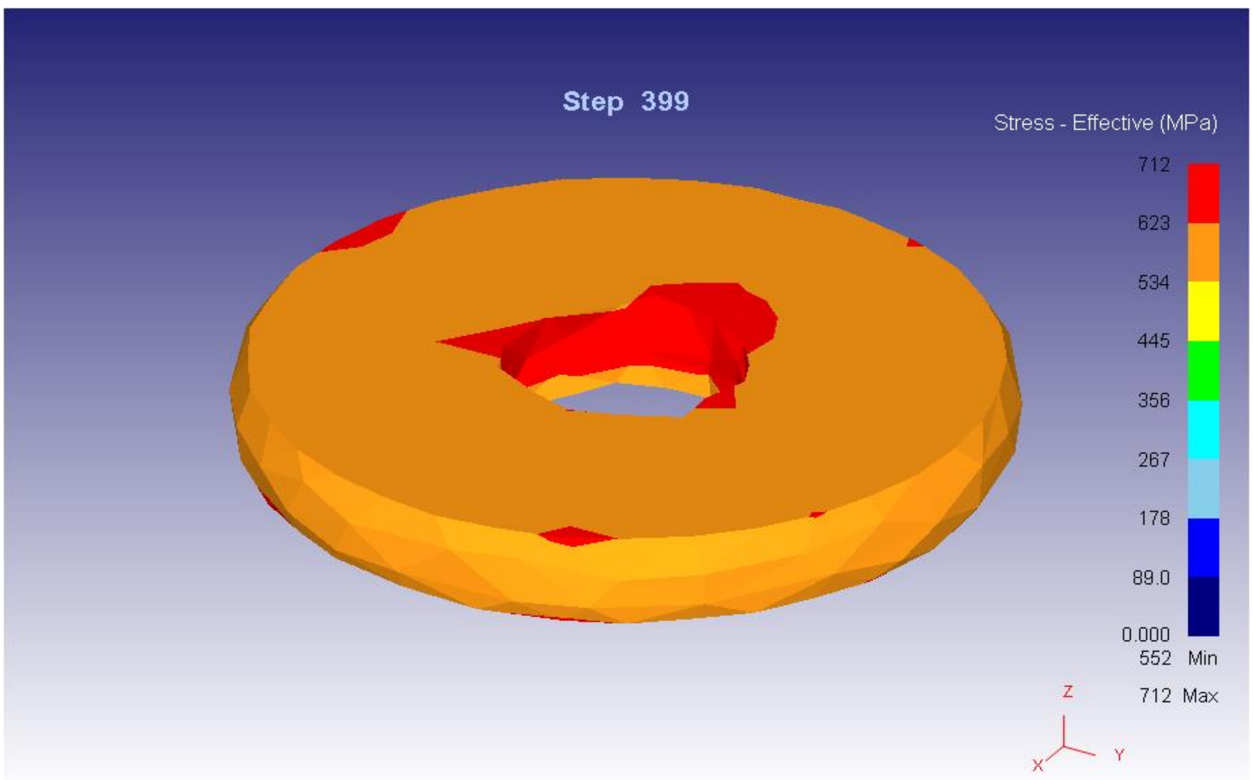

b) Grease

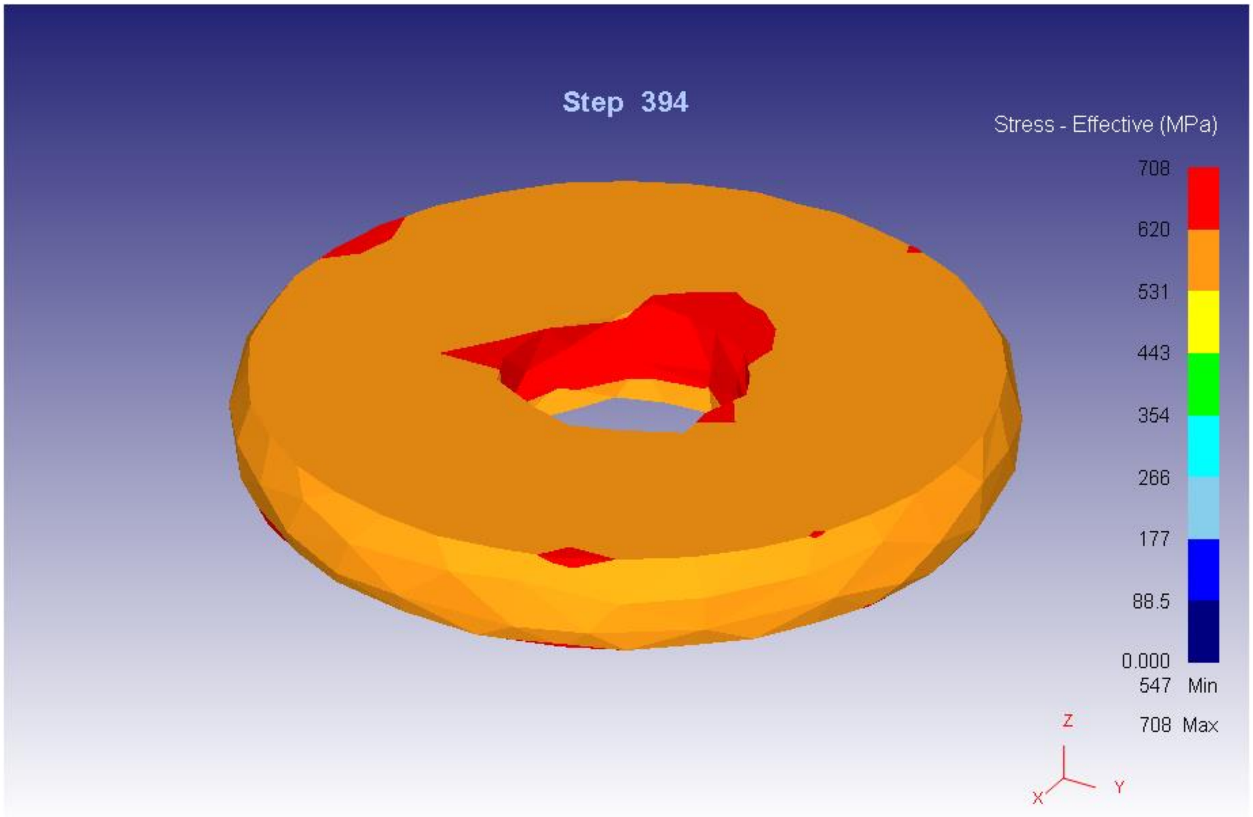

c) Emulsion oil

Figure 4. 17 FEM effective stress for various lubricating conditions

4.6 Validation of Simulation Results for Ring Compression Test

The specimen with ratio of standard ring compression test 6:3:2 has been taken for modeling as stated in the experimental procedure, and subsequently deformation test was carried out by using DEFORM 3D software. The simulation was carried out at different friction factor and height reductions that were obtained from ring compression experiment for various surface roughness and lubricating conditions. The effects of interface friction factor on effective strain and effective stress at various surface roughness and lubricating conditions can be validate by comparing the simulation results with that of the results found out by the ring compression experiments. From the general observation of ring compression test and finite element simulations, the obtained values from the experiment and simulations were more related to each other, as indicated in Table 4.3.

Table 4. 3 Comparison between ring compression test and finite element simulation results

Condition	Parameters			Ring compression test results		Finite element simulations	
		Friction factor	Height reduction (mm)	Effective strain	Effective stress (MPa)	Effective strain	Effective stress (MPa)
Surface roughness	1.5 µm	0.50	3.88	1.13	706.30	1.13	706
	2.5 µm	0.53	3.79	1.11	701.04	1.11	701
	3.5 µm	0.55	3.79	1.09	697.34	1.10	700
Lubricants	Palm oil	0.30	4.07	1.19	719.24	1.18	717
	Grease	0.35	3.99	1.16	711.64	1.16	712
	Emulsion oil	0.45	3.94	1.15	710.47	1.14	708

It is clear from the Table 4.3 that for all surface roughness and lubricants, the effect of friction factor on effective strain agrees well with simulation predictions at the final stage of the fracture detected where no large deformation happens. From Table 4.3, one can find out that the effective strain was increased as friction factor decrease for all experiment conditions and simulations. Looking back at Figures 4.6 and 4.14 that presented the relationship between friction factor and effective strain, a sharp increase in effective strain was observed for test conducted at the 0.50 friction factor, when smooth roughness used. The relationship between friction factor and effective strain for various lubricating conditions is presented in Figure 4.10 and Figure 4.15. Experimental results are agreed well with simulations.

An attempt was also made to correlate the ring compression test and finite element simulation under-prediction of effective stress with respect to interface friction factor. It can be seen from Table 4.3 that the effective stress was increased as friction factor decrease for all experiment conditions and simulations. Furthermore, Figure 4.7 and Figure 4.16 show a similar relationship between effective stress and friction factor under both experiment and simulations, when various roughness was used in the testing. Also, Figure 4.11 and Figure 4.17 show a similar relationship between effective stress and friction factor under both experiment and simulations, when various lubricating conditions was used in the testing.

Finally, using the above concepts, effects of various lubricant and surface roughness on interface friction, palm oil found to be suitable lubricant for successful forging AA 4032 alloy as it results in uniform and more metal flow between die-work pieces without fracture detected. Moreover, among the selected lubricants palm oil possess good lubrication with interface friction factor of 0.30. (Peterson, et al., 1998), correspondingly, justified that molybdenum disulphide act as a good lubricant with the friction factor value of 0.32 in which commercial aluminum has been used as base material. This reason has been verified from the current findings since viscosity of molybdenum disulphide is at least in comparison with other lubricant.

CHAPTER FIVE

CONCLUSIONS AND RECOMMENDATION

5.1 CONCLUSIONS

Based on the ring compression test and finite element simulation results on the frictional behavior of AA 4032 alloy under various surface roughness and lubricating conditions, the following conclusions have been drawn:

- Friction factor was increased with increasing the surface roughness of work piece, this was due to increase roughness (asperity peaks) on the work piece which restricts the metal flow at the die-work piece interfaces.
- It was observed that the contraction of inner diameter was increased with increase in the surface roughness, whereas, height reduction was decreased with increase in the roughness.
- The smoother surface roughness of work piece appear to be suitable roughness for dry condition, as it results in a more metal flow between die-work pieces.
- The inner diameters of ring specimen with various roughness were more contract than the inner diameter of ring specimen with various lubricating conditions. For various surface roughness and lubricating conditions, the reduction in height was increased with decreasing in the friction factor whereas, inner diameter expansion was increased with decreasing in the friction factor.
- Palm oil found to be a suitable lubricant for successful forging of AA 4032 alloy with smoother roughness, as results in a more metal flow between die-work pieces.
- Finite element simulation provided detailed and effective results in the analysis of effective strain and effective stress for various lubricating conditions and surface roughness, which were in a good agreement with the experimental results. Thus, integrating ring compression test with finite element simulation was simple and accurate tool to evaluate the friction behavior of AA 4032 alloy.

5.2 RECOMMENDATION

Moving beyond this study the potential exists for further investigation regarding the effect of various surface roughness and lubricating conditions on the interface friction factor. In this investigation all ring compression tests were completed using AA 4032 work pieces and H-13 tool steel dies. Because, only single die and work piece materials were investigated, it is recommended that additional ring materials and ring compression tests are performed with other die and work piece materials commonly used in cold forming processes. Possible alternatives to test specimen materials include aluminum alloy in the 1xxx, 2xxx, 3xxx, 5xxx, 6xxx, 7xxx series and carbon steels could be used. These additional compression tests will verify whether the relationships observed between various surface roughness and interface friction factor are applicable to the forming of alternative varieties of metals or alloys. In addition to, the use of alternative die and work piece materials, further investigation of the relationship between interface friction factor and work piece roughness is warranted. Presently, in this research a decrease in the friction factor was observed under dry test conditions when the work piece roughness's approximated at values of 1.5 μm. To verify this localized decrease in the friction factor observed was a result of work piece roughness conditions, ring compression tests should be repeated using ring test specimens having an alternative surface roughness than the 1.5 μm finish presently used. The use of a more abrasive finishing media, yielding an alternative average work piece roughness, may reveal whether this decrease in the friction factor noted at work piece roughness's is valid for other work piece finishes. The ability to control roughness by using emery paper grit size creates great opportunities to reduce interface friction for various lubricating conditions.

Another area of this study is recommended that all ring compression tests performed in this research were completed using hydraulic press machine (Toni Technik-2031 model). It was operated manually means that on each deformation load stage it was controlled by hand. In this research, a slight decrease in the deformation load was observed under ring compression test when compared with the finite element simulation results. The geometry dimensions of the ring was measured intermittently by stopping the hydraulic press machine on each deformation load level up to fracture detected. This could be performed with automatic hydraulic press machine, which is a more recommended for this kind of experiments to reduce measurement errors.

5.3 FUTURE WORK

This dissertation has provided an insight into investigation of friction behavior as well as corresponding experimental testing in metal forming area. From current study it was understood that further research could be undertaken in the following directions:

- One of the future further studies related to this research may be investigation of frictional behavior and selection of suitable lubricant for AA 4032 material at hot working conditions. In such a case, the effect of interface friction on metal forming process may be investigated by using both ring compression test and finite element simulations.
- Taking experimental results and frictional behavior into consideration and proposing a friction model that would give alternatives to the usual constant coefficient of friction, thus being possible having a more realistic and accurate model using updated and extended friction or lubrication data.
- Performing additional experiments on various material and lubricant characterization in order to obtain their frictional behavior.

References

Altan, T. & Boulger, F., 1973. Flow stress of metals and its applications in metal forming analysis. Journal of Engineering for Industry-Transactions of the American Society of Mechanical Engineers, Volume 95, pp. 1009-1019.

Altan, T., Oh, S. & Gegel, H., 1986. Metal forming, fundamentals and applications. ASM, Metals Park, pp. 131-141.

Avitzur, B., 1968. Metal forming, processes and analysis. New York: McGraw-Hill..

Babu Rao, J., Kamaluddin, S. & Bhargava, N., 2009. Finite element analysis of deformation behavior of aluminum-copper alloys. Materials and Design, 30(4), pp. 1298 -1309.

Bay, N., 1987. Friction stress and normal stress in bulk metal forming processes. Journal of Materials Production Technology, Volume 14, pp. 203 - 223.

Bay, N., 1994. The state of the art in cold forging lubrication. Journal of Material Process and Technology, Volume 46, p. 19.

Becker, P., Jeon, H. J. & Chang, C. C., 2003. A geometric approach to modeling friction in metal forming. CIRP Annals - Manufacturing Technology, 52(1), pp. 209-212.

Behrens, B., Doege, E. & Daehndel, H., 2007. Precision forging processes for high-duty automotive components. Journal of Material Process and Technology, Volume 185, p. 139 – 146.

Bonab, B., Sadeghi, M., Halimi, K. & Amiri, A., 2015. A study on hot working and frictional behavior of 6082 aluminum alloy during hot forming. Transactions of Famena , Issue 1333-1124.

Camachoa, A., Torralvoa, A., Bernala, C. & Sevillab, L., 2013. Investigations on friction factors in metal forming of industrial alloys. Manufacturing Engineering Society International, p. 564 – 572.

Cisson, M., Rausina, G. & Stonebraker, P., 1996. Human health and environmental hazard characterization of lubricating oil additives. Lubrication Science, Volume 8, p. 145 –177.

DePierrie, V. & Gurney, F., 1974. A method for determination of constant and varying friction factors during ring compression tests. Journal of Lubrication Technology, Volume 96, pp. 482-488.

Diehl, S., 2015. H-13 Air hardening tool steel. International Journal of Machine Tools and Manufacture, pp. 1637-1649..

Douglas, J. R. & Altan, T., 1975. Flow stress determination for metals at forging rates and temperatures. Journal of Engineering for Industry, pp. 66-76.

Dutton, R. E., Seetharaman, V. & Goetz, R. L., 1999. Effect of flow softening on ring test calibration curves. Materials Science and Engineering, 270(2), pp. 249-253.

Equbal, M., Alam, P., Ohdar, R. & Serfraj, A., 2016. Lubrication behavior of 35C8 steel using ring compression test and finite element simulation. International Journal of Mechanical And Production Engineering, 4(11), pp. 292-323.

Fereshteh-Saniee, F. & Fatehi-Sichani, F., 2006. An investigation on determination of flow curves at room temperature and under forming conditions. Journal of Materials Processing Technology, Volume 177, p. 478–482.

Fereshteh-Saniee, F., Pillinger, I. & Hartley, P., 2004. Friction modeling for the physical simulation of the bulk metal forming processes. Journal of Material Processing Technology, Volume 153, pp. 151-156..

Forcellese, A., Gabdellp, F., Barceilona, A. & Micafi, F., 1994. Evaluation of friction in cold metal forming. Journal of Materials Process Technology, Volume 45, pp. 619-624.

Fricker, D. C. & Wanheim, T., 1974. Low friction coefficient estimation for model material experiments. Journal of Materials Processing Technology, Volume 27, pp. 303-317.

Hartley, R. S., Cloete, T. & Nurick, G., 2007. An experimental assessment of friction effects in the split Hopkinson pressure bar using the ring compression test. International Journal of Impact Engineering, 34 (10), pp. 1705-1728.

Henning, H., 2007. Aluminum forging an overview, Forging. Industrial Tribology, 18(4), pp. 20-24.

Hill, R., 1985. The mathematical theory of plasticity. International Journal of. Mech. Sci., Volume 35, p. 19.

Hu, Z. & Dean, T., 2000. A study of surface topography, friction and lubricants in metal forming. International Journal of Machine Tools and Manufacture, pp. 1637-1649.

Isogawa, S., Kimura, A. & Tozawa, Y., 1992. Method for evaluating lubricants. CIRP Annals - Manufacturing Technology, Volume 41, pp. 263-266.

Kalpakjian, S. & Schmid, S., 2001. tribology, friction, wear and lubrication. Manufacturing engineering and technology, Volume 32, p. 884.

Kevorkijan, V., 2001. Production technology and use of aluminum drop forging components. Journal of Materials Processing Technology, Volume 35, p. 19.

Kobayashi, S., 1970. Deformation Characteristics and Ductile Fracture of 1040 Steel in Simple Upsetting of Solid Cylinders and Rings. Journal of Engineering for Industry-Transactions of the American Society of Mechanical Engineers, Volume 92, pp. 391-399.

Kochumman, L. & Sarathchandradas, M., 2014. Friction calibration in die metallic interface and stress analysis of steel AISI 1010 employing ring compression test under specified lubrication. International Journal of Scientific and Engineering Research, 5(6), p. 784.

Kudo, H. & Aoi, K., 1967. Effect of Compression Test Condition upon fracturing of a medium carbon steel-Study on Cold Forge ability Test. Journal of the Japan Society of Technical Plasticity, Volume 8, pp. 17-27.

Li, Y., Onodera, E. & Chiba, A., 2010. Friction coefficient in hot compression of cylindrical sample. Materials Transactions, 51(7), pp. 1210-1215.

Male, A. & Cockcroft, M., 1965. A method for the determination of the coefficient of friction of metals under condition of bulk plastic deformation. Journal of the Institute of Metals, Volume 93, p. 38 – 46..

Menezes, P., Kishore, K. & V.K., S., 2006. Influence of friction during forming processes using numerical simulation technique. Industrial Tribology, p. 560.

Menezes, P., Kishore, S. & Kailas, V., 2006. Influence of surface texture on coefficient of friction and transfer layer formation during sliding of pure magnesium pin on M40 steel plate. Wear, Volume 261, pp. 578-591.

Mondolfo, L., 1976. Aluminum alloys structures and properties. London: s.n.

Narayanasamy, R. & Pandey, K., 1997. Phenomenon of barreling in aluminum solid cylinders during cold upset-forming. Journal of Materials Processing Technology, Volume 70, pp. 17-21.

Narayanasamy, R., Ramesh, T. & Pandey, K., 2007. An experimental investigation on strain hardening behavior of aluminum under various stress states during cold upset forming. Materials and Design, 28(4), pp. 1211-1223.

Ohio, C., 2016. DEFORM v11.1 system documentation. Scientific Forming Technologies Corporation, p. 378.

Oh, S., Wu, W., Tang, J. & Vedhanayagam, A., 1991. Capabilities and application of FEM code DEFORM, the perspective of the Developer. Journal of Materials Processing Technology, Volume 27, pp. 25-42.

Peterson, M. B. & Ling, F. F., 1966. Friction and Lubrication at Extreme Pressures, Symposium on Friction and Lubrication in Metal Processing. American Society of Mechanical Engineers, p. 39.

Peterson, S., Martins, P. & Bay, N., 1998. An alternative ring-test geometry for the evaluation of friction under low normal pressure. Journal of Materials Processing Technology, 79(1), pp. 14-24.

Rahul, T., Manoj, G. & Prabhash, J., 2012. Development of new design of specimens for friction determination in metal forming. Journal of Mechanical and Civil Engineering, 3(5), pp. 21-26.

Rajesh, E. & Siva-Prakash, M., 2013. Analysis of Friction Factor by Employing the Ring Compression Test Under Different Lubricants. International Journal of Scientific and Engineering Research, Volume 4(5), p. 1163 – 1171.

Rao, K., Prasad, Y. & Hawbolt, E., 1998. Study of fractional softening in multi-stage hot deformation. Journal of Materials Processing Technology, Volume 77, p. 166 –174.

Rasp, W. & Wichern, C. M., 2002. Effects of surface-topography directionality and lubrication condition on frictional behavior during plastic deformation. Journal of Materials Processing Technology, Volume 3, p. 379.

Robinson, T., Ou, H. & Armstrong, C., 2004. Study on ring compression test using physical modelling and FE simulation. Journal of Materials Processing Technology, p. 54–59.

Ryo, M. & Kozo, O., 2004. Measurement of friction in cold upsetting with mist lubrication. Materials Transactions, 45(9), p. 2891– 2896.

Sahin, M., Cetinarslan, C. & Akata, H., 2007. Effect of surface roughness on friction coefficient during upsetting processes for different materials. Materials and design, Volume 28, p. 633–640..

Sahin, M., Cetinarslan, C. S. & Akata, H. E., 2007. Effect of surface roughness on friction coefficients during upsetting processes for different materials and design. Journal of Materials Processing Technology, 8(2), pp. 633-640..

Schey, J., 1983. Tribology in metalworking: friction, lubrication and wear. American Society for Metals, p. 443.

Schey, J. A., Venner, T. R. & Takomana, S. L., 1982. The effect of friction on pressure in upsetting at low diameter-to-height ratios. Journal of Mechanical Working Technology, 6(1), pp. 22-33.

Schroeder, W. & Webster, D. A., 1949. Press-forging thin sections: effect of friction, area and thickness on pressures required. Journal of Applied Mechanics, Volume 16, p. 289.

Semiatin, S., 1998. Introduction to Forming and Forging Processes. 9th Edition ed. USA: ASM Handbook Committee.

Shahriari, D., Sadeghi, M., Ebrahimi, G. & Kim, K., 2011. Effects of Lubricant and Temperature on Friction Coefficient During Hot Forging of Nimonic 115 Superalloy. Journal of Material Engineering and Performance, Volume 49, p. 375 –383.

Sofuoglu, H. & Rasty, J., 1999. On the measurement of friction coefficient utilizing the ring compression test. Tribology International, Volume 32, pp. 327-335.

Stahlmann, J., Nicodemus, E. R. & Sharma, S. C., 2012. Surface roughness evolution in FEA simulations of bulk metal forming process. Wear, Volume 288, pp. 78-87.

Stake, E. & Staley, J., 1996. Application of modern aluminum alloys to automotive and aircraft. Progress in Aerospace Sciences, Volume 32, p. 131–172.

Tamrakar, R. & Mittal, N., 2013. Finite element analysis of pistons made of steel and AA4032. Journal of Materials and Metallurgical Engineering, 3(2).

Tan, X., Martins, P., Bay, N. & Zhang, W., 1998. Friction studies at different normal pressures with alternative ring compression tests. Journal of Materials Processing Technology, 80(81), pp. 292-297.

Wagoner, R. & Chenot, J., 1996. Friction in fundamentals of metal forming. p. 313 – 338.

Wanheim, T., Bay, N. & Petersen, A., 1974. A theoretically determined model for friction in metal working processes. Volume 28, pp. 251- 258..

Wiklund, D., Rosen, B. & Gunnarsson, L., 2008. Frictional mechanisms in mixed lubricated regime in steel metal forming. Wear, Volume 264, p. 474 – 479.

Wogaso, D., Davidson, M. & Khanra, A., 2014. Friction Factor Evaluation Using Experimental and Finite Element Methods for Al-4%Cu Preforms. Journal of Materials Engineering and Performance, Volume 23(8), p. 3068.

Yoshimura, H. & Tanaka, K., 2000. Precision forging of aluminum and steel. Journal of Materials Processing Technology, Volume 98, pp. 196-204.

Zienkiewicz, O., 1971. The finite element method in Engineering Sciences. New York: McGraw Hill.

APPENDIX I

Experimental Data Recorded of Ring Compression Test for AA 4032 at Various Surface Roughness and Lubricating Conditions

The experimental data recorded before and after the compression test for the different specimen surface roughness and lubricating conditions are given in Table A and Table B, respectively. Tests were performed with 50 KN deformation load increment up to fracture detected for each AA 4032 ring specimen. For each load deformation, changes in ring geometry measurements were measured and recorded. Due to the non-homogeneous flow of metal during deformation, ring geometry were not perfect circle. Then, three measurements in different radial directions were carried out and their average was recorded. Compression tests were repeated at least three times to obtain reliable results for each parameters. Also, the measurement of surface roughness was carried out using the surface roughness tester (SRT-6210 type) instrument. In Table C all measured parameters of the different surfaces involved in this work. Tables contain results of measures taken before tests.

Table A_1: Experimental data recorded before and after ring compression test for surface roughness 1.5 µm at dry condition

Trial #1									
Load (KN)			0.00	50.00	100.00	150.00	200.00	250.00	328.00
OD	Measurements	#1	24.05	24.18	24.43	25.00	25.94	27.54	30.54
		#2	23.99	24.12	24.38	24.98	25.88	27.48	30.43
		#3	24.03	24.15	24.36	24.90	25.84	27.41	30.40
	Average		24.02	24.15	24.39	24.96	25.89	27.48	30.46
ID	Measurements	#1	12.01	12.01	11.92	11.77	11.42	10.60	9.57
		#2	12.00	11.99	11.87	11.69	11.22	10.51	9.48
		#3	12.03	12.00	11.90	11.75	11.20	10.46	9.53
	Average		12.01	12.00	11.90	11.74	11.28	10.52	9.53
H	Measurements	#1	8.01	7.84	7.60	7.08	6.34	5.32	4.10
		#2	7.97	7.89	7.64	7.15	6.39	5.38	4.14
		#3	8.02	7.92	7.67	7.18	6.40	5.42	4.17
	Average		8.00	7.88	7.64	7.14	6.38	5.37	4.14

Trial #2									
Load (KN)			0.00	50.00	100.00	150.00	200.00	250.00	331.00
OD	Measurements	#1	24.00	24.16	24.41	25.03	25.96	27.55	30.67
		#2	24.01	24.18	24.38	24.95	25.91	27.54	30.58
		#3	24.00	24.16	24.45	24.98	25.89	27.50	30.60
	Average		24.00	24.17	24.41	24.99	25.92	27.53	30.62
ID	Measurements	#1	12.01	11.98	11.94	11.80	11.25	10.55	9.57
		#2	12.01	12.00	11.85	11.71	11.35	10.63	9.85
		#3	12.01	11.98	11.86	11.64	11.28	10.56	9.89
	Average		12.01	11.99	11.88	11.72	11.29	10.58	9.77
H	Measurements	#1	8.00	7.86	7.61	7.11	6.36	5.36	4.11
		#2	8.00	7.87	7.63	7.11	6.37	5.38	4.14
		#3	8.02	7.83	7.58	7.08	6.33	5.32	4.07
	Average		8.01	7.85	7.61	7.10	6.35	5.35	4.11
Trial #3									
Load (KN)			0.00	50.00	100.00	150.00	200.00	250.00	328.00
OD	Measurements	#1	24.03	24.15	24.42	24.87	25.88	27.55	30.48
		#2	24.00	24.12	24.39	24.98	25.90	27.46	30.42
		#3	24.02	24.14	24.35	25.06	25.93	27.60	30.54
	Average		24.02	24.14	24.39	24.97	25.90	27.54	30.48
ID	Measurements	#1	12.01	11.99	11.94	11.81	11.45	10.86	9.82
		#2	12.02	12.02	11.86	11.74	11.34	10.76	9.77
		#3	12.03	12.01	11.96	11.77	11.40	10.70	9.68
	Average		12.02	12.01	11.92	11.77	11.40	10.77	9.76
H	Measurements	#1	8.01	7.91	7.66	7.16	6.41	5.40	4.16
		#2	8.04	7.89	7.65	7.12	6.38	5.38	4.14
		#3	8.02	7.93	7.68	7.18	6.44	5.42	4.18
	Average		8.02	7.91	7.66	7.15	6.41	5.40	4.16

Table A_2: Experimental data recorded before and after ring compression test for surface roughness 2.5 µm at dry condition

Trial #1									
Load (KN)			0.00	50.00	100.00	150.00	200.00	250.00	327.00
OD	Measurements	#1	24.03	24.15	24.42	24.98	25.89	27.45	30.38
		#2	24.01	24.10	24.37	24.92	25.80	27.42	30.30
		#3	24.03	24.16	24.35	24.88	25.78	27.38	30.29
	Average		24.02	24.14	24.38	24.93	25.82	27.42	30.32
ID	Measurements	#1	12.01	11.98	11.90	11.73	11.27	10.66	9.78
		#2	12.06	12.03	11.94	11.79	11.38	10.78	9.62
		#3	12.04	12.03	11.92	11.67	11.22	10.55	9.65
	Average		12.04	12.01	11.92	11.73	11.29	10.66	9.68
H	Measurements	#1	8.00	7.92	7.68	7.18	6.47	5.50	4.25
		#2	8.01	7.93	7.68	7.19	6.40	5.41	4.17
		#3	8.02	7.89	7.64	7.14	6.42	5.40	4.18
	Average		8.01	7.91	7.67	7.17	6.43	5.44	4.20
Trial #2									
Load (KN)			0.00	50.00	100.00	150.00	200.00	250.00	330.00
OD	Measurements	#1	24.04	24.13	24.36	24.96	25.84	27.38	30.12
		#2	24.01	24.10	24.34	24.84	25.77	27.35	30.09
		#3	23.98	24.11	24.29	24.87	25.75	27.34	30.06
	Average		24.01	24.11	24.33	24.89	25.79	27.36	30.09
ID	Measurements	#1	12.05	12.00	11.87	11.71	11.25	10.45	9.04
		#2	12.02	11.96	11.84	11.64	11.16	10.47	9.02
		#3	12.03	11.99	11.89	11.73	11.30	10.65	9.15
	Average		12.03	11.98	11.87	11.69	11.24	10.52	9.07
H	Measurements	#1	8.03	7.94	7.70	7.20	6.44	5.45	4.19
		#2	8.01	7.91	7.67	7.19	6.41	5.43	4.18
		#3	8.01	7.86	7.64	7.11	6.42	5.40	4.24
	Average		8.02	7.90	7.67	7.17	6.42	5.43	4.20
Trial #3									
Load (KN)			0.00	50.00	100.00	150.00	200.00	250.00	326.00

OD	Measurements	#1	24.04	24.17	24.38	24.95	25.86	27.38	30.28
		#2	24.02	24.12	24.34	24.85	25.81	27.33	30.22
		#3	24.03	24.11	24.38	24.90	25.74	27.34	30.16
	Average		24.03	24.13	24.37	24.90	25.80	27.35	30.22
ID	Measurements	#1	12.01	12.03	11.92	11.69	11.19	10.50	9.78
		#2	12.03	11.98	11.89	11.64	11.25	10.62	9.69
		#3	12.04	12.00	11.88	11.70	11.32	10.65	9.65
	Average		12.03	12.00	11.90	11.68	11.25	10.59	9.71
H	Measurements	#1	8.02	7.96	7.71	7.22	6.46	5.48	4.27
		#2	8.00	7.93	7.68	7.18	6.43	5.44	4.20
		#3	8.01	7.90	7.67	7.16	6.45	5.48	4.26
	Average		8.01	7.93	7.69	7.19	6.45	5.47	4.24

Table A_3: Experimental data recorded before and after ring compression test for surface roughness 3.5 µm at dry condition

Trial #1									
Load (KN)			0.00	50.00	100.00	150.00	200.00	250.00	326.00
OD	Measurements	#1	24.04	24.14	24.35	24.82	25.75	27.25	30.10
		#2	24.00	24.10	24.30	24.78	25.67	27.19	29.99
		#3	24.02	24.11	24.34	24.88	25.72	27.21	30.00
	Average		24.02	24.12	24.33	24.83	25.71	27.22	30.03
ID	Measurements	#1	12.05	12.01	11.91	11.78	11.33	10.42	9.27
		#2	12.04	11.98	11.88	11.64	11.24	10.59	9.66
		#3	12.06	12.00	11.87	11.53	11.16	10.38	9.52
	Average		12.05	12.00	11.89	11.65	11.24	10.46	9.48
H	Measurements	#1	8.01	7.92	7.70	7.26	6.52	5.55	4.32
		#2	8.02	7.95	7.71	7.21	6.49	5.51	4.27
		#3	8.01	7.93	7.70	7.20	6.47	5.44	4.24
	Average		8.01	7.93	7.70	7.22	6.49	5.50	4.28
Trial #2									
Load (KN)			0.00	50.00	100.00	150.00	200.00	250.00	325.00

OD	Measurements	#1	24.04	24.10	24.39	24.90	25.84	27.40	30.10
		#2	24.08	24.17	24.32	24.90	25.75	27.33	30.00
		#3	24.03	24.11	24.36	24.90	25.81	27.36	30.05
	Average		24.05	24.13	24.36	24.90	25.80	27.36	30.05
ID	Measurements	#1	12.02	11.98	11.85	11.68	11.32	10.82	9.25
		#2	12.00	11.97	11.87	11.74	11.27	10.75	9.12
		#3	12.03	11.98	11.89	11.66	11.20	10.53	9.15
	Average		12.02	11.98	11.87	11.69	11.26	10.70	9.17
H	Measurements	#1	8.03	7.96	7.72	7.25	6.50	5.52	4.28
		#2	8.01	7.93	7.69	7.19	6.46	5.48	4.25
		#3	8.00	7.95	7.71	7.20	6.45	5.49	4.24
	Average		8.01	7.95	7.71	7.21	6.47	5.50	4.26
Trial #3									
Load (KN)			0.00	50.00	100.00	150.00	200.00	250.00	327.00
OD	Measurements	#1	24.04	24.12	24.36	24.88	25.76	27.22	29.97
		#2	24.05	24.16	24.30	24.85	25.66	27.18	29.90
		#3	24.02	24.11	24.34	24.82	25.68	27.20	29.88
	Average		24.04	24.13	24.33	24.85	25.70	27.20	29.92
ID	Measurements	#1	12.03	11.99	11.84	11.60	11.11	10.37	9.37
		#2	12.04	12.00	11.86	11.65	11.17	10.40	9.32
		#3	12.03	11.96	11.90	11.74	11.24	10.49	9.16
	Average		12.03	11.98	11.87	11.66	11.17	10.42	9.28
H	Measurements	#1	8.01	7.90	7.69	7.20	6.49	5.52	4.30
		#2	8.03	7.95	7.72	7.23	6.52	5.47	4.26
		#3	8.00	7.94	7.71	7.24	6.47	5.54	4.34
	Average		8.01	7.93	7.71	7.22	6.49	5.51	4.30

Table B_1: Experimental data recorded before and after ring compression test for palm oil

Trial #1									
Load (KN)			0.00	50.00	100.00	150.00	200.00	250.00	335.00
OD	Measurements	#1	24.00	24.21	24.57	25.28	26.36	28.11	31.56

		#2	24.00	24.20	24.52	25.22	26.31	28.09	31.49
		#3	24.03	24.18	24.52	25.18	26.28	28.06	31.40
	Average		24.01	24.20	24.54	25.23	26.32	28.09	31.48
ID	Measurements	#1	12.02	12.02	12.01	12.00	11.84	11.32	10.64
		#2	12.02	12.01	12.03	12.03	11.80	11.25	10.62
		#3	12.02	12.04	12.08	11.96	11.73	11.31	10.45
	Average		12.02	12.02	12.04	12.00	11.79	11.29	10.57
H	Measurements	#1	8.00	7.85	7.60	7.09	6.29	5.27	3.98
		#2	8.01	7.85	7.55	7.00	6.25	5.23	3.94
		#3	8.01	7.84	7.55	6.98	6.21	5.19	3.88
	Average		8.01	7.85	7.57	7.02	6.25	5.23	3.93
Trial #2									
Load (KN)			0.00	50.00	100.00	150.00	200.00	250.00	337.00
OD	Measurements	#1	24.01	24.22	24.58	25.20	26.35	28.21	31.61
		#2	24.01	24.24	24.52	25.18	26.31	28.13	31.56
		#3	24.04	24.24	24.55	25.17	26.28	28.14	31.51
	Average		24.02	24.23	24.55	25.18	26.31	28.16	31.56
ID	Measurements	#1	12.03	12.00	11.98	11.90	11.73	11.23	10.46
		#2	12.03	12.03	12.01	11.95	11.75	11.16	10.57
		#3	12.03	12.04	12.02	11.92	11.77	11.38	10.44
	Average		12.03	12.02	12.00	11.92	11.75	11.26	10.49
H	Measurements	#1	7.99	7.80	7.54	7.03	6.25	5.18	4.01
		#2	8.03	7.84	7.56	7.08	6.25	5.20	3.96
		#3	8.01	7.78	7.50	6.96	6.20	5.18	3.92
	Average		8.01	7.81	7.53	7.02	6.23	5.19	3.96
Trial #3									
Load (KN)			0.00	50.00	100.00	150.00	200.00	250.00	334.00
OD	Measurements	#1	24.01	24.22	24.58	25.22	26.38	28.18	31.47
		#2	24.02	24.16	24.47	25.18	26.21	28.08	31.39
		#3	24.03	24.22	24.56	25.22	26.30	28.14	31.45

	Average		24.02	24.20	24.54	25.21	26.30	28.13	31.44
ID	Measurements	#1	12.00	12.00	11.98	11.92	11.64	11.12	10.38
		#2	12.03	12.01	11.98	11.87	11.68	11.23	10.21
		#3	12.01	12.01	12.00	11.94	11.71	11.30	10.34
	Average		12.01	12.01	11.99	11.91	11.68	11.22	10.31
H	Measurements	#1	8.01	7.87	7.59	7.09	6.27	5.22	3.96
		#2	8.02	7.86	7.56	7.02	6.22	5.18	3.92
		#3	8.00	7.82	7.53	6.96	6.24	5.22	3.91
	Average		8.01	7.85	7.56	7.02	6.24	5.21	3.93

Table B_2: Experimental data recorded before and after ring compression test for grease

Trial #1									
Load (KN)			0.00	50.00	100.00	150.00	200.00	250.00	334.00
OD	Measurements	#1	24.00	24.20	24.48	25.10	26.18	27.96	31.21
		#2	24.00	24.14	24.46	25.08	26.11	27.90	31.12
		#3	24.03	24.18	24.48	25.14	26.15	27.95	31.15
	Average		24.01	24.17	24.47	25.11	26.15	27.94	31.16
ID	Measurements	#1	12.01	11.98	11.90	11.81	11.52	11.15	10.57
		#2	12.02	11.96	11.87	11.77	11.38	11.25	10.65
		#3	11.97	11.98	11.96	11.89	11.68	11.11	10.63
	Average		12.00	11.97	11.91	11.82	11.53	11.17	10.62
H	Measurements	#1	8.00	7.84	7.56	7.01	6.25	5.28	4.08
		#2	8.01	7.88	7.60	7.10	6.30	5.31	4.05
		#3	8.02	7.85	7.58	7.08	6.32	5.26	3.98
	Average		8.01	7.86	7.58	7.06	6.29	5.28	4.04
Trial #2									
Load (KN)			0.00	50.00	100.00	150.00	200.00	250.00	331.00
OD	Measurements	#1	24.04	24.22	24.55	25.18	26.31	27.92	31.19
		#2	24.00	24.18	24.48	25.07	26.19	27.82	31.08
		#3	24.02	24.20	24.45	25.15	26.26	27.87	31.16
	Average		24.02	24.20	24.49	25.13	26.25	27.87	31.14

ID	Measurements	#1	11.99	11.98	11.94	11.90	11.78	11.06	10.14
		#2	12.03	12.03	11.98	11.92	11.84	11.13	10.48
		#3	12.01	11.98	11.98	11.89	11.80	10.94	10.42
	Average		12.01	12.00	11.97	11.90	11.81	11.04	10.35
H	Measurements	#1	8.03	7.85	7.58	7.05	6.28	5.27	4.01
		#2	7.99	7.83	7.58	7.06	6.30	5.32	4.00
		#3	8.01	7.86	7.60	7.11	6.33	5.29	4.04
	Average		8.01	7.85	7.59	7.07	6.30	5.29	4.02
Trial #3									
Load (KN)			0.00	50.00	100.00	150.00	200.00	250.00	330.00
OD	Measurements	#1	24.04	24.26	24.56	25.24	26.20	28.00	31.22
		#2	24.02	24.20	24.49	25.12	26.11	27.90	31.13
		#3	24.01	24.18	24.52	25.18	26.15	27.96	31.17
	Average		24.02	24.21	24.52	25.18	26.15	27.95	31.17
ID	Measurements	#1	12.00	11.98	11.97	11.89	11.54	11.15	10.23
		#2	12.01	12.00	11.96	11.95	11.48	11.10	10.54
		#3	12.00	11.99	11.94	11.90	11.59	11.00	10.05
	Average		12.00	11.99	11.96	11.91	11.54	11.08	10.27
H	Measurements	#1	8.04	7.82	7.57	7.07	6.32	5.24	4.05
		#2	8.00	7.86	7.59	7.09	6.30	5.31	4.01
		#3	8.00	7.85	7.55	7.00	6.28	5.26	3.96
	Average		8.01	7.84	7.57	7.05	6.30	5.27	4.01

Table B_3: Experimental data recorded before and after ring compression test for emulsion oil

Trial #1									
Load (KN)			0.00	50.00	100.00	150.00	200.00	250.00	332.00
OD	Measurements	#1	24.02	24.22	24.48	25.09	26.14	27.79	30.91
		#2	24.01	24.16	24.44	25.08	26.01	27.77	30.82
		#3	24.02	24.18	24.45	24.98	26.00	27.75	30.82
	Average		24.02	24.19	24.46	25.05	26.05	27.77	30.85
ID	Measurements	#1	12.00	11.98	11.94	11.81	11.40	10.78	9.94

		#2	12.01	12.01	11.84	11.73	11.36	10.70	9.77
		#3	12.00	11.99	11.89	11.75	11.40	10.76	10.16
	Average		12.00	11.99	11.89	11.76	11.39	10.75	9.96
H	Measurements	#1	8.01	7.86	7.61	7.10	6.33	5.23	4.01
		#2	8.00	7.84	7.58	7.09	6.29	5.32	4.10
		#3	8.01	7.86	7.56	7.06	6.31	5.30	4.08
	Average		8.01	7.85	7.58	7.08	6.31	5.28	4.06
Trial #2									
Load (KN)			0.00	50.00	100.00	150.00	200.00	250.00	329.00
OD	Measurements	#1	24.01	24.20	24.44	25.16	26.05	27.65	30.74
		#2	23.99	24.14	24.39	25.00	25.98	27.60	30.69
		#3	24.01	24.12	24.40	25.02	25.95	27.55	30.65
	Average		24.00	24.15	24.41	25.06	25.99	27.60	30.69
ID	Measurements	#1	12.02	12.02	11.92	11.85	11.52	10.75	10.00
		#2	12.01	11.98	11.95	11.83	11.34	10.71	9.78
		#3	12.03	12.01	11.88	11.76	11.37	10.68	9.98
	Average		12.02	12.00	11.92	11.81	11.41	10.71	9.92
H	Measurements	#1	8.00	7.88	7.62	7.07	6.35	5.38	4.08
		#2	8.05	7.86	7.62	7.10	6.34	5.30	4.10
		#3	8.01	7.90	7.64	7.09	6.35	5.37	4.13
	Average		8.02	7.88	7.63	7.09	6.35	5.35	4.10
Trial #3									
Load (KN)			0.00	50.00	100.00	150.00	200.00	250.00	330.00
OD	Measurements	#1	24.02	24.15	24.37	24.98	25.90	27.75	30.91
		#2	24.01	24.16	24.42	25.02	25.98	27.71	30.92
		#3	24.03	24.18	24.45	25.08	26.11	27.64	30.88
	Average		24.02	24.16	24.41	25.03	26.00	27.70	30.90
ID	Measurements	#1	12.03	12.01	11.93	11.85	11.43	10.75	9.79
		#2	12.01	11.99	11.89	11.73	11.32	10.95	10.10
		#3	12.02	12.00	11.90	11.77	11.35	10.79	9.86

	Average		12.02	12.00	11.91	11.78	11.37	10.83	9.92
H	Measurements	#1	8.01	7.86	7.62	7.11	6.36	5.34	4.09
		#2	8.03	7.92	7.67	7.12	6.32	5.33	4.00
		#3	7.95	7.80	7.55	7.05	6.30	5.29	4.02
	Average		8.00	7.86	7.61	7.09	6.33	5.32	4.04

Table C: Measured Surface Roughness before Test

Types of emery paper used	Sample (#)	Trial #1	Trial #2
Grinding and 380 grit size	1	1.497	1.537
	2	1.545	1.561
	3	1.492	1.545
grit size with 60,120,240,320 &360	1	2.621	2.571
	2	2.558	2.484
	3	2.482	2.497
grit size with 60,120 & 240	1	3.437	3.527
	2	3.494	3.469
	3	3.472	3.546
Grinding and grit size 380	1	1.539	1.374
	2	1.601	1.521
	3	1.398	1.483
	4	1.41	1.457
	5	1.54	1.62
	6	1.593	1.531
	7	1.50	1.576
	8	1.43	1.475
	9	1.611	1.676

APPENDIX II

HIBRET MANUFACTURING AND MACHINE BUILDING INDUSTRY

DOC. No.HMMBI HMMBI/ / SPI/LB/-02

Chemical composition Laboratory Test Result Form | Issue No. 01 | Page 1 of 1

Date: 10/07/10

Requested by; ADAMA SCIENCE AND TECHNOLOGY UNIVERSITY

Sample type: ALUMINUM

Purpose: IDENTIFICATION

S/N	Sample Name	Chemical composition											
		Si	Fe	Cu	Mn	Mg	Zn	Ni	Cr	Pb	Sn	Al	CSN
1	A	11.51	1.12	1.65	0.31	0.31	1.42	1.77	0.062	0.13	0.14	81.3	Aluminum
2	B	9.07	1.77	2.58	0.22	0.88	2.69	1.52	0.059	0.13	0.17	80.06	Aluminum

Prepared by: Alemitu
Sign:
Date: 10/07/10

Checked by: Saba
Sign:
Date: 10/07/10

Approved by: SGADA
Sign:
Date: 10/07/10

የኢትዮጵያ የተስማሚነት ምዘና ድርጅት
Ethiopia Conformity Assessment Enterprise

ቁጥር (No.) 2/R/16-2/4307/18
ቀን (Date) 14 SEP 2018

Head Quarters
House No.: New:
Woreda 6, Bole Sub-City
P.O.Box: 1145
Addis Ababa, Ethiopia
Tel:- 251 (0)11 647 0193-Ex140,122
Fax: +251 (0)11 645 9720
Fax: +251 (0)11 667 0245
Email: info-cp@eca-e.com
(Complain Handling)
Web site: www eca-e.com
Bank Account
Commerical Bank of Ethiopia (CBE)
megenagna branch
Account no 100005054366
Tin no. 0020245227

Director General Office
Tel: +251 (0)11 8695041
Fax: +251 (0)11 6670245
Email info-cp@ eca-e.com

Customer Service
Tel:- +251 (0)11 651 6468
Tel:- +251 (0)11 896 0258
Fax:- +251 (0) 11 6670249
Email info-cp@ eca-e.com

Certifecation Services
Tel:- +251 (0)11 646 0548
Email info-cp@ eca-e.com

Inspction Services
Tel:- +251 (0)11 896 0261
Email info-cp@ eca-e.com

Testing Laboratory Services
Tel:- +251 (0)11 6670246
Email info-cp@ eca-e.com

Corporation Communcation
Tel:- +251 (0)11 6460683
Email info-cp@ eca-e.com

Finance and Supplies
Tel:- +251 (0)11 8695044

Admin. Human Res. Dev
Tel:- +251 (0)11 896 0263

Addis Ababa Branch
Tel:- +251 (0)11 651 7988
Email addisababa-br@ eca-e.com

Centeral Branch (Adama)
Tel:- +251 (0) 22 1112278
Fax:- +251(0) 22 1128066
Email addisababa-br@ eca-e.com

Southern Branch (Hawassa)
Tel:- +251 (0)46 221 4732
Fax:- +251(0)46 220 4488
Email addisababa-br@ eca-e.com

North Western Branch (Baher Dar)
Tel:- +251 (0)58 220 0724
Fax:- +251(0)58 220 0724
Email addisababa-br@ eca-e.com

North Eestern Branch (Desele)
Tel:- +251 (0)33 111 1664
Fax:- +251(0)33 111 9069
Email addisababa-br@ eca-e.com

Estern Branch (Dera Dewa)
Tel:- +251 (0)25 111 3159
Fax:- +251(0)25 111 1426
Email addisababa-br@ eca-e.com

Northern Branch (Mekele)
Tel:- +251 (0)34 440 6280
Fax:- +251(0)34 440 6280
Email addisababa-br@ eca-e.com

To: Mohammed Hamda

Adama

On your letter dated 21/06/2018 and 25/06/2018 you have requested for the analysis on Aluminum 4026 Ring samples.

Accordingly, the analysis is completed as per your request and hence you find the report attached here with.

Regards,

Tesfaye Solomon
Head, Branch Coordination and Customer's Service

THE FEDERAL DEMOCRATIC REPUBLIC OF ETHIOPIA ETHIOPIAN CONFORMITY ASSESSMENT ENTERPRISE

Enc: 1 Page of test reports MTR/2110/18

CC. ECAE

- Customer's Service
  Addis Ababa

ወደ ላቀ ብቃት የሚያደርስ!
Moving you forward!

ECAE ኢተምድ	የኢትዮጵያ የተስማሚነት ምዘና ድርጅት Ethiopian Conformity Assessment Enterprise	Document No. TLD/F5.10-1	
		Copy No: -	Rev No: 1
Title:	TEST REPORT ይህ የናሙና ፍተሻ ሪፖርት እንጂ ሰርተፍኬት አይደለም	Page No: 1 of 5	Effective Date: 1Jan 13

Report No: MTR/2110/18
Test order No: ---

1	Name and address of client	Mohammed Hamda Tel: +251-924-48-42-93, Adama
2	Date and place of sampling	Not Specified
3	Sampled and submitted by	Client
4	Date sample received	25/06/18
5	Client's sample code	-
6	Laboratory designated sample No.	10284036,10284037,10288003,10288004,10288005 & 10288006
7	Type of sample	Aluminum 4026 ring
8	Test method	As per client agreement
9	Test date(s)	28/06/18-29/06/18
10	Date of Submission of test report	10/09/18

Test result

RO. No.	LDS. NO.	Type Of Sample	Parameters tested	Number of test specimens
1	10284036	1.5 µm surface rough dry	Dimension changes(deformations) in Outside diameter,Inside diameter,Thickness	3
2	10288003	2.5 µm surface rough dry		3
3	10288004	3.5 µm surface rough dry		3
4	10288005	1.5 µm SR grease		3
5	10284037	1.5 µm SR palm oil		3
6	10288006	1.5 µm SR emulision		3

Remark:

1. This test report relates only to the specific sample product which has been tested by ECAE testing laboratory.

Test report authorized by, Name Yohannes Kedir Position Analyst V Sign

✉ 11145 ☎ 011 6 46-05-69, Fax. 011 6 45-97-20, E-mail info-cs@eca-e.com Web site: www.eca-e.com
BOLE SUBCITY, WOREDA 6
ADDISABABA. ETHIOPIA